

**Elastic tethers remain functional during anaphase arrest in partially-lysed crane-fly spermatocytes, and in non-lysed spermatocytes treated with microtubule inhibitors**

Aisha Adil

A Thesis submitted to the Faculty of Graduate Studies in Partial Fulfillment of the Requirements for the Degree of Master of Science

Graduate Program in Biology, York University, Toronto, Ontario

November 2023

© Aisha Adil, 2023

## **Abstract**

Elastic tethers connect corresponding arms (telomeres) of partner chromosomes during anaphase segregation; they exert anti-poleward (backward) forces on the poleward-moving chromosomes. This thesis examined how arresting anaphase chromosomal segregation affected elastic tether function. Various dilutions of a standard immunofluorescent lysis buffer were used to partially lyse anaphase-I spermatocytes of crane flies. Partial cell lysis deactivated the anaphase spindle apparatus and arrested anaphase chromosomal segregation. Elastic tethers remained functional, and backward tether forces acting on chromosomes were able to cause backward chromosomal movements. Backward-moving chromosomes were attached to their kinetochore microtubules (kMTs) which might have been slowing them down. To test whether detaching chromosomes from their kMTs could enable their faster backward movements, anaphase spermatocytes were treated with various microtubule inhibitors to disassemble kMTs. The inhibitors led to anaphase segregation arrest, and backward chromosomal movements. However, the drugs were unable to disassemble the stable, acetylated kMTs, and allow faster backward movements.

## Acknowledgement

First of all, I was honored to have received the prestigious Natural Sciences and Engineering Research Council of Canada Graduate Scholarship-Master's Program (NSERC-CGSM). I am deeply indebted to the funding council for this financial endowment, and hope my research work meets their high standards.

Next, I would like to express my utmost appreciation to my research supervisory committee; my master's supervisor Dr. Arthur Forer, and my committee member Dr. Terrance Kubiseski. Art has promoted my scientific knowledge and research prowess since we started working together. I learnt a lot from Art as his data analyst and research assistant with an NSERC undergraduate student research award (NSERC-USRA) during the summer of 2020. That work led to my first research publication as a third author. Art then took me on as his MSc student, further boosting my career in research. We have had a plethora of scientific exchanges, research brainstorming, and medical discussions. Yet my favorites have been our personal chats, including his anecdotes from his extensive life experiences that he has generously shared with me. I have nothing but respect and admiration for him and the work he does, on a professional and personal level. As for Dr. Kubiseski, I feel lucky to have had him as my other scholarly guide through my master's journey; he has taught me how to be a professional, thorough researcher, and his valuable advice has always helped me improve my work. I would especially like to thank Dr. Kubiseski for the patience he has shown me during my MSc thesis submission, as I struggled with immense personal and health-related issues in the last year of my master's.

I would also like to thank my MSc thesis defense committee examiners, Dr. Peter Backx and Dr. Christopher Perry; they took me on a critical thinking journey during my exam and opened up mind to alternative modes of analysis of my own research! I thoroughly enjoyed our session.

Of course, my MSc lab experience would have been incomplete if not for my super-supportive colleagues: Eleni, Divya, Maral, and Demetra. They brought fun into what was often a tedious and endless hunt for good cells at the microscope. Thanks guys!

And last but certainly not the least, from the bottom of my heart I cannot thank enough my husband and kids who make every day of my life a blessing, and support me unconditionally through all my endeavors, no matter how unachievable they may seem. Thank you.

## Table of Contents

<b>Abstract.....</b>	<b>ii</b>
<b>Acknowledgement.....</b>	<b>iii</b>
<b>Table of contents.....</b>	<b>iv</b>
<b>Chapter 1. Thesis Introduction.....</b>	<b>1</b>
Life cycle of a cell.....	1
A brief background on tethers.....	6
Historical evidence pointing to tethers.....	6
Establishment of tethers as cell components.....	7
Tether characteristics defined presently.....	9
Research project background.....	12
Detergent-based cell lysis.....	13
Research objective.....	18
Research material and outline.....	18
<b>Chapter 2. Elastic tethers remain functional during anaphase arrest in partially-lysed crane-fly spermatocytes: A possible system for studying tethers .....</b>	<b>20</b>
Abstract .....	20
Introduction.....	21
Materials and methods .....	26
Results.....	29
Discussion.....	52
<b>Chapter 3. Elastic tethers remain functional during microtubule inhibition, but do not cause faster backward chromosomal movements than the backward movements seen in partially-lysed cells.....</b>	<b>56</b>
Abstract .....	56
Introduction.....	57
Materials and methods .....	60
Results.....	62
Discussion.....	79
<b>Chapter 4. Summary Discussion.....</b>	<b>84</b>
<b>References.....</b>	<b>88</b>

## Chapter 1. Thesis Introduction

### Life Cycle of a Cell

Many multicellular eukaryotes have diploid somatic cells with nuclei having two sets of chromosomes, homologous paternal and maternal sets. Each diploid cell goes through a life cycle that has four major phases (Alberts *et al.*, 2002); First is the G1 phase during which cell grows and produces cell components like proteins to prepare for DNA replication; second is the S phase during which DNA is synthesized as each chromosome replicates to become sister chromatids held together at centromere; third is the G2 phase during which cell continues to grow and produce cell components like proteins in preparation for cell division; and fourth is the cell division or M phase during which cell divides either by mitosis or meiosis. Mitosis involves a single round of division that produces two new identical diploid somatic cells, both of which start the G1 phases of their own life cycles. Meiosis involves two rounds of division that produce four new non-identical haploid reproductive cells, also called gametes, which fertilize their counterpart gametes resulting in the formation of new diploid organisms (McIntosh and Hays, 2016). Usually, the first meiotic division (meiosis-I) is the reduction division which results in two new cells having half the number of chromosomes as the parent cell. The second meiotic division (meiosis-II) is the equational division where the two resultant cells of first division produce four new cells, each containing half the number of chromosomes as the parent cell that started meiosis-I (Sato, 2013).

There is evolutionary diversity among the cell divisions of various organisms such that a single universal mechanism cannot be assigned to all (McIntosh and Hays, 2016). Still, the most common processes involved in division are described herein (McIntosh, 2016). The general stages of cell division in mitosis and meiosis of animal cells are similar and comprise of the following:

[1] **Prophase:** Decondensed chromosomes are present as long strands of DNA extending diffusely throughout the nucleus at the end of the G2 phase. Cell division starts with prophase where chromosomes are packed into tight loops, and shortened lengthwise while broadened in breadth. This makes chromosomes compact and condensed with distinct sister chromatids and centromeres. Meanwhile, microtubule organizing centers (MTOCs), which are usually the duplicated centrosomes, move through the cytoplasm to occupy two opposite ends of the cell outside the nucleus. They assemble tubulin polymers called microtubules into spindle fibers which form the mitotic/meiotic spindle apparatus. The spindle apparatus, a cytoskeletal

structure that is composed of a variety of protein molecules, coordinates the movement of chromosomes during cell division (Fabian *et al.*, 2007b). Spindle construction continues between the two opposite MTOCs, which are now the two spindle poles, and surrounds the nucleus. Nuclear envelope disperses marking the end of prophase.

[2] **Prometaphase:** The bipolar spindle apparatus now has direct access to the condensed chromosomes. Spindle fiber microtubules have their one end at the pole (the minus end) and one end free (the plus end). Sister chromatids of each chromosome have specialized protein structures on their centromeres called kinetochores. Spindle fiber plus ends interact with the chromosomal kinetochores to establish attachment; for mitosis and meiosis-II, sister kinetochores of each chromosome attach to spindle fibers of opposite poles. For meiosis-I, homologous kinetochores of homologous chromosomes attach to spindle fibers of opposite poles (Ohkura, 2015). Such accurate attachments are rarely achieved on first attempts; kinetochores usually end up binding to microtubule walls rather than the plus ends resulting in imbalanced forces acting on the chromosomes. Moreover, inadequate binding of chromosomes to spindle fibers of only one pole also leads to imbalanced forces acting on the chromosomes. Such improper attachments are unstable and quickly dissolve to give another chance for proper binding. When sister kinetochores or homologous kinetochores are bound to the plus ends of spindle microtubules of opposite poles, the forces acting on the kinetochores are balanced making their attachment to the microtubules stable. Such proper attachments are followed by chromosomes migrating along the spindle axis; sometimes they move up towards the pole, but then move back towards their ultimate destination which is the midpoint between spindle poles called the spindle equator. This central migration is driven partly by microtubule plus ends polymerizing away from both the poles and towards the spindle equator, pushing the chromosomes along with them (polar ejection force). Additionally, kinesin motors bind chromosomes and move them as they walk along microtubule walls towards their plus ends at the spindle equator. Prometaphase ends once chromosomes have congressed to the spindle equator.

[3] **Metaphase:** Spindle attached chromosomes line up at the spindle equator to form the metaphase plate, initiating metaphase. In case of mitosis and meiosis-II, sister chromatids attached to opposite spindle poles line up along the metaphase plate, and they are held together at their centromeres by special protein complexes called cohesins (Ohkura, 2015). In case of meiosis-I, homologous chromosomal pairs attached to opposite spindle poles line up along

the metaphase plate and are held together at their chiasmata, and via cohesins (Buonomo *et al.*, 2000; Ohkura, 2015). The kinetochore microtubules are in constant flux towards the poles during metaphase (Wilson *et al.*, 1994; Silverman-Gavrila and Forer, 2000); their plus ends polymerize while their minus ends depolymerize causing them to treadmill away from the kinetochore and towards the pole. However, the rates of polymerization/depolymerization are balanced maintaining the steady length of kinetochore microtubules, thereby maintaining the metaphase plate position of chromosomes (LaFountain *et al.*, 2004). Complex biochemical pathways involving multiple regulatory proteins control the transition from metaphase to anaphase; one key event is the activation of separase enzyme that degrades the cohesin connections between chromosomes ending metaphase and starting anaphase (Buonomo *et al.*, 2000).

- [4] **Anaphase:** Separase enzyme breaks the cohesion between sister chromatids in mitosis and meiosis-II, or between homologous chromosomes in meiosis-I, signaling anaphase onset. Sister chromatids, or homologous chromosomes, separate as partners move towards their respective poles at opposite ends of the cell. The poleward movement of partner chromosomes is driven by a combination of mechanisms; kinetochore microtubule flux increases during anaphase when compared to metaphase, and minus end depolymerization is faster than plus end polymerization leading to overall movement of chromosomes towards the poles (LaFountain *et al.*, 2004). In addition, spindle matrix components push chromosomes poleward (Johansen *et al.*, 2011), and their activity is independent of the kinetochore microtubule activity (Forer *et al.*, 2018). Besides the poleward segregation of chromosomes, spindle elongation also occurs as poles move further apart causing interpolar distance to increase. Chromosomes reach their respective poles and form two groups at opposite ends of the cell bringing anaphase to an end.
- [5] **Telophase:** Telophase begins when a nuclear membrane starts forming around each chromosomal group formed at the end of anaphase. Nuclear proteins surround the chromosomes to rebuild the nuclear membrane and reestablish the boundary between genetic material and cell cytoplasm. The spindle apparatus disassembles as chromosomes inside the newly formed nucleus decondense and cytokinesis starts. Some cases of meiosis-I have no telophase as each chromosomal group formed at the end of anaphase enters meiosis-II to complete cell division.

[6] **Cytokinesis:** Once the new nuclei have formed, cell cytoplasm divides during cytokinesis. This usually initiates with a cleavage furrow forming at the equatorial region of the cell (Barr and Gruneberg, 2007); the furrow is a contractile ring of actin and myosin assembled from the cytoskeleton at the cell cortex. It contracts inwards towards the cell center causing the cell membrane to fuse along and ultimately become two separate membranes enclosing the two new daughter cells (Barr and Gruneberg, 2007). Formation of new daughter cells brings cell division to an end in mitosis and meiosis-II; however, daughter cells of miosis-I need to enter meiosis-II to complete cell division. Therefore, mitosis and meiosis-II are alike and involve the separation and distribution of sister chromatids into new cells. Contrarily, meiosis-I involves the separation and distribution of homologous chromosomes into new cells.

This thesis presents research work conducted on male meiosis-I cells, primary spermatocytes, of crane flies. These primary spermatocytes undergo anaphase-I following the general description presented earlier, i.e., their 3 pairs of homologous autosomes (bivalents) separate into partner chromosomes (half bivalents) that move towards their respective poles. Each homologue moves poleward led by its kinetochore while all four of its arms usually trail behind. In crane-fly meiosis-I, there are 2 unpaired sex chromosomes (univalents) which do not segregate while the homologous autosomes are segregating (Forer, 1980). Once homologous partners have reached near their poles, the unpaired sex chromosomes segregate (Figure 1.1).

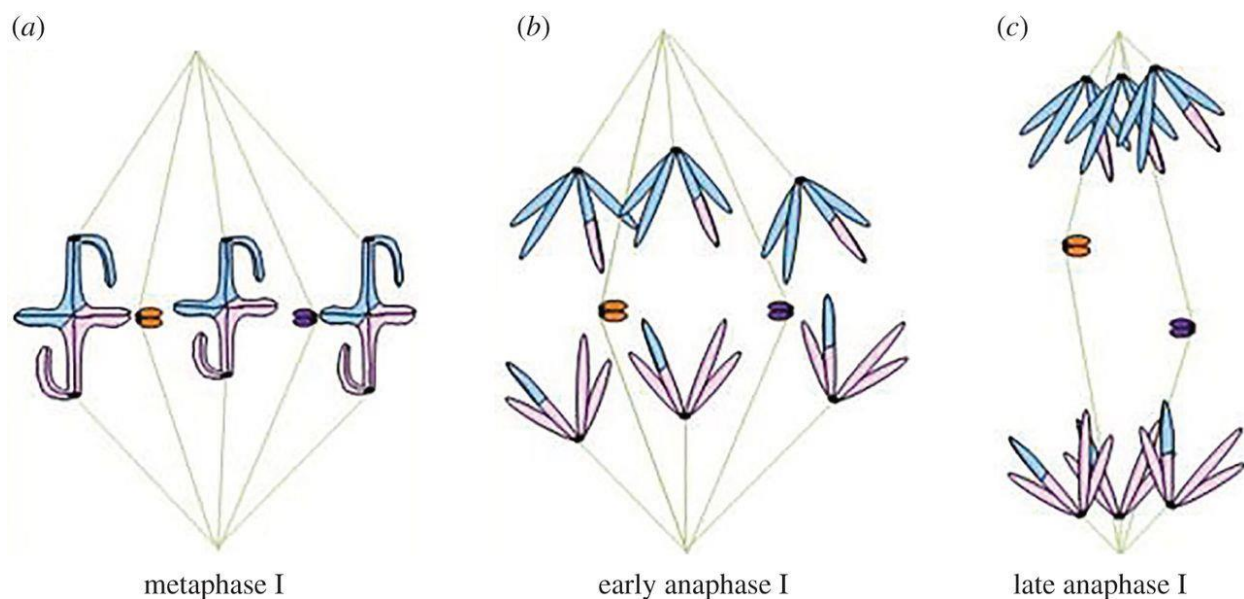


**Figure 1.1.** Meiosis-I set up and segregation of 3 paired homologous autosomes and 2 unpaired sex chromosomes in primary spermatocytes of crane flies. (a) metaphase-I: the 3 pairs of homologous chromosomes (pink and blue partners) and 2 separate sex chromosomes (orange and purple individuals) line up at the metaphase plate. Partner kinetochores of each homologous pair are attached to spindle fibers of opposite poles, while the kinetochore of each sex chromosome is attached to spindle fibers of both poles. (b) early anaphase-I: the homologous autosomes start segregating such that each partner moves poleward led by its kinetochore while all its arms trail behind. Both sex chromosomes remain at the equator. (c) late anaphase-I: once all the autosomes are near their respective poles, each sex chromosome starts segregating towards one pole in opposite directions to each other such that only one sex chromosome ends up at one pole. (Adapted from Brady and Paliulis, 2015)

My research focuses on tethers that physically connect tips of chromosomal arms (telomeres) of the segregating homologous autosomes during anaphase-I of crane-fly spermatocytes. To further explain my work, I will first give a brief account of what tethers are, what we already know about them, and what is yet to be explained regarding these cell components.

## A Brief Background on Tethers

### Historical evidence pointing to tethers

Tethers are cell components that have been recently established by LaFountain *et al.* in 2002; however, their existence had been hinted upon by many researchers of cell division starting as early as the 1800s (Carnoy, 1885; Montgomery, 1899; Wilson, 1905; Andrews, 1915; Schrader, 1935; and others reviewed in Paliulis and Forer, 2018). Initial research on cell division described the presence of “fibers” or “tubes” that connected partner chromosomes while they segregated towards their respective poles during anaphase of mitosis and meiosis. Researchers illustrated these “interzonal connections” that extended from one partner chromosome to the other in many animal (Carnoy, 1885; Montgomery, 1899; Wilson, 1905; Schrader, 1935), and plant cells (Andrews, 1915; Schaede, 1930). Still, no one commented on the possible function of these connections until 1953; Carlson (1953) showed that in grasshopper neuroblasts, if an arm of any one segregating chromosome was pulled by applying force from the side, its partner’s corresponding arm also moved in the direction of the pulling force. Similar effect was seen in grasshopper spermatocytes (Paliulis and Nicklas, 2004). In crane-fly spermatocytes, if a segregating chromosomal arm was pushed to the side, its partner’s corresponding arm also moved towards the direction of the push as if connected to it (Forer and Koch, 1973). Thus, it had been shown by 1973 that there are interzonal connections between segregating partner chromosomes during anaphase, and that they probably exert tension on the partner chromosomal arms such that moving one causes the other to move along with it.

The function of interzonal connections between segregating anaphase chromosomes was further defined by studies of Forer (1966), Sillers and Forer (1981), and Ilagan and Forer (1997); they proposed that the interzonal connections coordinate the poleward movements of partner chromosomes during anaphase in crane-fly spermatocytes. Ultraviolet (UV) microbeam irradiation of the kinetochore fiber of one segregating chromosome caused not only that chromosome to stop moving poleward but also its partner. If the UV irradiation of kinetochore fiber was preceded or proceeded by UV irradiation of interzonal connection region, then only the one chromosome whose kinetochore fiber was irradiated stopped poleward movement while its partner continued unaffected (Yin and Forer, 1996). Therefore, there was suggestion by 1996 that partner chromosomal movements during anaphase are not independent of each other; altering the

interzonal linkage between the partners unlinks them and alters their coordinated anaphase movements.

UV microbeam irradiation experiments also indicated that the mechanical linkages between partner chromosomes can be elastic and cause anti-poleward movement of partners once their poleward movement is interrupted. UV irradiation of one spindle pole in telophase-I of silkworm spermatocytes led to that pole's chromosomes moving towards the opposite pole (Nakanishi and Kato, 1965). Additionally, UV irradiation of spindle fibers of separating anaphase chromosomes in newt fibroblasts caused transient anti-poleward (backward) movement of those chromosomes (Spurck *et al.*, 1997). Furthermore, UV irradiation of chromosomal kinetochores in anaphase crane-fly spermatocytes resulted in those chromosomes moving antipoleward (backward) towards their partners at the opposite pole (Ilagan *et al.*, 1997). Hence, it was hypothesized by 1997 that the mechanical linkages between partner chromosomes can be elastic and cause anti-poleward movement of partners once the poleward movement is interrupted.

More details about the mechanical connections between chromosomes were given by experiments on anaphase-I crane-fly spermatocytes which illustrated that only two of the four corresponding arms of segregating half bivalents seem to be linked to each other (Adames and Forer, 1996; Forer and Pickett-Heaps, 1998). Anaphase-I segregation of each half bivalent towards its respective pole is led by its kinetochore while all four of its arms usually trail behind. When chromosome segregation speeds were decreased by irradiating their kinetochore fibers or treating them with anti-actin drugs, one or two of the chromosomal arms moved ahead of their kinetochore towards the pole while the other two did not. This phenomenon had been seen even in some untreated (control) cells. So, it was postulated by 1998 that two of the four chromosomal arms must be linked to their corresponding partner arms during anaphase-I, thereby being physically unable to move ahead of the kinetochores towards their pole.

### **Establishment of tethers as cell components**

All the evidence collected by the end of the twentieth century was at best circumstantial, yet highly indicative of mechanical, perhaps elastic, connections existing between partner arms of segregating anaphase chromosomes in various animal and plant cells. In 2002, LaFountain *et al.* gave definite confirmation that elastic connections are present between partner arms of segregating anaphase chromosomes in crane-fly spermatocytes, and called them "tethers". They first pointed

out that as partner chromosomes started separating poleward during early anaphase, their trailing arms often stretched anti-poleward (backward) towards their partners in the opposite half spindle (Figure 1.2A). The backward stretching of partner arms seemed to be due to elastic tension created on them as if they were tethered together. Next, they used laser microbeam surgery to cut the arms of segregating chromosomes at different times during anaphase, and observed the movements of the cut arm fragments (Figure 1.2B-D). When a chromosomal arm was cut in early anaphase, the resultant arm fragment moved backwards in the anti-poleward direction, telomere quickly reaching its partner telomere in the opposite half spindle. Meanwhile, the rest of the intact chromosome, minus a terminal piece of its arm, continued moving poleward (Figure 1.2B). Laser-cut arm fragments produced in mid-anaphase moved backward to a lesser extent (Figure 1.2C). In fact, the later in anaphase the cut was made, the lesser was the backward movement of the arm fragment, if any at all (Figure 1.2D). These results indicated that tethers either became less elastic as anaphase progressed, or detached from the arms at later times of anaphase.

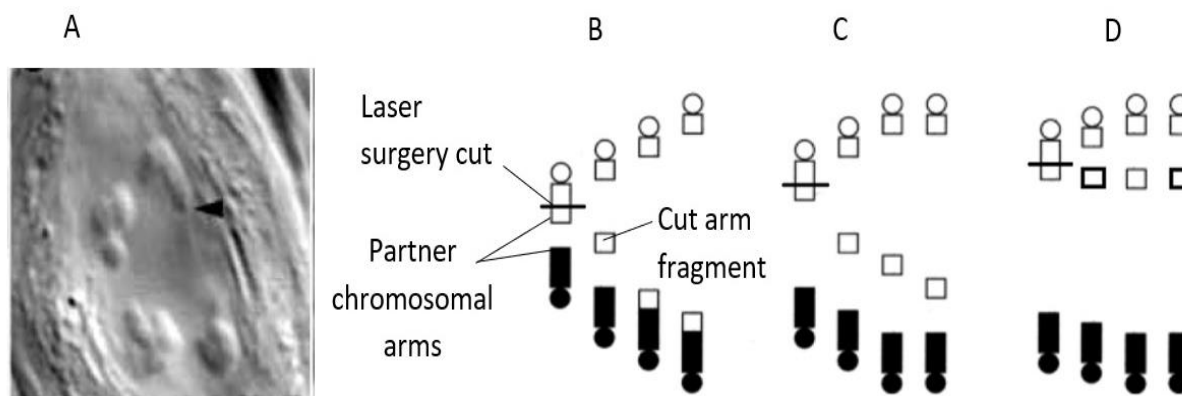


**Figure 1.2.** (A) DIC image with arrowhead showing transient stretching of trailing partner chromosomal arm during crane-fly spermatocyte anaphase. (B-D) diagram showing arm fragments cut at different anaphase times; (B) fragment cut in early anaphase moves backward rapidly to its partner (C) fragment cut in mid anaphase moves backward partially (D) fragment cut in late anaphase moves backward slightly if at all. (Adapted and modified from LaFountain *et al.*, 2002)

LaFountain's group (2002) further elaborated that elastic tethers connect the tips of partner chromosomal arms, telomeres, and that it is elastic tethers, rather than interzonal microtubules, that cause backward movement of cut arm fragments. They produced backward moving arm fragment by laser microsurgery, then further cut that fragment to separate its telomere into another fragment; the telomeric fragment continued moving backward while rest of the arm fragment

stopped. Moreover, they laser ablated either the backward moving arm fragment's telomere or its partner's telomere; in either case, backward moving fragment stopped. These experiments proved that backward forces acting on chromosomal arm fragments, making them move backwards, need intact undamaged partner telomeres. Movements caused by microtubules do not. Thus, LaFountain *et al.* (2002) concluded that elastic tethers, and not microtubules, connect partner telomeres and cause their backward movements.

### **Tether characteristics defined presently**

The research findings of LaFountain *et al.* (2002) led to other extensive studies on tether characteristics. It also rationalized many of the previous research findings that had suggested the probable existence of connections between segregating anaphase chromosomes, their characteristic features and possible functions. For instance, LaFountain *et al.* (2002) used laser microsurgery to cut the arms of segregating anaphase chromosomes, and the arm fragments thus produced moved backwards. This matched the findings of earlier experiments where disabling poleward movement of segregating chromosomes enabled their backward movements (Spurck *et al.*, 1997; Ilagan *et al.*, 1997). Moreover, when LaFountain *et al.* cut more than two of the four arms from half bivalents during anaphase, only two moved backward at most. This corroborated the theory proposed earlier that only two of the four trailing arms of partner chromosomes are tethered to each other (Adames and Forer, 1996; and Forer and Pickett-Heaps, 1998). Additionally, LaFountain *et al.*'s confirmation that tethers physically connect segregating partner chromosomes underpinned earlier speculations that these connections maybe playing a role in coordinating anaphase chromosomal movements (Forer, 1966; Sillers and Forer, 1981; Ilagan and Forer, 1997; Yin and Forer, 1996). This coordination function of tethers was further investigated by other researchers. Sheykhani *et al.* (2017) used laser microbeam to cut the kinetochore fiber of segregating anaphase chromosomes, after which the chromosome and its partner continued moving poleward with their original pre-cut speeds. However, when they laser cut the interzone tether region first and then the kinetochore fiber of the chromosome, then the affected chromosome sped up while its partner continued moving with its original speed. Also, Forer and Berns (2020) laser cut the tethered arm of a segregating chromosome and then cut its kinetochore fiber, and again only that chromosome sped up while its partner continued moving with its original speed. Both these studies concluded that tethers coordinate the poleward movements of partner chromosomes during anaphase in crane-fly spermatocytes, and uncoupling partner chromosomes

by disconnecting their tethers abolishes their coordinated poleward movement. Therefore, some characteristic features of tethers are that they exert anti-poleward forces on anaphase chromosomal arms which can cause their backward movement; that they connect only two out of the four chromosomal arms to their corresponding partner chromosomal arms; and that they play a role in coordinating anaphase movements of partner chromosomes.

Tether elasticity was highlighted when laser microsurgery during early anaphase produced chromosomal arm fragments that moved backwards further than arm fragments produced in later anaphase (LaFountain *et al.* 2002). The researchers suggested that this difference might have been due to either tethers becoming less elastic as anaphase progressed, or tethers disconnecting from their chromosomal telomeres at later times during anaphase. Sheykhani *et al.* (2017), and Forer *et al.* (2017) distinguished between the two possible explanations; they laser cut tethers at different times during anaphase in crane-fly spermatocytes and PtK cells. This resulted in the chromosomal arms of cut tethers shortening by almost 90% of their original, pre-cut length. Such arm shortening was seen even when tethers were cut in late anaphase when tethers did not normally cause backward movements. So, it was concluded that tethers remain connected to their partner chromosomal telomeres continuously until late anaphase, but, become less elastic as anaphase progresses.

A defining feature of tethers is their elasticity, which is due to their phosphorylation. Fabian *et al.* (2007a) introduced the concept of tether phosphorylation; they studied the effect of Calyculin A (CalA), a serine-threonine protein phosphatase 1 (PP1) and 2A (PP2A) inhibitor, on anaphase segregation. They added CalA to early anaphase cells which caused the chromosomes to speed up, to complete anaphase faster, and then to move backwards towards their partners. Fabian *et al.* (2007a) speculated that such backward movements may be due to hyperphosphorylated myosin working in conjunction with actin or may be due to the elastic tethers. So, they added myosin or actin inhibitor to these CalA treated cells as soon as backward movement started. Blocking myosin or actin did not affect the backward chromosomal movements which proceeded in the presence of myosin or actin inhibition. Hence elastic tethers seemed to be the most likely candidates responsible for the backward chromosomal movements. This research finding suggested that tethers are dephosphorylated during anaphase; by adding CalA, tether dephosphorylation is prevented, thereby allowing tethers to be able to cause backward chromosomal movements at the end of anaphase.

The relationship between tether phosphorylation/dephosphorylation and elasticity was elucidated by Kite and Forer in 2020. They added CalA to cells at different times after the start of anaphase and observed chromosomal motion. Early anaphase CalA addition led to chromosomal segregation followed by backward movement of separated partner chromosomes. The later in anaphase CalA was added, the fewer were the chromosomes that moved backwards at the end of anaphase. The interpretation of these results given by Kite and Forer (2020) was that most likely tethers are phosphorylated at the beginning of anaphase, hence are elastic. As anaphase progresses, tethers gradually dephosphorylate such that towards the end of anaphase tethers are dephosphorylated and inelastic. Addition of CalA at the beginning of anaphase prevents the dephosphorylation of tethers during anaphase and preserves their elasticity till anaphase end. This in turn enables the tethers to move chromosomes backward at the end of anaphase when their poleward movement stops. Therefore, tethers are phosphorylated and elastic at the start of anaphase, and gradually become dephosphorylated and inelastic by the end of anaphase.

In 2021, Forer *et al.* substantiated the direct relationship between tether elasticity and phosphorylation, expounding certain features of tethers and how they function. All their experimental cells were treated with CalA at early anaphase to maintain tether phosphorylation till anaphase end. As soon as chromosomes completed anaphase segregation or just began backward movement, tethers directly were disabled by laser-cutting either the tethers themselves or the chromosomal arms, or ablating the telomeres to which the tethers were connected. This ensured that tethers themselves were deactivated. In all instances, backward chromosomal movement stopped; in cases where chromosomal arm was cut off, the arm fragment continued to move backwards while the rest of the chromosome did not. This proved that it is tethers, and not some other spindle interzone components, that exert anti-poleward force on the chromosomes causing their backward movements once poleward forces dissipate. The work by Forer *et al.* (2021) highlights some key tether characteristics and functional capabilities. Firstly, as anaphase progresses, tethers become longer and less elastic and less likely to cause backward chromosomal movements over long distances. Secondly, although shorter tethers are more elastic, they do not cause faster backward movements as compared to longer tethers. Also, CalA addition in early anaphase maintains tether elasticity till the end of chromosomal segregation with longest tether

lengths remaining elastic, but, it does not increase elasticity and, as such, does not cause faster backward movements of chromosomes.

All the research conducted so far has uncovered some of the salient features and functions of tethers. Still, much more needs to be understood about these cell components. For example, we know tethers are elastic (Fabian *et al.*, 2007b) but what is it about their composition that makes them elastic? Also, we know tether elasticity is due to its phosphorylation state most likely caused by PP1 (Kite and Forer, 2020), but when does that phosphorylation occur, and can it be enhanced or diminished? Would enhancing tether phosphorylation cause greater frequency and velocity of chromosomal backward movements? Answers to such questions can be vital in improving our comprehension of aberrant cell division pathogenesis leading to abnormal cell death, cancer, and fatal birth defects like Edwards syndrome. Thus, we need a system for analyzing tethers in further detail, and this formed the backdrop of my research project presented in the next section.

### **Research Project Background**

Some of the details about tether mechanics could be easily studied if there was a way of getting enhancer/ inhibitor enzymes into the anaphase spindle interzone of living cells during their cell division. Therefore, I wanted to create a partially permeabilized (partially lysed) living cell system wherein the spindle apparatus is deactivated, yet tethers remain functional. Then the effects of different kinases and phosphatases on tethers could be studied by allowing the enzymes to enter the partially permeabilized cell and directly enhance or diminish tether phosphorylation.

Permeabilizing a cell means manipulating its cell membrane such that the membrane allows the desired molecules to pass through which would not be able to do so normally. The cell membrane is a phospholipid bilayer having a variety of protein molecules dispersed throughout its structure (Figure 1.3). It functions as a partially permeable barrier which separates the intracellular contents from the extracellular environment. It only allows extracellular molecules needed by the cell to pass through and enter the cell, and allows intracellular molecules not needed by the cell to pass through and exit the cell. Thus, it helps maintain optimum intracellular conditions needed to promote efficient cell operations. If the cell content needs to be accessed for research purposes, then depending on the research objective, different techniques are employed to either permeate the cell membrane (Yang and Hinner, 2015), or break it down completely

(Islam *et al.*, 2017). The latter, also referred to as cell lysis, can be achieved by mechanical or non-mechanical (physical, chemical, biological) methods; each of these methods is further categorized according to the agent used to cause membrane breakdown (Islam *et al.*, 2017). One of the common chemical methods of cell lysis uses detergents, and this is the one I used to devise a partially permeabilized/lysed living cell system for studying tethers.

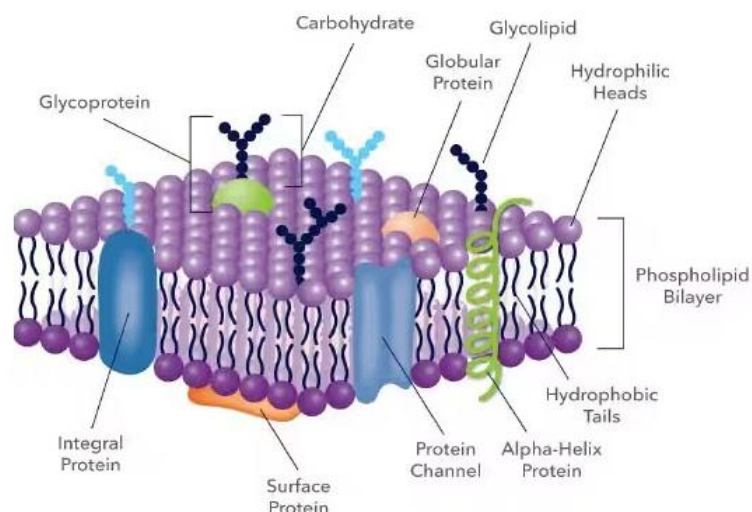


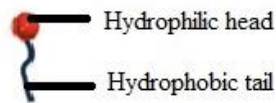
**Figure 1.3.** Structure of a cell membrane (Adapted from Novus Biologicals, 2023)

### Detergent-based cell lysis

Detergents are made up of amphipathic molecules (monomers) having a hydrophilic head and a hydrophobic tail (Thermofisher, 2023). When a sufficient concentration of detergent is mixed with water, the detergent monomers aggregate into micelles (Garavito and Ferguson-Miller, 2001). Monomer hydrophobic tails are compactly packed together and mostly oriented inwards at the micelle core, while their hydrophilic heads face outwards surrounded by water (Figure 1.4). Le Maire *et al.* (2000) and Sudbrack *et al.* (2011) explain that detergent micelles approach cell membranes and get incorporated into the lipid bilayer; their hydrophilic heads facing the water and hydrophobic tails embedded in between the hydrophobic tails of the lipid bilayer. Detergent monomers keep assimilating into the lipid bilayer until the layer becomes fully saturated with detergent. This way, detergent monomers disrupt the lipid-lipid and lipid-protein interactions of the bilayer. They remove sections of the bilayer as mixed micelles and protein-detergent complexes creating holes in the bilayer (partial cell lysis). Mixed lipid-detergent micelles have the bilayer's phospholipid molecules at their core grouped with the hydrophobic tails of detergent monomers.

Mixed protein-detergent complexes have the bilayer's protein molecules at their center where the protein's hydrophobic regions interact with the hydrophobic tails of the detergent monomers (Figure 1.5). Sections of the bilayer keep solubilizing into mixed micelles and protein-detergent complexes until the entire membrane is dissolved away (complete cell lysis).

**(A) Detergent monomer**



**(B) Detergent micelle**



**Figure 1.4.** (A) Parts of a detergent monomer. (B) Structure of a detergent micelle (Adapted from Anandan and Vrielink, 2016)

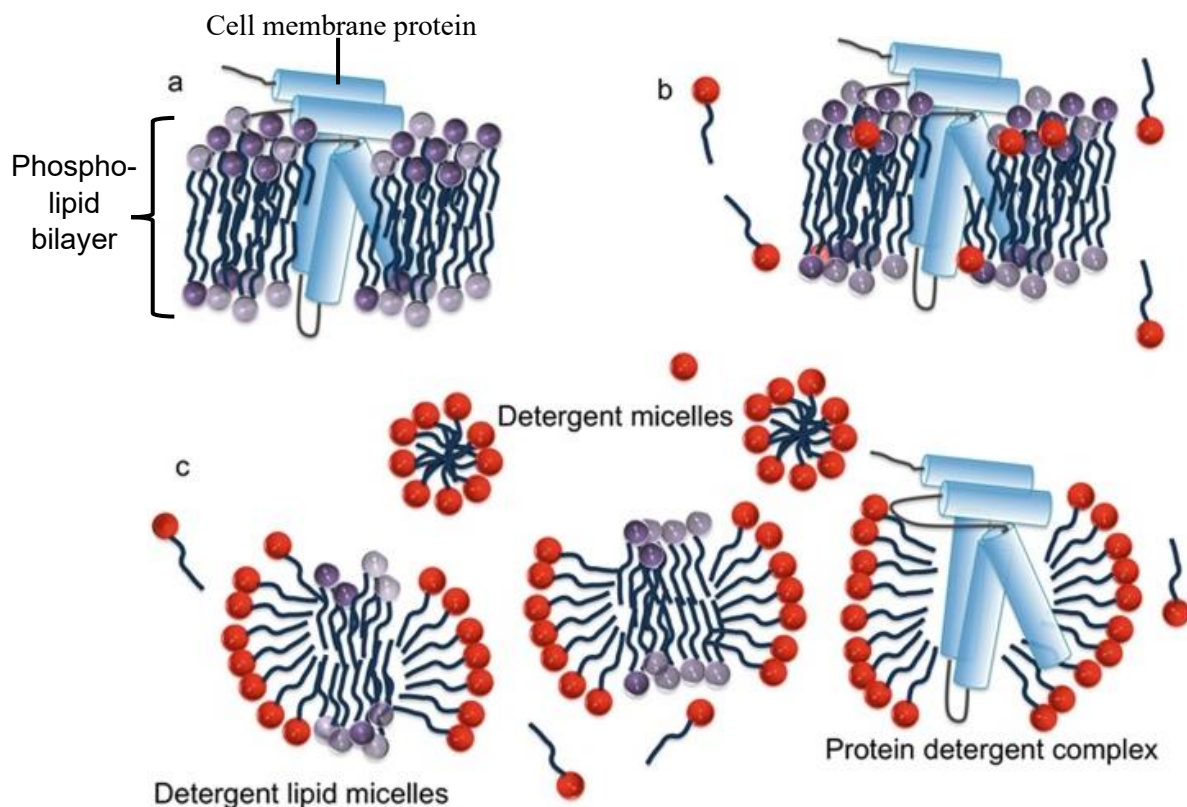


**Figure 1.5.** General mechanism of cell lysis caused by detergent. (a) cell membrane made of phospholipid bilayer and membrane protein. (b) detergent molecules near cell membrane get incorporated into the membrane disrupting the membrane lipid-lipid and lipid-protein interactions. (c) membrane breaks, releasing lipid-detergent mixed micelles and protein-detergent complex. Unused detergent micelles also remain. (Adapted from Anandan and Vrielink, 2016)

Detergents can be classified as ionic, non-ionic or zwitterionic based on the charge on their monomer heads (Caligur, 2023; Thermofisher, 2023). They can also be classified as denaturing or non-denaturing depending upon their protein denaturing abilities. Taken together, ionic detergents are denaturing, while non-ionic and zwitterionic are non-denaturing. Figure 1.6 illustrates some examples of detergents commonly used in each category, and highlights some of their key features and uses (Brown and Audet, 2008; Caligur, 2023; Thermofisher, 2023).

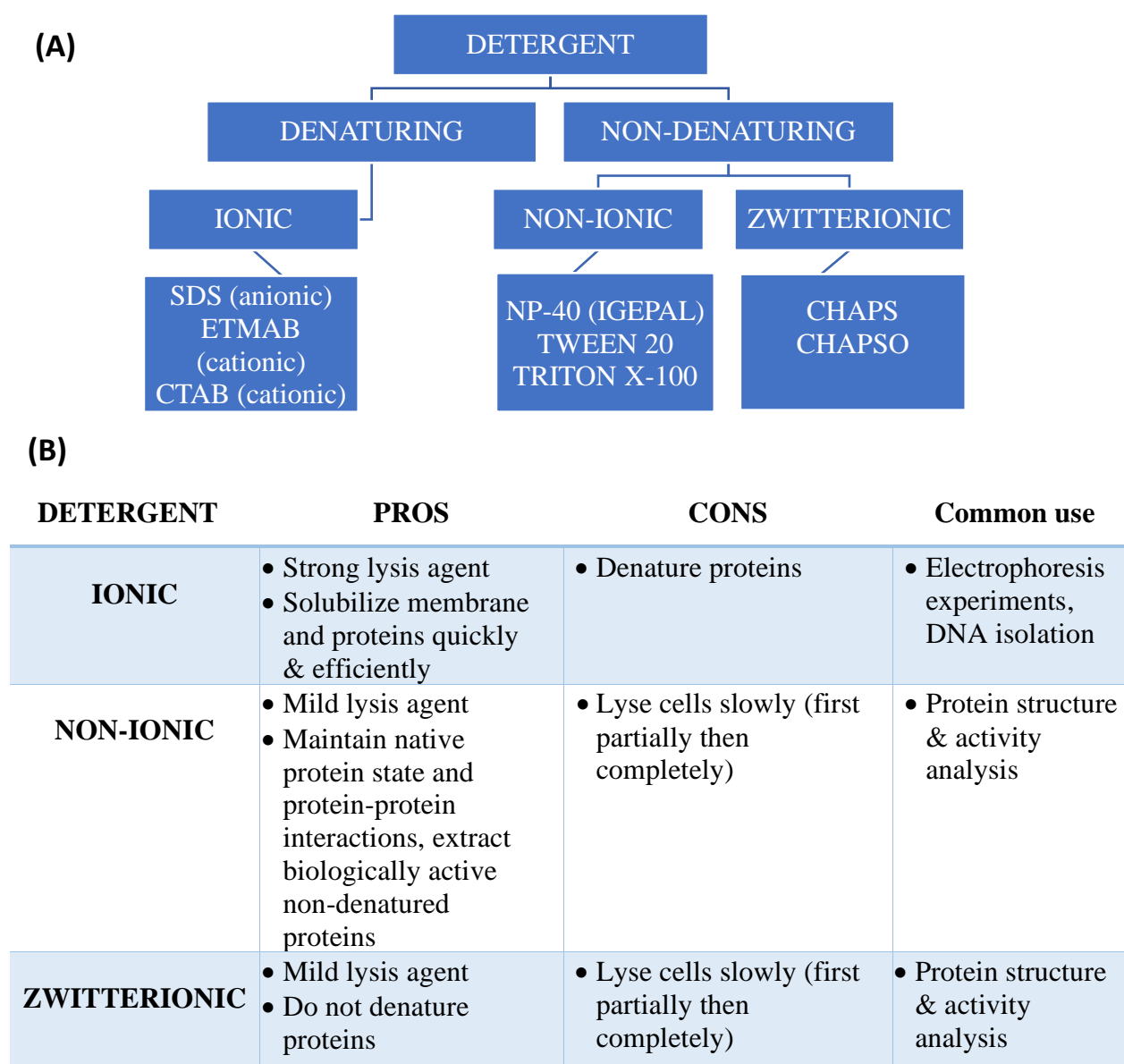


**Figure 1.6.** (A) Detergent classification based on charge and denaturation ability, and commonly used examples of each. (B) Key features of different types of detergents and their common use.

Non-ionic detergents are mild and cause cell lysis slowly as described by Sudbrack *et al.*, (2011); their monomers distribute in both layers of the cell membrane phospholipid bilayer by flip-flopping between the two. They saturate both layers, increase the cell membrane area, and disrupt the lipid-lipid and lipid-protein interactions. This causes parts of the bilayer to break off as mixed micelles and protein-detergent complexes creating holes in the membrane (partial lysis) before the entire membrane disintegrates (Figure 1.7). Contrarily, ionic detergents are strong and cause cell lysis quickly (Sudbrack *et al.*, 2011); their monomers distribute only in the one outer layer of the phospholipid bilayer, facing the extracellular environment. Monomers do not flip-flop due to their charged heads. They saturate only the outer layer, increase its area making it disproportionate to the inner layer of the phospholipid bilayer, and cause the cell membrane to curve outward. They also disrupt the lipid-lipid, lipid-protein, and protein-protein interactions, causing the proteins to denature. Cell membrane becomes tense, and either parts of it break off or entire membrane bursts to release mixed micelles and denatured protein-detergent complexes (Figure 1.7).

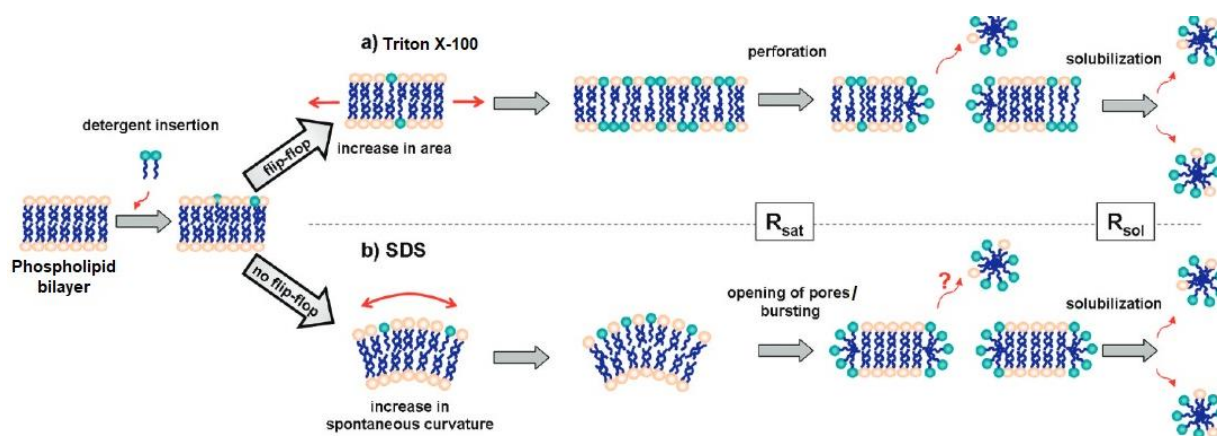


**Figure 1.7.** Mechanism of cell lysis caused by non-ionic and ionic detergent. **(a)** non-ionic Triton X-100 mechanism of action. **(b)** ionic SDS mechanism of action.  $R_{sat}$  and  $R_{sol}$  represent respectively the saturation and solubilization thresholds of the ratio between bound detergent and total lipids. (Adapted from Sudbrack *et al.*, 2011)

Non-ionic detergents are non-denaturing, so, they are the usual choice for extracting cell proteins in their native, biologically active form, with their protein-protein interactions intact (Seddon *et al.*, 2004; Orwick-Rydmark *et al.*, 2016). Many proteome analysis studies, including mitotic spindle proteome analysis studies, use non-ionic detergents to extract proteins for detailed

structural and functional analysis (Churchward *et al.*, 2005). In case of mitotic spindle studies, the entire spindle apparatus remains intact upon extraction, with all its protein-protein interactions preserved (Sauer *et al.*, 2005). In fact, with highly controlled experimental conditions, the mitotic spindle can be extracted such that not only are its proteins preserved, but all the chromosomes remain attached to their KT fibers (Salmon and Segall, 1980). Furthermore, the controlled experimental conditions allow such spindles to remain intact and preserved for more than one week without deteriorating (Salmon and Segall, 1980).

Another important application of non-ionic detergents is in fluorescent tagging of intracellular proteins and RNA for flowcytometry and Immunohistochemistry. This involves first fixing the cell and then partially permeabilizing it to allow the antibodies/fluorochromes to enter and bind their intracellular targets (Unity Health Toronto, 2023). Many non-ionic detergents like NP-40, Triton X-100, Tween-20, and saponin partially permeabilize cells effectively enough to allow the required amount of antibodies/fluorochromes to enter the cells (Amidzadeh *et al.*, 2014). They do not compromise the cell membrane integrity and do not alter its overall architecture. Moreover, saponin causes partial permeabilization of cells that is transient; this indicates that cell function is not compromised by saponin as it is able to ultimately patch up the broken areas (holes) in its membrane (Behbehani *et al.*, 2014; Unity Health Toronto, 2023). Therefore, non-ionic detergents seem to be effective in partially lysing cells and making them more permeable for experimental agents without killing them. This is why I used a non-ionic detergent to partially lyse anaphase-I spermatocytes of crane-flies. Once they were partially lysed, I observed the effect of lysis on anaphase spindle and tether activity.

## **Research Objective**

My research objective was to create a partially permeabilized (partially lysed) living cell system where the anaphase spindle apparatus was deactivated, but the tethers still worked so they could be studied. I hypothesized that partially lysing cells should deactivate the anaphase spindle apparatus, but should not affect tether function. Thus, tether function in the partially lysed cells was assessed against previously documented benchmarks of tether activity to ensure tethers were not altered by the partial lysis treatment of cells. Also, certain markers of tether activity in partially lysed cells were compared with corresponding markers in non-lysed cells where microtubules were inhibited. This further clarified how tethers were working, and the factors affecting tether activity during the partial cell lysis-induced anaphase arrest.

## **Research Material and Outline**

I conducted my research on anaphase in primary spermatocytes of crane flies (*Nephrotoma suturalis* Loew). Forer (1982) has described how primary spermatocytes of crane flies have certain characteristics which make them ideal for studying cell division. Firstly, crane flies can be reared in the lab all year round, so the cells are available any time as per need. Secondly, preparing living cells for experiments and microscopic observations requires adhering the cells onto coverslips in fibrin clots bathed in insect Ringer's solution (Forer and Pickett-Heaps, 1998). This simple procedure maintains viable cells for at least 2-3 hours until experiment is completed. Thirdly, a large number of cells are in the same stage of division which means it easy to find the cell of choice. Lastly, the anaphase-I spermatocyte size is about 25-30  $\mu\text{m}$  pole-to-pole on average, and it has only three pairs of homologous autosomes (bivalents) and 2 unpaired sex chromosomes (univalents). Thus, the spindle size is relatively large as compared to the size and number of chromosomes occupying the spindle space. This makes it easy to follow the chromosomes during anaphase segregation, and to observe the effects of experimental conditions on anaphase chromosomal behavior. For these reasons, I carried out my research on tethers in anaphase-I spermatocytes of crane flies.

For my first set of experiments detailed in chapter 2 of this thesis, I partially lysed anaphase-I spermatocytes using different dilutions of our standard immunofluorescence lysis buffer; this buffer preserves the cytoskeleton and contains the detergent IGEPAL CA-630. I

studied anaphase spindle deactivation and tether function in the partially lysed cells. I also used the IGEPAL CA-630 detergent alone to partially lyse cells and study them. IGEPAL CA-630 is a non-ionic, non-denaturing detergent used as a substitute for NP-40 detergent since NP-40 is no longer manufactured (Sinha *et al.*, 2017). In a few experimental cells, I first added CalA in early anaphase to preserve tether elasticity, and then did partial cell lysis. This was to confirm that tethers which remained elastic throughout anaphase did not alter their behavior due to partial lysis effect.

My next set of experiments, explained in chapter 3 of this thesis, involved microtubule inhibitors. I used three different microtubule inhibitors at various concentrations in anaphase-I spermatocytes to inhibit microtubule function, and then study tether behavior. Tether activity in microtubule inhibited cells was compared to tether activity in partially lysed cells to investigate any similarities/differences that would highlight any possible role of microtubules in tether activity during anaphase arrest.

## **Chapter 2. Elastic tethers remain functional during anaphase arrest in partially-lysed crane-fly spermatocytes: A possible system for studying tethers**

### **Abstract**

Elastic tethers connect partner telomeres of segregating anaphase chromosomes in animal cells. They exert anti-poleward forces on the separating chromosomes; hence they could play a role in anomalous cell divisions that lead to fatal disorders. They need to be studied in detail in a living-cell system into which different proteins, like enzymes, can be introduced, and their effect on tether activity can be analyzed. So, I used dilutions of our standard immunofluorescent lysis buffer to partially lyse anaphase crane-fly spermatocytes, to consistently arrest the anaphase spindle apparatus, and to study elastic tether function. To ensure that partial cell lysis did not alter tethers, I compared markers of tether activity in partially lysed cells with those in control cells. I found that elastic tethers cause backward chromosomal movements with typical characteristics in partially lysed cells, like as they do in non-lysed (control) cells. These include: shorter tethers causing more frequent backward movements than longer tethers; shorter tethers causing backward movements over greater fractional distances than longer tethers; tethers of different lengths causing backward movements with statistically similar velocities. Some early anaphase cells were treated with Calyculin A (CalA), a serine-threonine protein phosphatase 1 and 2A inhibitor which maintains tether elasticity throughout anaphase; partial lysis of these cells led to tethers always moving chromosomes backward completely at all tether lengths. Therefore, partial cell lysis arrests anaphase segregation, but does not affect tether function; such partially lysed system can be used to study tether activity in detail.

## **Introduction**

Most theories and textbooks explain anaphase chromosomal segregation as being driven primarily by microtubules and their associated motor proteins (Coue *et al.*, 1991; Sharp *et al.*, 2000; Rogers *et al.*, 2005). Such explanations have been countered in recent years by studies that highlight the roles of actin, myosin, titin, and other spindle matrix proteins as valuable contributors to the anaphase mechanics (Forer *et al.*, 2003; Fabian *et al.*, 2007a, 2007b; Johansen *et al.*, 2011; Sheykhan *et al.*, 2013; Forer *et al.*, 2018). In fact, the anaphase spindle apparatus is a cytoskeletal structure composed of a variety of protein molecules interacting with each other and with the chromosomes via complex mechanisms to achieve successful chromosomal segregation (Silverman-Gavrila and Forer, 2000; Fabian and Forer, 2005; Pimm and Henty-Ridilla, 2020). Tethers, newly-discovered components of the spindle apparatus, also play a part in anaphase segregation dynamics (Sheykhan *et al.*, 2017; Forer and Berns, 2020). They exist in a wide variety of animal cells ranging from flatworms to humans (Forer *et al.*, 2017), and may even exist in plant cells (Paliulis and Forer, 2018).

Tethers are structural connections between separating anaphase chromosomes (Montgomery, 1899; Wilson, 1905; Andrews, 1915; and many others). As partner chromosomes separate during anaphase, they move towards their respective poles led by their kinetochores while their arms trail behind; in anaphase-I, two of the four partner arms seem to be physically linked to each other (Adames and Forer, 1996). In 2002, LaFountain *et al.* established that tethers connect the corresponding arms (telomeres) of partner anaphase chromosomes (Figure 2.1.A). They used laser microsurgery to cut a chromosomal arm in early anaphase; the resultant arm fragment moved backwards in the anti-poleward direction, telomere quickly reaching its partner telomere in the opposite half spindle, while the rest of the intact chromosome continued moving poleward. The later in anaphase the cut was made, the lesser was the backward movement of the arm fragment, indicating that perhaps tethers become less elastic as anaphase progresses (Figure 2.1.B-D).

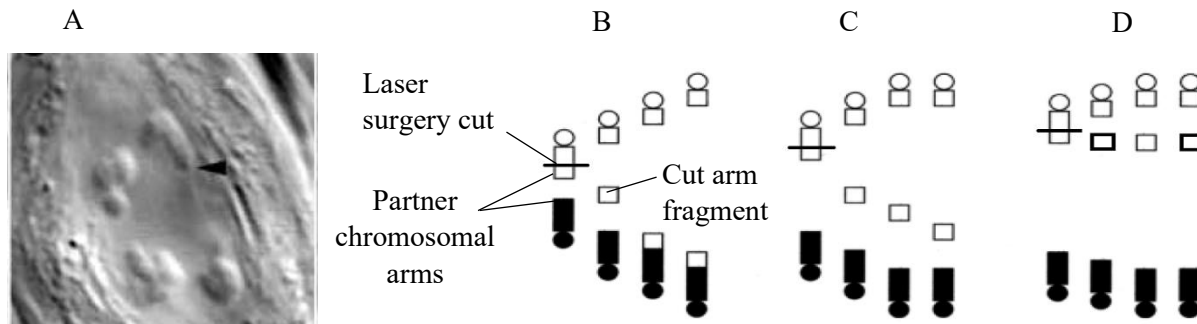


**Figure 2.1.** (A) DIC image with arrowhead showing transient stretching of trailing partner chromosomal arm during crane-fly spermatocyte anaphase. (B-D) diagram showing arm fragments cut at different anaphase times; (B) arm cut in early anaphase moves backward rapidly to its partner (C) arm cut in mid anaphase moves backward partially (D) arm cut in late anaphase moves backward slightly if at all. Adapted and modified from LaFountain *et al.*, 2002.

Surgically cut arm fragments of partner anaphase chromosomes move backward due to elastic tethers and not due to other spindle components like microtubules, or ultra-fine DNA bridges. Microtubules cannot be causing the anti-poleward movement, because even though they can cause poleward-directed movement of cut arm fragments (LaFountain *et al.*, 2001), the anti-poleward movement requires both partner telomeres intact. Ablating either of the two partner telomeres stops the arm fragment movement (LaFountain *et al.*, 2002; Forer *et al.*, 2021), and cutting the telomere off the moving fragment causes only the telomere part to continue moving while rest of the fragment stops (LaFountain *et al.*, 2002). Moreover, Taxol treatment of cell stabilizes microtubules and slows down chromosomal poleward movement by 80% as compared to control cells (LaFountain *et al.*, 2001). Nevertheless, arm fragment backward movement occurs with the same speed in Taxol-treated anaphase as seen in control cell anaphase (Forer *et al.*, 2018). Therefore, microtubules cannot be the force generators for backward movement. As for the ultra-fine DNA bridges, they sometimes connect partner telomeres; however, they are not elastic, are found only in a small number of the anaphase chromosomes, mostly at the centromeric regions rather than at telomeres, and generally retard or stop anaphase segregation (Chan *et al.*, 2007; Barefield and Karlseder, 2012; Gemble *et al.*, 2015; Su *et al.*, 2016). This contrasts with tethers which are elastic and cause chromosomal stretching, are found connecting two out of the four arms of all partner anaphase chromosomes, always present at the partner telomeres, and do not slow down anaphase segregation since cutting them does not affect anaphase speed (LaFountain *et al.*, 2002; Forer *et al.*, 2017; Sheykhan *et al.*, 2017; Forer *et al.*, 2018; Forer and Berns, 2020). Thus, ultra-fine DNA bridges do not fit the profile of backward movement mediators as these movements seem to be due to elastic tethers.

Actin and myosin too are not the anti-poleward force generators causing backward movements during anaphase, as demonstrated by Fabian *et al.* in 2007a. They added Calyculin A (CalA), an inhibitor of serine-threonine protein phosphatase 1 (PP1) and 2A (PP2A), to early anaphase cells. This caused the chromosomes to complete anaphase faster, and then move backwards towards their partners. Such backward movements proceeded in the presence of actin and myosin inhibition, hence were most likely caused by elastic tethers.

Fabian *et al.* (2007a) suggested that tethers are dephosphorylated during anaphase; adding CalA at the start of anaphase prevents tether dephosphorylation allowing tethers to remain phosphorylated, and cause backward chromosomal movements at the end of anaphase. Kite and Forer (2020) elucidated a possible relationship between tether phosphorylation/dephosphorylation and elasticity. They added CalA to cells at different intervals of anaphase and observed chromosomal motion; early anaphase CalA addition led to chromosomal segregation followed by backward movement of separated partner chromosomes. The later in anaphase CalA was added, the fewer were the chromosomes that moved backwards. Kite and Forer (2020) posited that most likely tethers are phosphorylated at the beginning of anaphase, hence are elastic. As anaphase progresses, tethers gradually dephosphorylate such that towards the end of anaphase tethers are dephosphorylated and inelastic. Addition of CalA at the beginning of anaphase prevents dephosphorylation of tethers during anaphase, and preserves their elasticity till anaphase end.

In 2021, Forer *et al.* substantiated the direct relationship between tether elasticity and phosphorylation, explaining certain features of tethers and how they function. They added CalA at early anaphase, and allowed chromosomes to complete their segregation. Then, just before or right after backward movement started, they disabled tethers directly by laser-cutting either the tethers themselves or the chromosomal arms, or ablating the telomeres to which the tethers were connected. This ensured that tethers themselves were deactivated and, in all instances, backward chromosomal movement stopped; in cases where a chromosomal arm was cut off, the arm fragment continued to move backwards while the rest of the chromosome did not. This proved directly that it is tethers that exert anti-poleward force on the chromosomes causing their backward movements once poleward forces dissipate. The work by Forer *et al.* (2021) highlights some key tether characteristics and functional capabilities. Firstly, as anaphase progresses and

tethers become longer, they become less elastic and less likely to cause backward chromosomal movements over long distances. Secondly, although shorter tethers are more elastic, they do not cause faster backward movements as compared to longer tethers. Also, CalA addition in early anaphase maintains tether elasticity till the end of chromosomal segregation with longest tether lengths remaining elastic, but, it does not increase elasticity and, as such, does not cause faster backward movements of chromosomes.

The anti-poleward force exerted on anaphase chromosomes by elastic tethers is much smaller than the poleward force which causes anaphase chromosomal segregation (Sheykhani *et al.*, 2017; Forer *et al.*, 2017). This is why most tether function studies use laser surgery to cut the tethered arm fragment of chromosome, release it from poleward force, and thereby allow elastic tether force to become effective. The work by Forer *et al.* (2021) verified that the backward movements seen with early anaphase CalA treatment (Fabian *et al.*, 2007a; Kite and Forer, 2020) are due to the same elastic tether forces that cause backward movements of cut arm fragments (LaFountain *et al.*, 2002; Forer *et al.*, 2017). This means that tethers can be studied at any point during anaphase using non-invasive protocols which do not depend on laser cutting partner chromosomal arms to visualize tether effects. Therefore, in my research presented herein, a non-invasive procedure was devised in which anaphase spindle apparatus was deactivated by partially lysing the cell, and then tether function was assessed. The objective was to test whether elastic tethers continue generating anti-poleward force causing backward chromosomal movements despite the arrested anaphase segregation. If they do so, then this partially lysed system can be further developed for studying tether function in detail; for example, by adding different phosphorylation promoters/inhibitors directly to permeabilized cells and analyzing their effect on tether elasticity.

My primary experiment aimed to deactivate the anaphase spindle apparatus, arrest anaphase segregation at different anaphase stages, and evaluate tether activity thereafter. Various dilutions of our standard immunofluorescence lysis buffer were applied to cells at different anaphase stages to stabilize the cytoskeleton and arrest spindle activity, while maintaining the cell membrane intact by only partially lysing the cells. Tether functioning was examined under such conditions by measuring how much tether shortening and backward chromosomal movements occurred while the tethers were elastic during the earlier stages of anaphase. Additionally, immunofluorescence study was conducted on the partially-lysed cells to assess

whether spindle microtubules were still intact during the lysis treatment. As an extension of the primary experimental procedure, a secondary experimental protocol was developed that incorporated CalA addition to cells at the start of anaphase to maintain tether elasticity throughout segregation. This was followed by the addition of dilute lysis buffer in combination with CalA at later stages of anaphase to arrest segregation in CalA presence. Assessments were made as to how much tether shortening and backward chromosomal movements occurred even at late anaphase stages when tethers would normally be inelastic in non-CalA treated cells. A final experiment tested each ingredient of the lysis buffer individually in order to identify which one was responsible for the results obtained with the lysis buffer preparations.

## Materials and Methods

### **Living cell preparation**

Crane flies (*Nephrotoma suturalis* Loew) were reared in the lab as described by Forer (1982), and IV-instar larvae of the proper stage were selected. Using procedures explained in detail by Forer and Pickett-Heaps (1998), larval testes were dissected out in a drop of halocarbon oil to prevent their dehydration, then washed thrice in insect Ringer's solution (IR) (0.13 M NaCl, 5mM KCl, 1.5 mM CaCl<sub>2</sub>, 3mM phosphate buffer, pH 6.8). Next, each testis was placed in a 2.5  $\mu$ L drop of IR containing fibrinogen (10mg/mL) on a coverslip, and broken up to spread out the cells. These cells were then fixed in place by adding 2.5  $\mu$ L thrombin to the fibrinogen making a fibrin clot (Forer and Pickett-Heaps, 2005). The coverslip with cells embedded in the fibrin clot was inverted over a drop of IR in a perfusion chamber (Forer and Pickett-Heaps, 2005), and sealed with a molten mixture of 1:1:1 Vaseline, lanolin, and paraffin. IR was then perfused through the chamber covering the fibrin-clot-held cells as they continued their routine division. Finally, the perfusion chamber was set up on the stage of a phase-contrast microscope for observation.

### **Different cell treatments**

The dividing cells in the perfusion chamber were studied using the phase-contrast microscope, and once the cells were at the required stage of division (different times during anaphase-I like early, mid, or late), they were perfused according to the treatment group they belonged to. Control cells were perfused with IR, while the experimental cells were subjected to various dilutions in IR of our lysis buffer (100 mM piperazine-N, N-bis (2-ethanesulfonic acid) [PIPES]; 10 mM EGTA; 5 mM MgSO<sub>4</sub>; 5% DMSO; 1% IGEPAL CA-630; pH 6.9). The lysis buffer was diluted in IR according to the following factors; 5 $\mu$ L lysis buffer in 5 mL IR (1:1000), 7.5 $\mu$ L lysis buffer in 5mL IR (1.5:1000), 10 $\mu$ L lysis buffer in 5mL IR (2:1000), 12.5 $\mu$ L lysis buffer in 5 mL IR (2.5:1000), 20 $\mu$ L lysis buffer in 5 mL IR (4:1000), 25 $\mu$ L lysis buffer in 5 mL IR (5:1000), 30 $\mu$ L lysis buffer in 5 mL IR (6:1000). Each lysis concentration was studied separately, one at a time, by perfusing it through the chamber having the cells which were observed using the phase-contrast microscope. 10-15 minutes after lysis buffer treatment, some cells were perfused with IR to washout the lysis buffer, and test whether the effects of the lysis buffer were reversible. For experiments using Calyculin A (CalA) (LC Laboratories, Woburn, MA), 50 $\mu$ M CalA stock prepared in DMSO and stored frozen as aliquots were thawed and diluted in IR by 1000-fold,

yielding final working concentrations of 50nM CalA; first, cells were perfused with the 50nM CalA in early anaphase to preserve tether phosphorylation, and then later on a combination of 50nM CalA and diluted lysis buffer (lysis +CalA) was added to ensure that tethers continued to remain phosphorylated while lysis buffer produced its effects. For testing individual lysis buffer components, each one was prepared separately in IR according to its final working concentration found in 6:1000 lysis buffer, which was as follows: 0.56% PEM (PIPES, EGTA and MgSO<sub>4</sub> combination), 0.006% IGEPAL, and 0.03% DMSO. Thus, 5.6 $\mu$ L PEM/ 1mL IR, and 0.06  $\mu$ L IGEPAL/ 1 mL IR were prepared for study. DMSO was used at 1% as 10 $\mu$ L DMSO/ 1 mL IR although its final working concentration in 6:1000 lysis was 0.03%; the higher concentration was used as a control to verify that up to 1% DMSO in experimental solutions had no effect on the anaphase segregation (LaFountain, 1985; Silverman-Gavrila and Forer, 2000). Some of the 6:1000 dilute lysis buffer treated cells were saved for immunofluorescence study. 25-35 minutes after adding 6:1000 dilute lysis buffer, cells were completely lysed using our full-strength lysis buffer as described later in the fluorescent staining and confocal microscopy section.

## **Microscopy and data analysis**

The living cell preparations mounted in perfusion chambers and inserted on the stage of the phase-contrast microscope were studied using *Nikon* 100X, 1.25 NA phase-contrast oil immersion objective lens. Real-time video images were recorded on DVDs which were later converted into time-lapse video sequences (.avi files) using freeware *VirtualDub 2*. Individual video sequence frames were analyzed and measurements of chromosomal movements were made using an in-house program *WinImage* (Wong and Forer, 2003). Chromosomal movement graphs were plotted using the commercial software *SlideWrite Plus 7.0* (Forer and Berns, 2020).

## **Fluorescent staining and confocal microscopy**

Immunostaining procedure of Fabian and Forer (2005) was modified and followed. First, control cells and 6:1000 dilute lysis buffer treated cells on cover slips were lysed in our full-strength lysis buffer for 15 minutes. Next, the cells were fixed in 0.25% glutaraldehyde in phosphate-buffered saline (PBS) for 2-3 minutes. Then, cells were rinsed twice in PBS (5 minutes each rinse), placed in 0.05M glycine for 10 minutes (to neutralize the free aldehyde groups), and again rinsed four times in PBS (5 minutes each rinse). Finally, the coverslips with the fixed cells

were stored in PBS-glycerol 1:1 (v/v) mixture at 4°C. When ready to immunostain, stored coverslips were first washed in PBS to remove all the PBS-glycerol mixture. Cells were then rinsed with 0.1% Triton X-100 in PBS to ensure antibodies spread evenly over the cell preparation. All the cells were double-stained for tyrosinated  $\alpha$ -tubulin, and for acetylated  $\alpha$ -tubulin; tyrosinated  $\alpha$ -tubulin was stained with rat monoclonal antibody YL1/2 (Abcam) diluted 1:200, followed by mouse-absorbed Alexa 488-conjugated goat anti-rat antibody (Molecular Probes) diluted 1:50. Acetylated  $\alpha$ -tubulin was stained with mouse monoclonal antibody 6-11B-1 (Millipore Sigma) diluted 1:50, followed by rat-absorbed Alexa 568-conjugated donkey anti-mouse antibody (Invitrogen) diluted 1:200. All antibodies were diluted in PBS, and cells were incubated in each antibody for 1 hour kept in the dark to prevent fluorochrome inactivation by light. At the end of every antibody incubation, cells were rinsed twice in PBS (5 minutes each rinse), then rinsed with 0.1% Triton X-100 in PBS to ensure the next antibody spread evenly over the cell preparation as well. After the last antibody staining, coverslips were rinsed twice in PBS (5 minutes each rinse), and then placed in PBS-glycerol 1:1 (v/v) for 2-3 minutes to prepare for mounting. Finally, coverslips were mounted in Mowiol solution (Osborn and Weber, 1982) containing 0.2 g/L paraphenylene diamine (PPD) antifading agent, and left to dry in the dark for 24-48 hours. Once dry, coverslips with the stained cells were stored at 4°C. When ready to analyze, cells were studied using an LSM 700 Zeiss Observer confocal microscope, with a Zeiss Plan-Apochromat 63X 1.4 NA oil-immersion objective lens. Images were collected using ZEN Black software, and further processed using FIJI Image J software.

## Results

### Control cells

Primary spermatocytes of crane flies have three pairs of homologous autosomes and two unpaired sex chromosomes. Normal meiosis-I entails the bivalent autosomes and the univalent sex chromosomes lining up at the equator to achieve metaphase-I, as illustrated in Figure 2.2. Anaphase-I begins as the three bivalents disjoin into six half-bivalents (partner homologues) which then move towards their respective poles in opposite directions while the spindle length remains constant (Forer, 1966). As the partner homologues move poleward, both sex chromosomes remain stationary at the equator (Forer *et al.*, 2013). The homologues reach near their respective poles in about 20-30 minutes after which the spindle starts elongating, the sex chromosomes start segregating, and the cleavage furrow ingresses.

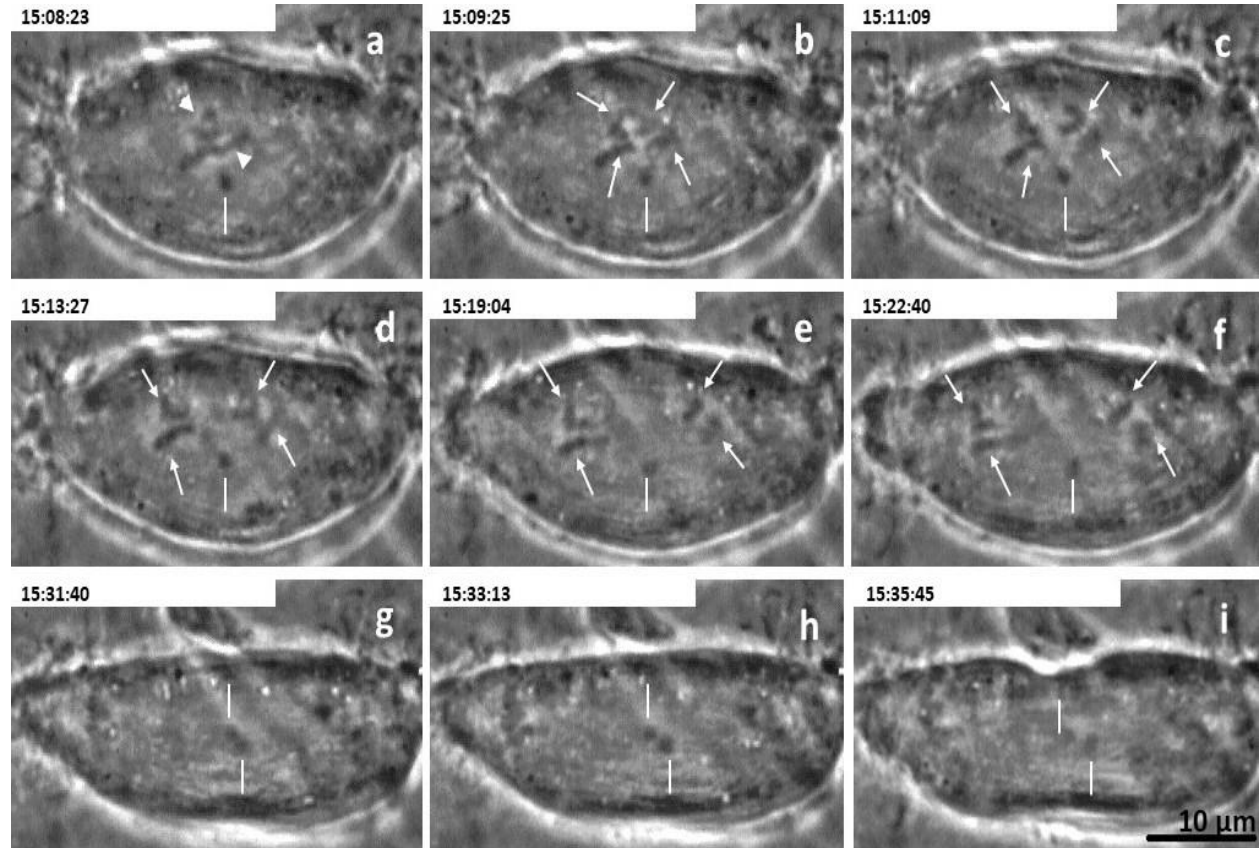


**Figure 2.2.** Meiosis-I in primary spermatocyte of crane flies. Time (hrs:min:sec) is presented at the top of each image panel (a-i). **(a)** Two arrowheads point to two bivalents in metaphase. Lines point to sex chromosomes. **(b–f)** Arrows follow the positions of separating half-bivalents during anaphase as they move apart from each other and travel to their respective poles in opposite directions. Lines indicate the position of sex chromosomes which remain stationary. **(g)** Autosomes reach near the poles **(g–i)** Spindle elongates as both sex chromosomes separate, and the cleavage furrow appears at the equatorial region of the cell cortex. Scale bar in (i) represents 10  $\mu\text{m}$ .

## Experimental cells

### 1) Dilute lysis buffer preparations stop anaphase segregation, after which chromosomes move backward; more concentrated dilutions are more effective at consistently arresting anaphase segregation than less concentrated dilutions

To test whether the different lysis buffer preparations were able to deactivate spindles, and thereby cause anaphase segregation arrest, cells at different stages of anaphase were treated with the lysis buffer. Then, the following parameters were measured for each of the homologous chromosomal pairs: distance between partner telomeres which quantified initial tether length immediately after lysis treatment; halt or no halt in the separation of partner kinetochores which indicated anaphase arrest or no arrest respectively; and in case of anaphase arrest, whether partner telomeres and kinetochores moved anti-poleward towards each other which gauged backward movement. The distance that remained between partner telomeres at the end of their backward movement was measured to be the final tether length; subtracting this final length from the initial gave the total distance that partners travelled backwards. This total distance travelled backward was taken as a fraction of the initial tether length that the elastic tether shortened and pulled backward its partner telomeres. In order to obtain an objective analysis of each parameter, a fixed reference point near one spindle pole was chosen from which distance measurements were made at regular intervals for each of the two kinetochores and telomeres of partner homologues. These were then plotted as graphs of distance from the reference point versus time. Slopes of the kinetochore graphs represented corresponding movement velocities. Figures 2.3A and 2.3B illustrate an example of how such analyses were performed on homologous chromosomal pairs in a cell treated with 6:1000 lysis buffer. Figure 2.3A shows two chromosomal pairs that were segregating during anaphase when 6:1000 lysis buffer was added, after which both pairs stopped their segregation and moved backward. A fixed point was chosen near the right spindle pole from where the distances of right and left partner kinetochores and telomeres for each chromosomal pair were measured at regular intervals. These were plotted as graphs of distance versus time. Figure 2.3B shows the graph for one of the chromosomal pairs; immediately after lysis treatment, the distance between partner telomeres was 3  $\mu\text{m}$  which was taken as the initial tether length. Additionally, the partner telomeres and kinetochores stopped moving apart from each other indicating arrest of anaphase segregation due to spindle deactivation. Furthermore, the right and left counterparts converged towards each other verifying that the partner homologues moved

backwards. The distance remaining between partner telomeres at the end of their backward movement was 0  $\mu\text{m}$ , so, the partners moved backward by 3  $\mu\text{m}$  due to the anti-poleward force exerted on them by their elastic tether. The tether shortened by 3/3 $\mu\text{m}$  or 100%, which means partners moved backward by a fractional distance of 1. Figures 2.4A and 2.4B give another example of how a homologous chromosomal pair in a cell treated with 1:1000 lysis stopped its anaphase segregation and moved backwards.

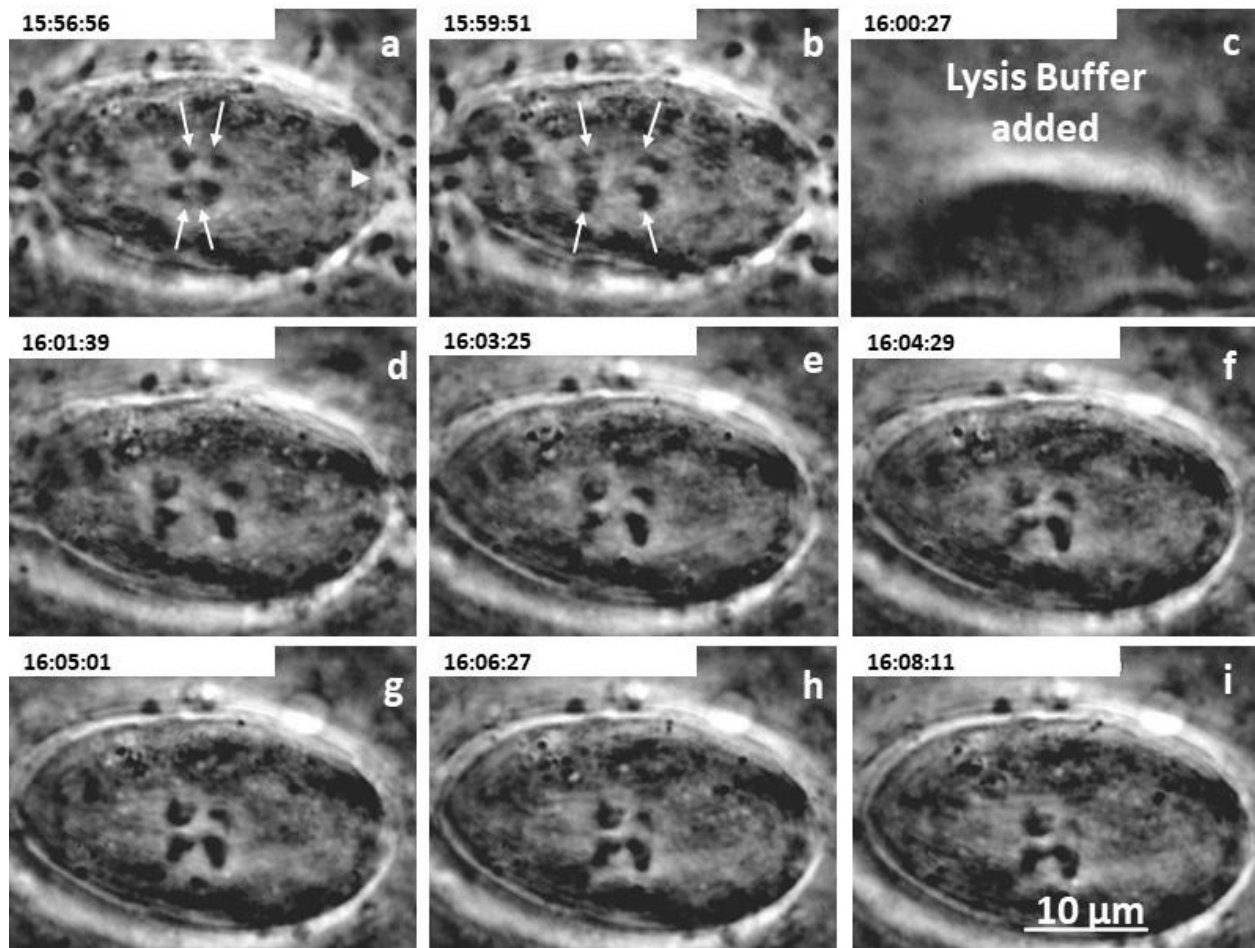


**Figure 2.3A.** 6:1000 lysis buffer-treated cell montage. Time (hr:min:sec) is presented at the top of each panel (a-i). **(a)** Two homologous pairs start anaphase separation; each partner homologue is marked by arrows. Single arrowhead points to the fixed point near the right spindle pole used as a fixed reference point for measurements. **(b)** Partner homologues continue separating. **(c)** Lysis buffer added. **(d-g)** Homologues stop separating and start moving backwards towards each other. **(h)** Backward movement stops as partners meet up with each other. **(i)** Partners remain as they are. Scale bar in (i) represents 10  $\mu\text{m}$ .

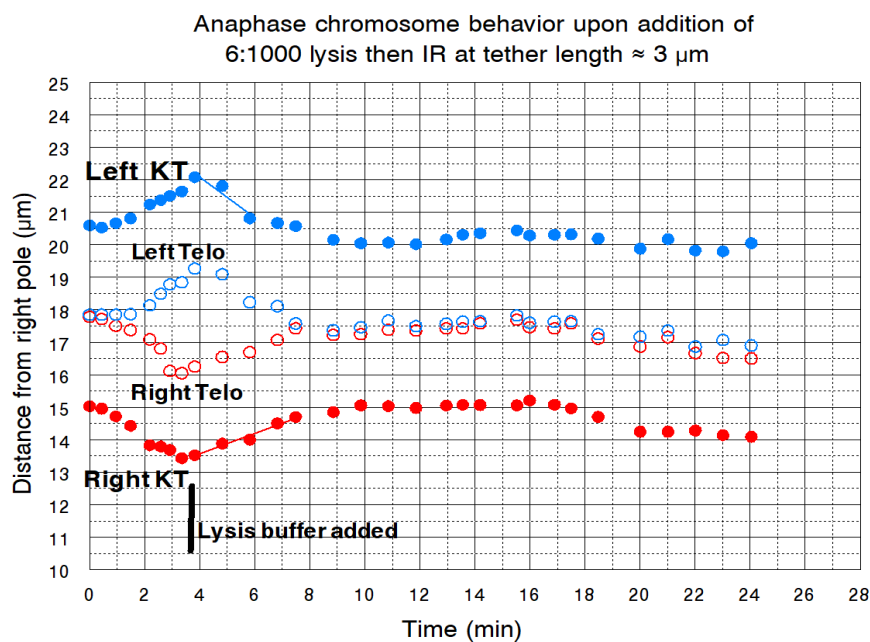


**Figure 2.3B.** Movement graph for the bottom homologous pair illustrated in Figure 2.3A cell montage. The graph time=0 min corresponds to the montage panel (a) image time=15:56:56 (hr:min:sec). Distance measurements were made from a fixed point near the right pole. Partner kinetochores are marked as Right KT and Left KT, partner telomeres are Right Telo and Left Telo. Partners were moving apart when lysis buffer was added after which they stopped separating and moved backwards all the way to meet each other. Slopes of the kinetochore graphs represent backward movement velocities.

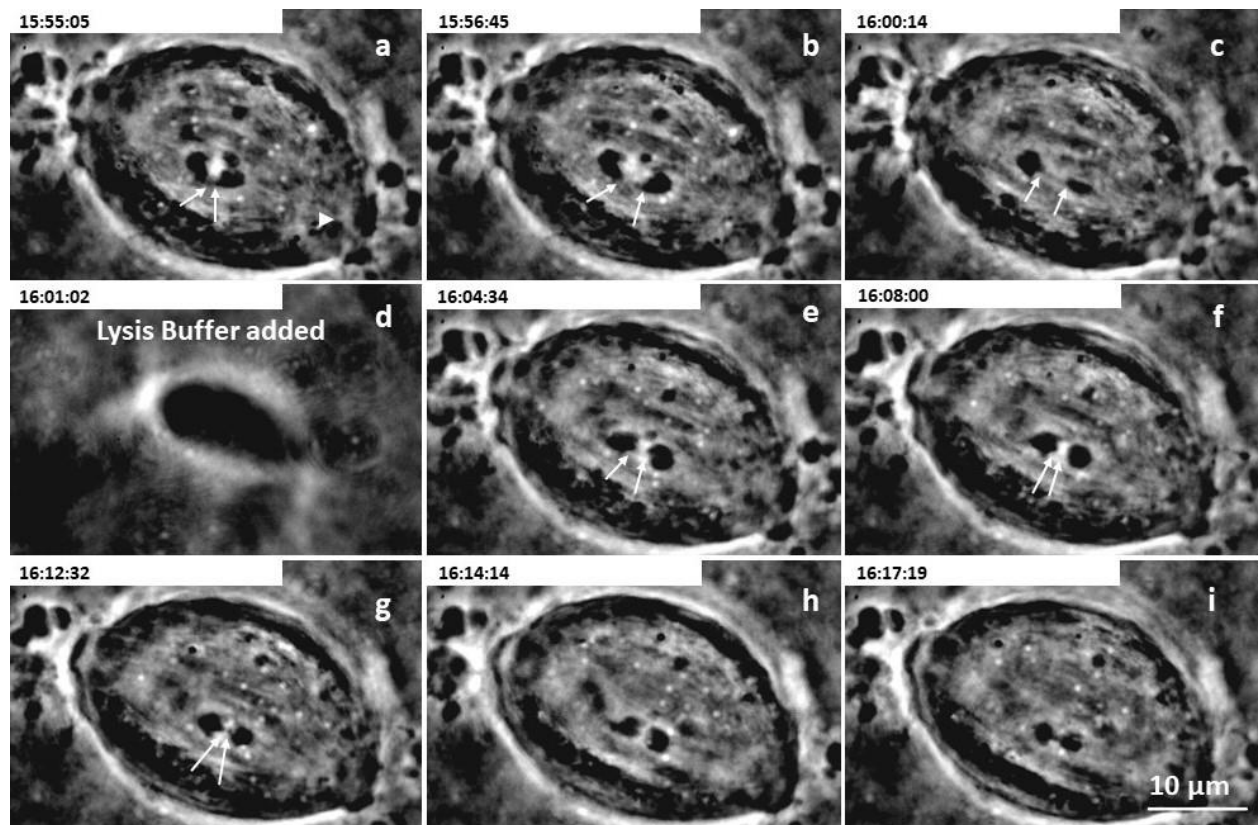


**Figure 2.4A.** 1:1000 lysis buffer-treated cell montage. Time (hr:min:sec) is presented at the top of each panel (a-i). **(a)** One homologous pair starts anaphase separation; each partner homologue is marked by arrows. Single arrowhead points to the fixed point near the right spindle pole used as a fixed reference point for measurements. **(b-c)** Partner homologues continue separating. **(d)** Lysis buffer added. **(e-f)** Homologues stop separating and start moving backwards towards each other. **(g)** Backward movement stops as partners meet up with each other. **(h-i)** Partners remain as they are. Scale bar in (i) represents 10  $\mu\text{m}$ .

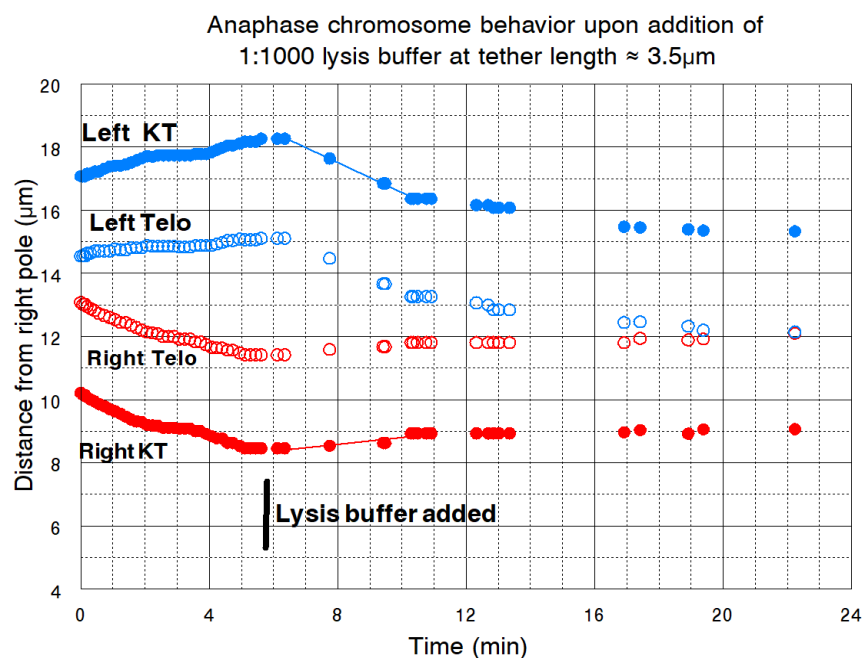


**Figure 2.4B.** Movement graph for the homologous pair illustrated in Figure 2.4A cell montage. The graph time=0 min corresponds to the montage panel (a) image time=15:55:05 (hr:min:sec). Distance measurements were made from a fixed point near the right pole. Partner kinetochores are marked as Right KT and Left KT, partner telomeres are Right Telo and Left Telo. Partners were moving apart when lysis buffer was added after which they stopped separating and moved backwards all the way to meet each other. Slopes of the kinetochore graphs represent backward movement velocities.

Not all the homologous pairs treated with 1:1000 lysis buffer stopped their anaphase segregation and moved backwards. Figures 2.5A and 2.5B present one of three homologous pairs in a cell treated with 1:1000 lysis where all partners continued their anaphase separation moving towards their respective poles, albeit at reduced speeds. A similar phenomenon was seen in another cell treated with 2:1000 lysis where all three homologous pairs failed to stop segregating post-treatment and just slowed down their separation speed.

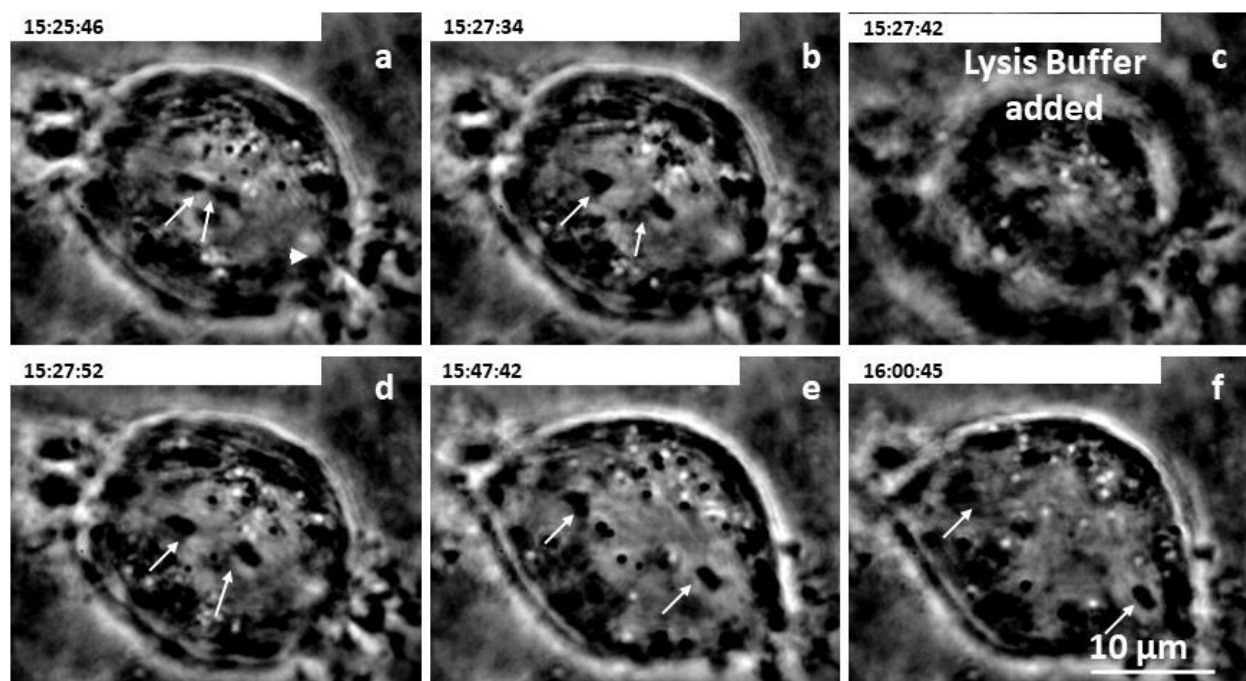


**Figure 2.5A.** 1:1000 lysis buffer-treated cell montage. Time (hr:min:sec) is presented at the top of each panel (a-f). **(a)** One homologous pair starts anaphase separation; partner homologues are marked by arrows. Single arrowhead points to the fixed point near the right spindle pole used as a fixed reference point for measurements. **(b)** Partner homologues continue separating. **(c)** Lysis buffer added. **(d)** Homologues slow-down. **(e)** Homologues continue separating at reduced speeds. **(f)** Homologues reach close to their respective poles. Scale bar in (f) represents 10  $\mu\text{m}$ .

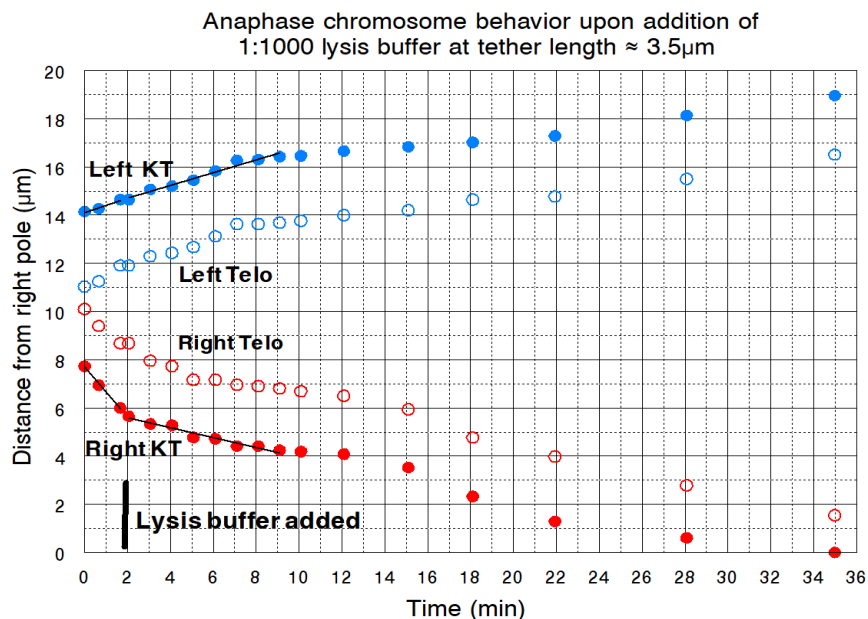


**Figure 2.5B.** Movement graph for the homologous pair illustrated in Figure 2.5A cell montage. The graph time=0 min corresponds to the montage panel (a) image time=0=15:25:46 (hr:min:sec). Distance measurements were made from a fixed point near the right pole. Partner kinetochores are marked as Right KT and Left KT, partner telomeres are Right Telo and Left Telo. Partners were moving apart when lysis buffer was added after which they slowed down but continued separating. Slopes of the kinetochores graphs represent corresponding movement velocities.

19 cells were treated with various lysis buffer preparations of <3:1000 dilutions; in 13 cells all 36 chromosomal pairs stopped anaphase segregation within 1 minute of treatment. In the other 6 cells all 15 homologous pairs continued anaphase segregation at slower speeds. Higher lysis buffer concentrations of 4, 5, and 6:1000 dilutions were applied to 24 cells which caused anaphase segregation arrest of all their 65 homologues within 1 minute (Table 2.1, Figure 2.6). These findings lead to two inferences; the first is that lysis treatment of a cell affects all its chromosomes similarly such that all either stop anaphase separation or slow down. This in turn reinforces the presumption that the lysis buffer affects the entire spindle of a cell the same way rather than having partial effects in different areas. The second conclusion is that higher lysis buffer concentrations of 4,5, and 6:1000 dilutions are consistently effective in deactivating the entire spindle apparatus in a cell resulting in anaphase arrest of all the chromosomal pairs therein. Lower lysis buffer concentrations of <3:1000 dilutions are ineffective in consistently deactivating the anaphase spindle, and instead retard it leading to decreased speeds of all segregating chromosomes present there (Figure 2.6).

Interestingly, when CalA was added in early anaphase followed by CalA+Lysis addition at any later stage in anaphase, spindle deactivation and anaphase arrest always occurred (Table 2.1, Figure 2.6). The arrest was achieved either within 1 minute or at most within 5 minutes of treatment.

**Table 2.1.** Anaphase segregation arrest or slow-down in cells treated with various lysis buffer dilutions, and CalA then CalA+Lysis buffer dilutions.

Lysis buffer dilution ( $\mu\text{L}/1000 \mu\text{L}$ IR)	Anaphase spindle deactivated & anaphase arrested		Anaphase spindle activity retarded & anaphase slowed down (not arrested)	
	Treated cells	Homologous pairs arrested/ homologous pairs observed	Treated cells	Homologous pairs slowed down/ homologous pairs observed
< 3	13	36/36	6	15/15
4-5	4	10/10	0	0
6	20	55/55	0	0
<b>CalA then CalA+Lysis buffer dilution (<math>\mu\text{L}/1000 \mu\text{L}</math> IR)</b>				
< 3	4	9/9	0	0
6	3	8/8	0	0

**Efficacy of various lysis buffer concentrations in arresting anaphase segregation (N= 133)**

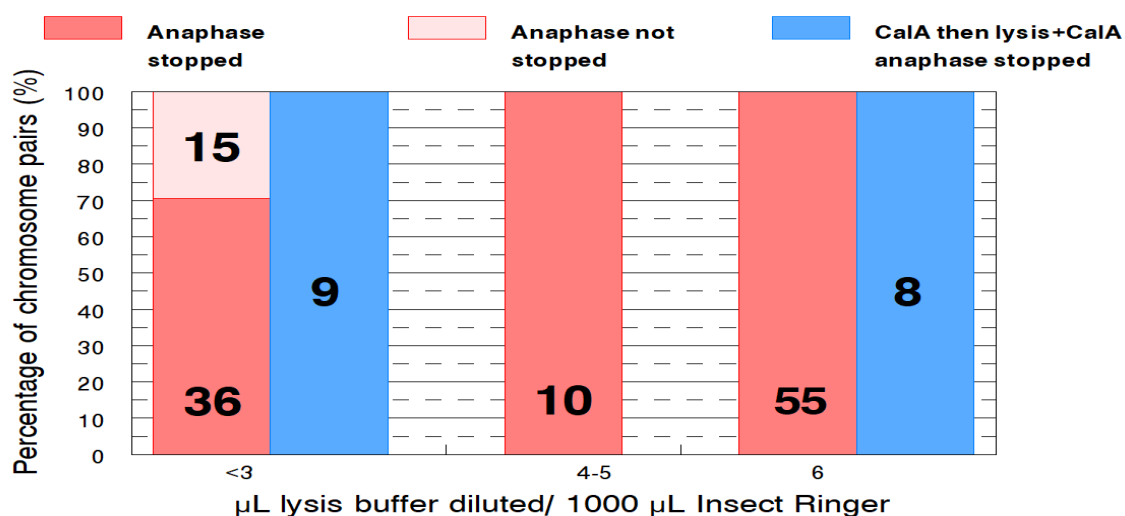


**Figure 2.6.** Effectiveness of the different strengths of lysis buffer at stopping anaphase segregation measured as percentage of chromosome pairs that stopped/did not stop segregation with different lysis buffer concentrations (pink bars), and with early anaphase CalA addition followed later by lysis +CalA treatment (blue bar). 133 homologous pairs were examined in total (N) and numbers tested with each lysis concentration are written on the respective bars.

## 2) The lysis-arrested cells recover with IR washout, resuming anaphase as normal

It could be argued that the lysis treatments might not just be arresting anaphase by deactivating spindles, rather they might be killing the cells or causing some irreparable damage to some part of the cell spindle or elsewhere. This issue was addressed through the results of IR washout as displayed in Table 2.2 and Figure 2.7; 9 cells treated with 1-5 parts lysis buffer/1000 IR were washed with IR which caused complete recovery of all the homologous pairs in 7 cells (more than 75% of all the homologous pairs washed). However, out of the 17 cells that had been treated with 6 parts lysis buffer/1000 IR then washed with IR, homologous pairs of only 5 cells recovered (only 28% of all the homologous pairs washed). In case of recovery, the entire cell recovered with all its homologues restarting their anaphase segregation within 5-15 minutes of IR washout, average recovery time being 8 minutes post-wash, and many cells finished their cell divisions as normal. Otherwise, none of the homologues in a cell recovered, reaffirming the theory that lysis deactivates the entire spindle which recovers as a complete unit once lysis effect is removed. The low recovery fraction of 6:1000 lysis buffer-treated cells could possibly be explained as 6:1000 concentration being potent enough to cause more permanent and irreversible anaphase spindle deactivation with anaphase arrest in most cells.

**Table 2.2.** Recovery with IR washout in cells treated with various lysis buffer dilutions.

Lysis buffer dilution ( $\mu\text{L}/1000 \mu\text{L}$ IR)	Recovered with IR		Did not recover with IR	
	Washed cells	Homologous pairs recovered/ homologous pairs observed	Washed cells	Homologous pairs not recovered/ homologous pairs observed
< 3	4	10/10	1	3/3
4-5	3	8/8	1	2/2
6	5	13/13	12	33/33

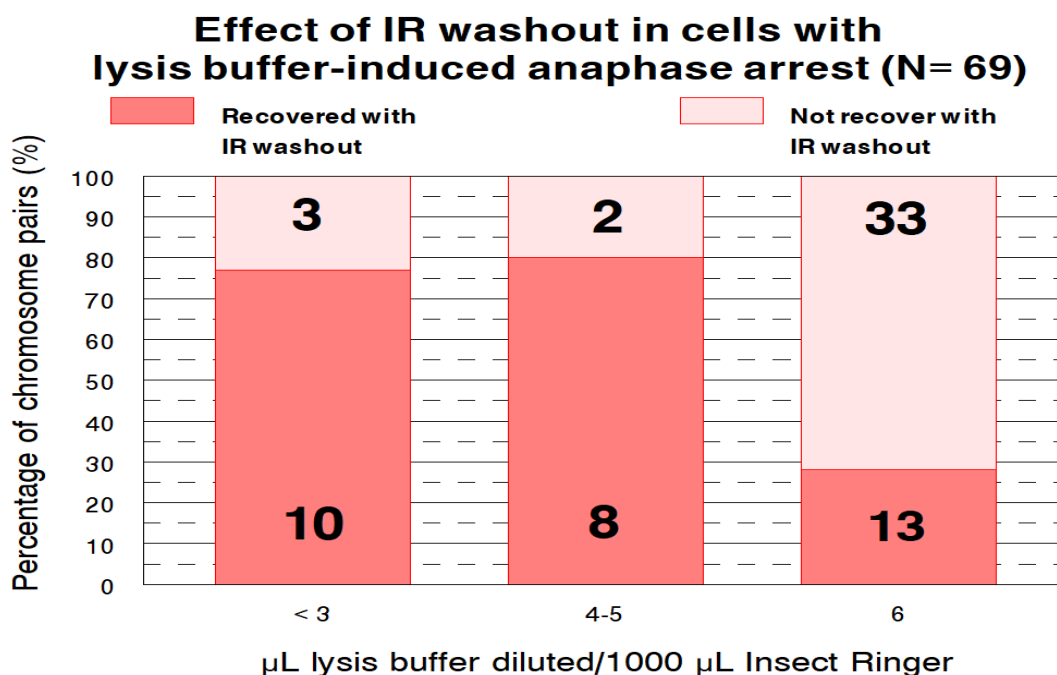


**Figure 2.7.** Anaphase recovery post-IR washout was measured as percentage of chromosome pairs that restarted anaphase segregation after IR washout at the different lysis buffer concentrations. 69 homologous pairs were examined in total (N) and numbers tested with each lysis concentration are written on the respective bars.

### 3) Shorter tethers are more consistently elastic and move chromosomes backward more often than longer tethers do during lysis-induced anaphase arrest

Once a lysis treatment stopped anaphase chromosomal separation, tether functionality was assessed to determine whether tethers were still capable of moving partner homologues backward. Functioning tethers which are shorter and more elastic cause backward chromosomal movements more often than tethers which are longer and less elastic (Forer *et al.*, 2021). To verify whether this was true during lysis-induced spindle deactivation as well, I assumed that any backward movements of  $\geq 0.5 \mu\text{m}$  seen after lysis addition were caused by the elastic tethers and not some other factor associated with the lysis treatment. Tether lengths at the time of anaphase arrest were measured and plotted against the percentage of homologous chromosomal pairs that moved backwards by  $\geq 0.5 \mu\text{m}$ . Backward movements started within 1 minute of anaphase arrest, and as illustrated in Figure 2.8, chromosomes moved backwards more than 85% of the times at tether lengths of  $< 5 \mu\text{m}$ , about 70% at lengths of 5-8  $\mu\text{m}$ , 37% at lengths of 9-10  $\mu\text{m}$ , and only 26% at lengths  $\geq 11 \mu\text{m}$ . So, in lysis-treated cells, shorter tethers are more elastic causing more frequent backward movements than longer tethers, just as is seen in non-treated cells.

Adding further, when CalA was applied at start of anaphase to maintain tether elasticity, followed by lysis +CalA application later in anaphase, then backward movements occurred 100% of the times no matter what the tether length was (Figure 2.8). These movements started either within 1 minute or maximum within 5 minutes of treatment, except in case of one homologous pair treated with CalA then <3:1000 lysis+ CalA which moved backward after 8 minutes. Since the treatment sample sizes of lysis+ CalA groups were smaller than those of their counterpart lysis buffer groups (Figure 2.8), were the differences between the two treatments statistically significant? There was 100% probability of backward movement with lysis+ CalA treatment at all tether length categories  $\geq 5\mu\text{m}$ . The chances of 100% backward movement occurring with lysis buffer treatment having the same sample size as its corresponding lysis+ CalA treatment at each tether length category was calculated and multiplied with each other as follows:-

<b>Tether length (<math>\mu\text{m}</math>)</b>	<b>Homologous pairs moved backward with lysis+ CalA treatment</b>	<b>Homologous pairs moved backward with lysis buffer treatment</b>	<b>Chances of backward movement probabilities being the same with both treatments</b>
5-6.99	4/4	12/17	$(12/17)^4$
7-8.99	8/8	13/18	$(13/18)^8$
$\geq 11$	5/5	5/19	$(5/19)^5$

$$\therefore (12/17)^4 * (13/18)^8 * (5/19)^5 = 0.000023$$

There was a 0.000023 chance of 100% backward movement occurring with lysis buffer treatment similar to that seen with lysis+ CalA treatment, which was highly unlikely. Thus, differences between the two treatments were statistically significant (Figure 2.8).

Therefore, in lysis treated cells, frequencies of backward movement follow the same patterns as those seen in untreated cells which provides support to the deduction that tether functioning remains intact under the various dilute lysis treatments.

## Backward movement of chromosomes during lysis buffer-induced anaphase arrest (N=118)

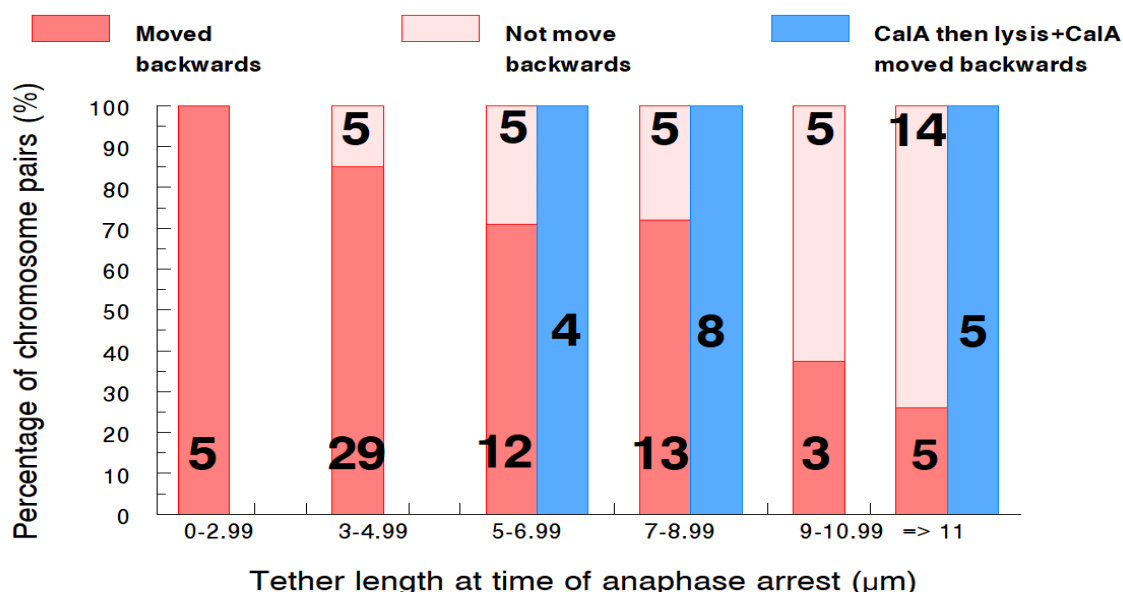


**Figure 2.8.** Frequencies of backward movement with different tether lengths at time of anaphase arrest upon treatment with lysis buffer (pink bars) and with CalA then lysis buffer+CalA (blue bar). 118 homologous pairs were examined in total (N) and numbers tested in each category are written on the respective bars. Differences between lysis and Lysis+ CalA treatments are statistically significant since the probability of them being due to chance is  $<0.01$

#### 4) Shorter tethers are more consistently elastic causing backward movements over greater distances than longer tethers during lysis-induced anaphase arrest

Another key parameter that evaluates tether functioning is the extent of its elasticity, i.e., how much the tether shortens and pulls backward its homologous chromosomal pair (Forer *et al.*, 2021). The distance moved backward by partner homologues when taken as a fraction of the initial tether length reflects how much the elastic tether shortens after being stretched, like an elastic spring, and consequently pulls backward its partner homologue (Forer *et al.*, 2021). Hence, distance moved as a fraction of initial tether length was used to represent how much backward chromosomal movement occurred during lysis treatment, indicating the extent of tether elasticity causing that much motion. Figure 2.9A displays all the measurements; homologous pairs treated with lysis buffer at tether lengths of  $<5 \mu\text{m}$  often moved the complete tether length backward (partner telomeres meeting up with each other); while most of the pairs treated with lysis at tether lengths  $\geq 11 \mu\text{m}$  moved 0 fractional distance backward (partners not moving at all). Thus, shorter tethers seem to be more elastic and shorten a larger fraction of their initial length causing greater

extent of backward movements than longer tethers. These findings are consistent with those of Forer *et al.* (2021), further corroborating that tether elasticity and functioning remains unaffected with the different lysis treatments.

Moreover, CalA applied at beginning of anaphase to maintain phosphorylated elastic tethers followed by lysis +CalA treatment resulted in all tethers shortening 100% of their initial length no matter what the initial length was (Figure 2.9A). Thus, tethers which have their elasticity fully preserved at the time of lysis +CalA addition remain unaffected by it and shorten completely, buttressing the conclusion that lysis treatment has no effect on tether elasticity and functioning.

### Anaphase arrested chromosomes' backward movement as fractional distance of tether length at time of arrest (N=118)

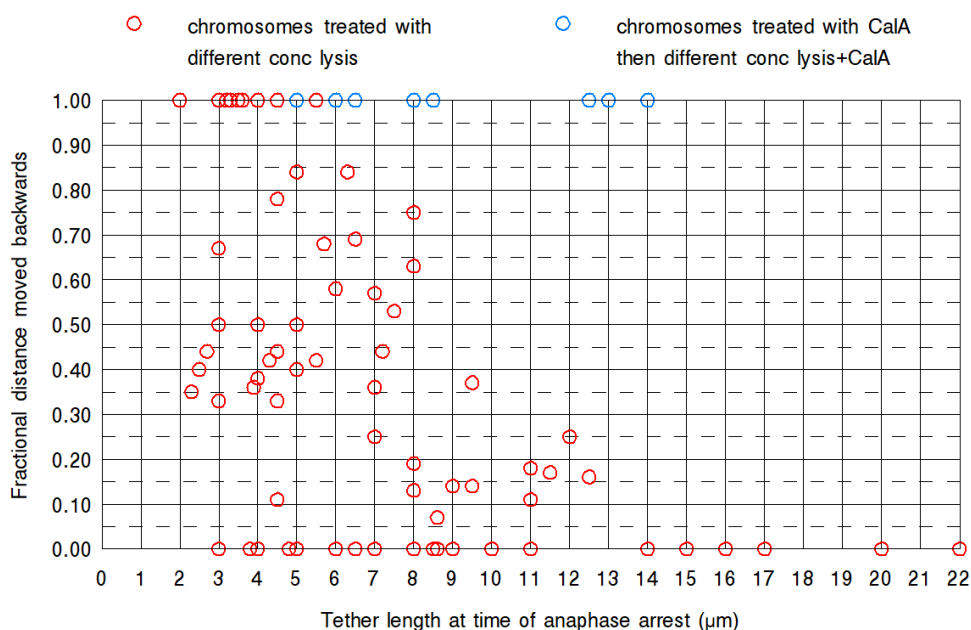


**Figure 2.9A.** Distances moved backwards by chromosomes as fractions of their initial tether length in cells treated with lysis buffer (pink circles), and with CalA then lysis buffer +CalA (blue circles). 118 homologous pairs were examined in total (N).

Tether shortening after Lysis+ CalA treatment was different than the tether shortening seen after treatment with lysis buffer alone (Figure 2.9A); Tethers having preserved elasticity with CalA then lysis +CalA treatment always caused complete backward movement of partner chromosomes to meet up with each other. However, short elastic tether lengths of  $<5 \mu\text{m}$  treated with lysis buffer alone did not always produce such complete backward movements. There were

chromosomal pairs in this short tether length category that had 0 fractional backward movement while others in the longer less elastic tether length category moved more. So, the question arose, was there a statistically significant correlation between tether length and fractional distance moved backward with lysis treatment alone? Was shorter tether elasticity truly different than longer tether elasticity during lysis conditions? To address this query, the 101 chromosome pairs treated with lysis buffer alone were statistically analyzed. One of these homologous pairs at tether length of 8.6  $\mu\text{m}$  had fractional backward movement of less than 0.10; such transient movement might not have been due to tether elasticity, rather might have been due to partner homologues briefly propelling backwards as poleward-directed anaphase forces were deactivated releasing the chromosomes from their poleward tension. Thus, the one homologous pair that moved backwards by <10% (Figure 2.9A) was excluded from the statistical analyses presented in Figure 2.9B. Fractional distance moved backwards and tether length at time of anaphase arrest were the two variables analyzed, and since the two were non-parametric, i.e. not normally distributed and having large variability, Spearman's rank correlation was computed to assess the relationship between them. Spearman's correlation coefficient ( $r_s$ ) worked out to be -0.610, and with  $P \leq 0.01$ , the critical value for  $r_s$  at the given sample size of 100 was 0.257. Therefore, during lysis treatment, fractional distance moved backward by chromosomes due to their tether elasticity is negatively correlated to the tether length more than 99% of the times (Figures 2.9B, 2.9C). Hence, shorter tether elasticity is significantly different from longer tether elasticity, and so is the backward movement caused by them. This highly significant statistical result further validates that lysis treatment does not affect tether function, and tethers work in lysis treated cells as they do in untreated (control) cells. If tether elasticity is maintained throughout anaphase, as with early anaphase CalA treatment, then fractional distance moved backwards is always the same no matter how long the tethers become as anaphase progresses (Figure 2.9D).

### Anaphase arrested chromosomes' backward movement as fractional distance of tether length at time of arrest (N=100)

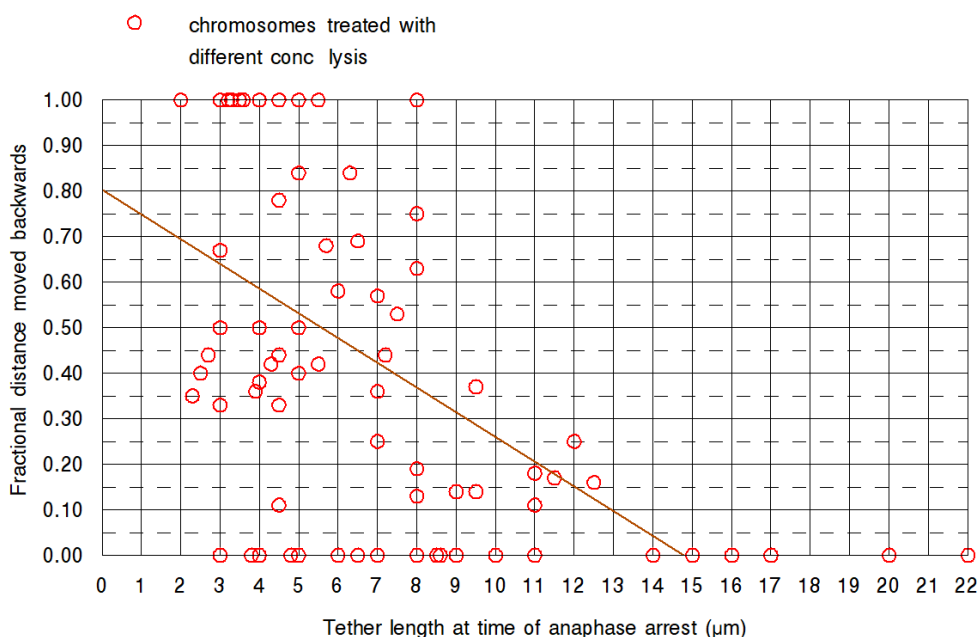


**Figure 2.9B.** Distances moved backwards by chromosomes as fractions of their initial tether length in cells treated with lysis buffer. 100 homologous pairs were examined in total (N). Spearman's rank correlation ( $r_s$ ) was calculated to assess the relationship between fractional distance moved backwards and tether length at time of anaphase arrest. A negative correlation was found with  $r_s = -0.610$  and critical value at  $P \leq 0.01$  as  $r_{s(0.01, 100)} = 0.257$

### Anaphase arrested chromosomes' backward movement as fractional distance of tether length at time of arrest (N=100)

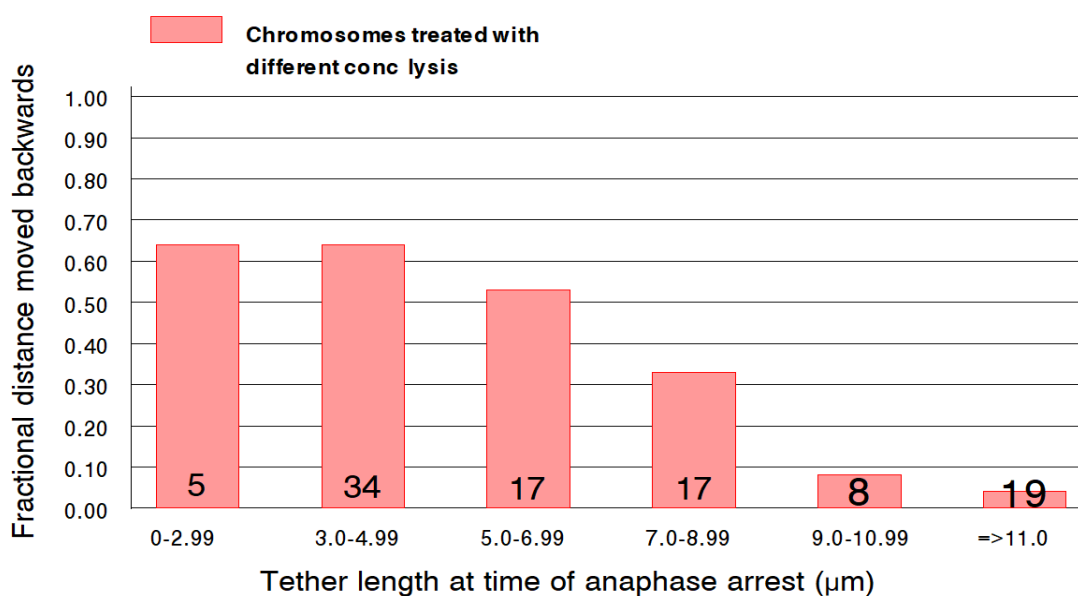


**Figure 2.9C.** Scatter plot data from Figure 2.9B grouped into categories of tether lengths plotted against average fractional distances moved backwards in each category. 100 homologous pairs were examined in total (N); numbers tested in each category are written on the respective bars.

## Anaphase arrested chromosomes' backward movement as fractional distance of tether length at time of arrest (N= 117)

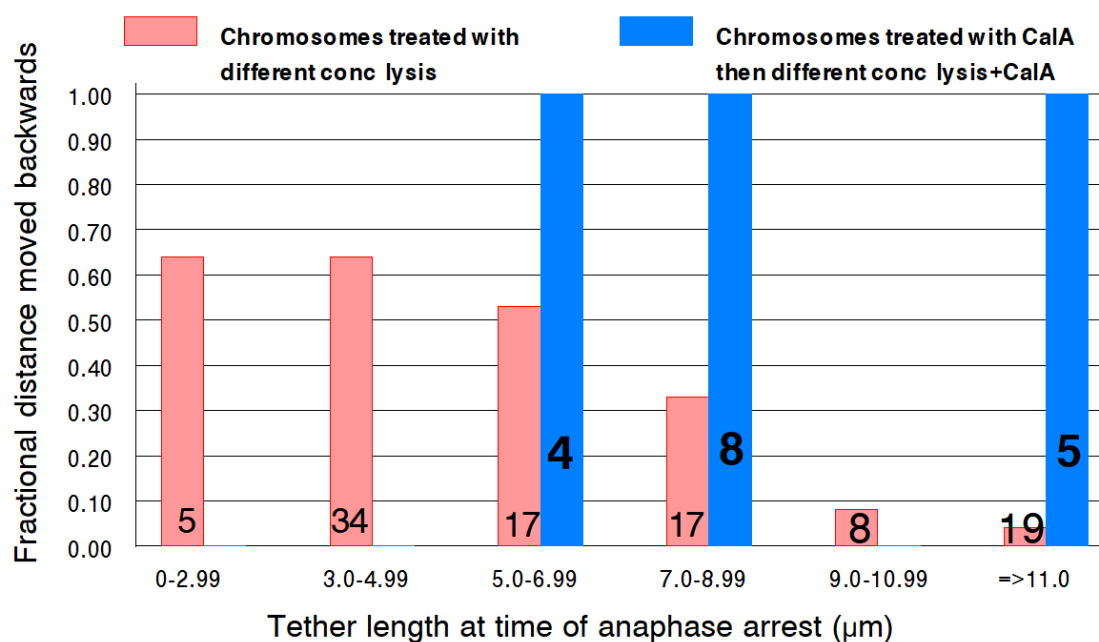


**Figure 2.9D.** Average fractional distance moved backwards under each tether length category in cells treated with lysis buffer (pink bars) and with CalA then lysis +CalA (blue bar). 117 homologous pairs were examined in total (N) and numbers tested in each category are written on the respective bars.

### 5) There is no statistically significant difference between the backward velocities seen with tethers of different lengths during lysis-induced anaphase arrest.

Forer *et al.* (2021) have reported that there were no statistically significant differences in backward velocities of chromosomal arm fragments cut at different tether lengths in untreated (control) cells. They reported the same findings in their CalA-treated (experimental) cells. Furthermore, backward velocities in untreated cells compared with backward velocities in CalA-treated cells were also statistically the same. This trend exists in the present study of lysis-induced anaphase arrest as exhibited in Figure 2.10. The average backward velocity during lysis treatment ranged from 0.4 to 1.1 µm/min; maximum velocity was with 7-8 µm long tethers. Yet Student's t-test yielded statistically insignificant differences between the velocities at the different tether lengths. This was also true for the CalA then lysis+CalA treatment velocities at different tether lengths. Moreover, backward velocities in lysis-treated cells compared with backward velocities in lysis+CalA-treated cells were also statistically the same. Therefore, tethers of different lengths cause backward movements with statistically similar velocities in partially lysed cells as they do in non-lysed cells.

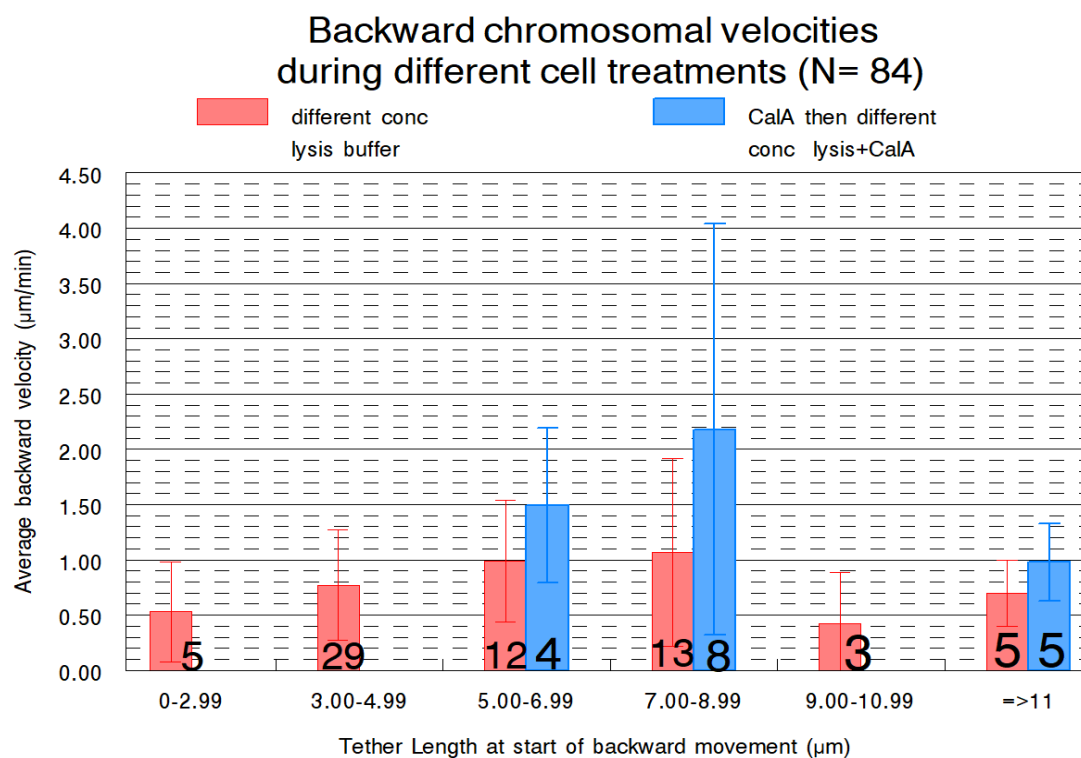


**Figure 2.10.** Average backward velocities with their standard deviations (capped bars) shown at different tether length categories during treatments with lysis buffer (pink bars), and CalA then lysis buffer +CalA (blue bars). 84 homologous pairs were examined in total (N) and numbers tested in each category are written on the respective bars. Student's t-test was performed on all data sets and all differences were statistically insignificant (alpha level  $\leq 0.01$ ).

Average backward chromosomal velocities measured in lysis buffer-treated cells were compared to the average backward arm fragment velocities measured in untreated (control) cells of Forer *et al.* (2021); they reported the average as about 4-7  $\mu\text{m}/\text{min}$  while the average in lysis treatment was 0.4-1.1  $\mu\text{m}/\text{min}$  (Figure 2.10). Similarly, average backward velocities of arm fragments with CalA treatment in Forer *et al.* (2021) were almost 6-10  $\mu\text{m}/\text{min}$ , while average backward velocities of chromosomes with lysis+ CalA treatment in present study were 1-2.2  $\mu\text{m}/\text{min}$  (Figure 2.10). It seems that although elastic tethers exert anti-poleward forces on chromosomes, pulling them backward in cells treated with lysis alone and with CalA then lysis+CalA, their effective velocities are much smaller than those of backward moving arm fragments. Contrarily, Fabian *et al.* (2007a) have documented backward chromosomal velocities with CalA treatment as ranging between 0.62-4.11  $\mu\text{m}/\text{min}$  (average of 2.13  $\mu\text{m}/\text{min}$ ), which seems to be comparable to the backward chromosomal velocities of 0.47-4.41  $\mu\text{m}/\text{min}$  (average of 1.66  $\mu\text{m}/\text{min}$ ) with lysis+ CalA treatment.

**6) The backward moving chromosomes remain attached to their kinetochore microtubules (kMTs) during lysis-induced anaphase arrest**

Why is backward chromosomal movement velocity less than backward chromosomal arm-fragment movement velocity? One possible answer to this question may lie in the meiotic spindle microtubules (MTs) attached to chromosome kinetochores (kMTs) (McIntosh, 2016). In crane-fly spermatocytes, kMTs are incompletely acetylated near their kinetochore ends during metaphase and early anaphase; kMTs become more acetylated as anaphase progresses, such that they are completely acetylated by late anaphase once the chromosomes have reached near their poles (Wilson and Forer, 1989; Wilson *et al.*, 1994). To check whether backward moving chromosomes were attached to their kMTs during the lysis-induced anaphase arrest, metaphase control and 6:1000 lysis buffer-treated cells were immunostained for  $\alpha$ -tyrosinated ( $\alpha$ -TYR) and  $\alpha$ -acetylated ( $\alpha$ -AC) tubulin (Figure 2.11). The fluorescent intensity of each immunostain was measured along a line drawn across one kinetochore fiber starting from the equator side of its kinetochore and ending near its pole (Figures 2.11A.c-d, 2.11B.c-d). The metaphase control cell, about to start anaphase, had both non-kinetochore MTs (non-acetylated), and kMTs (acetylated); the kMTs were less acetylated near their kinetochore ends and more acetylated further along their length towards their poleward ends (Figure 2.11A). The 6:1000 lysis buffer cell in early anaphase arrest also had both non-kinetochore MTs (non-acetylated), and kMTs (acetylated); however, their kMTs were completely acetylated starting from their kinetochore ends all the way to their poleward ends (Figure 2.11B). Thus, acetylated kMTs remain attached to anaphase arrested chromosomes during lysis buffer treatment, and may resist the backward chromosomal movements leading to slower backward chromosomal velocities as compared to the backward chromosomal arm fragment velocities.

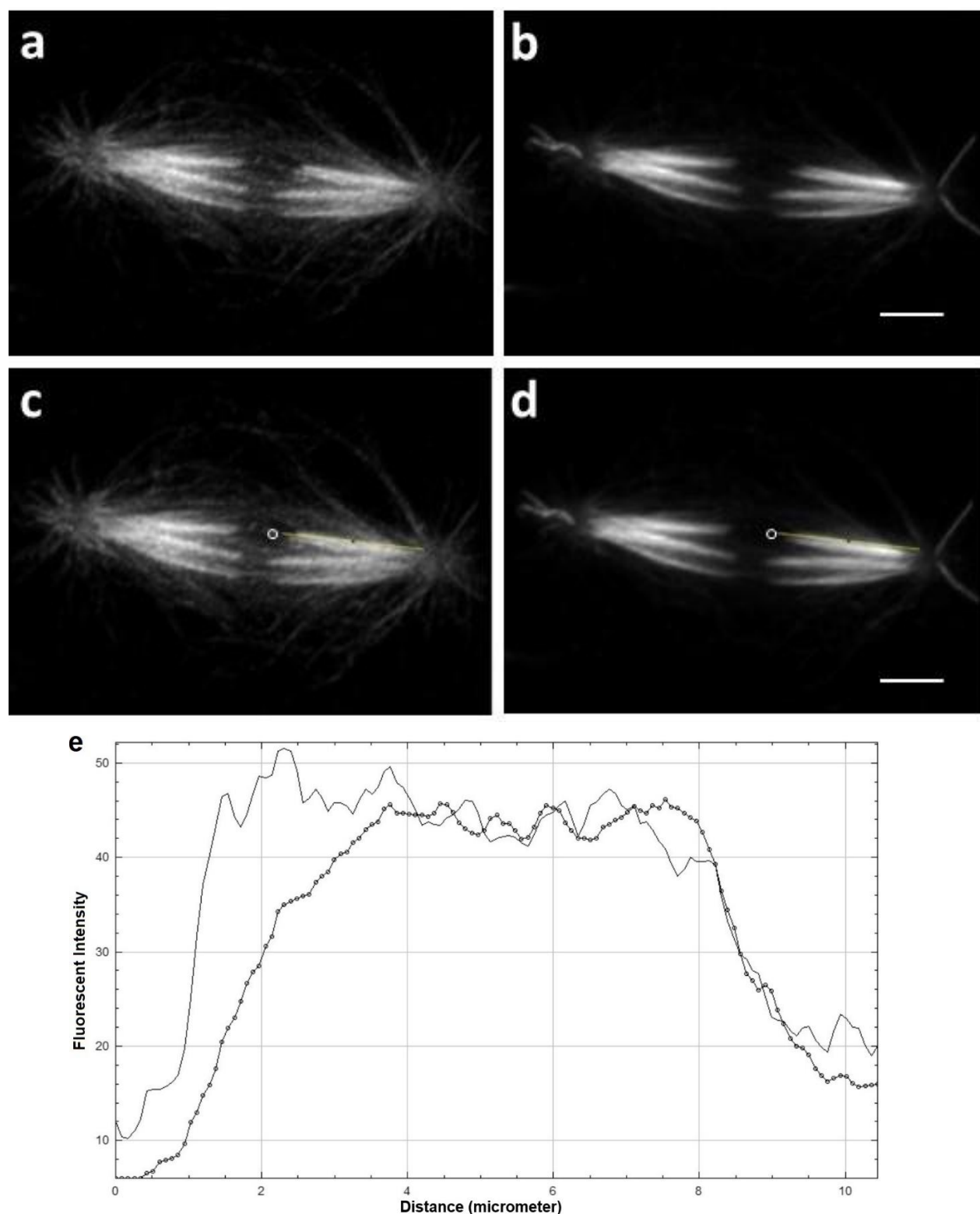


**Figure 2.11A.** Control metaphase spindle dual labeled with  $\alpha$ -TYR (image panels a & c), and  $\alpha$ -AC (image panels b & d). (a-b) 19 optical slices were taken through the cell; slices 3-17 were superposed to form a z-series. (c-d) Same z series as a-b with a line drawn along one kinetochore fiber to measure intensity of the immunostain; O marks the equator side of the kinetochore from where intensity measurement was started (time=0 of graph e). (e) Fluorescent intensity plotted against distance along the measuring line for  $\alpha$ -TYR (smooth line graph) and  $\alpha$ -AC (speckled line graph);  $\alpha$ -TYR was at maximum intensity all the way from kinetochore till the end of the fiber near the pole;  $\alpha$ -AC was less intense near kinetochore and more intense in the rest of the fiber until the pole. Scale bar= 5  $\mu$ m.

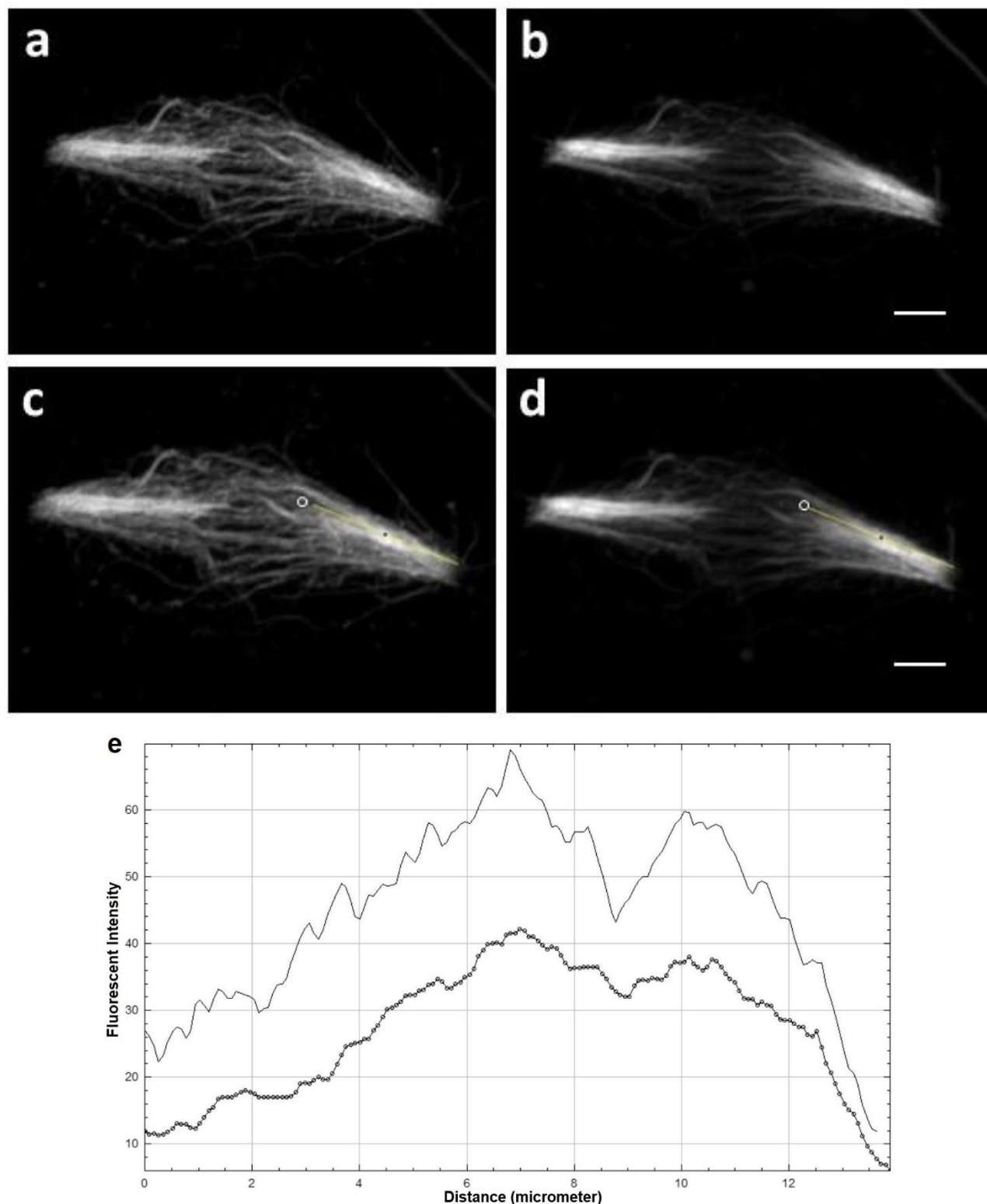


**Figure 2.11B.** 6:1000 Lysis buffer-treated early anaphase spindle dual labeled with  $\alpha$ -TYR (image panels a & c), and  $\alpha$ -AC (image panels b & d). **(a-b)** 19 optical slices were taken through the cell; slices 4-16 were superposed to form a z-series. **(c-d)** Same z series as a-b with a line drawn along one kinetochore fiber to measure intensity of the immunostain; O marks the equator side of the kinetochore from where intensity measurement was started (time=0 of graph e). **(e)** Fluorescent intensity plotted against distance along the measuring line for  $\alpha$ -TYR (smooth line graph) and  $\alpha$ -AC (speckled line graph); both  $\alpha$ -TYR and  $\alpha$ -AC stained similarly indicating kinetochore fiber was completely acetylated from its kinetochore end till its poleward end. Scale bar= 5 $\mu$ m.

## 7) The lysis buffer component most likely responsible for all the results discussed thus far is IGEPAL

Which component of lysis buffer is responsible for deactivating anaphase spindle apparatus and arresting anaphase segregation while maintaining tether function? Each lysis component was tested separately to check its influence on anaphase dynamics. As evident in Figure 2.12A, IGEPAL consistently stopped anaphase segregation when used at the concentration found in 6:1000 lysis buffer preparation. In addition, backward frequencies seen at different tether lengths with IGEPAL treatment (Figure 2.12B) were statistically the same as those previously seen with the full-composition lysis buffer treatment (Figure 2.8). The probabilities of backward moving chromosomes in the two treatments being from the same distribution at tether lengths 3-4, 5-6, and 7-8  $\mu\text{m}$  were 0.45, 0.18, and 0.20 respectively. Thus, shorter tethers cause more frequent backward movements than longer tethers in IGEPAL treated cells in the same manner as observed in full-composition lysis buffer treated cells. Interestingly though, IR washout in IGEPAL treated cells led to the complete recovery of 20 out of 20 homologous pairs within 5-7 minutes of washout, allowing them to finish their anaphase segregation. This contrasted with the recovery statistics of full composition 6:1000 lysis treatment which had the same concentration of IGEPAL as used separately (Table 2.2, Figure 2.7). Perhaps the IGEPAL effect is completely reversible when by itself, but is less so when combined with the PEM of the full-composition lysis buffer.

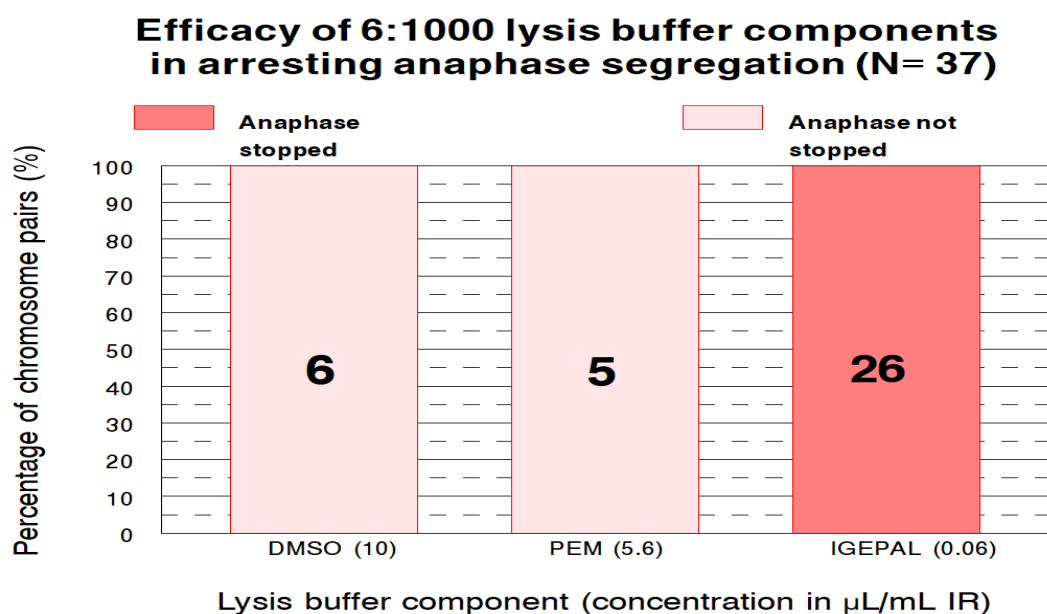


**Figure 2.12A.** Components of 6:1000 lysis buffer tested individually to measure their effectiveness at deactivating spindle apparatus and arresting anaphase segregation; concentration of each component in  $\mu\text{L/mL}$  IR is written in brackets. 37 homologous pairs were examined in total (N) and numbers tested with each lysis component are written on the respective bars.

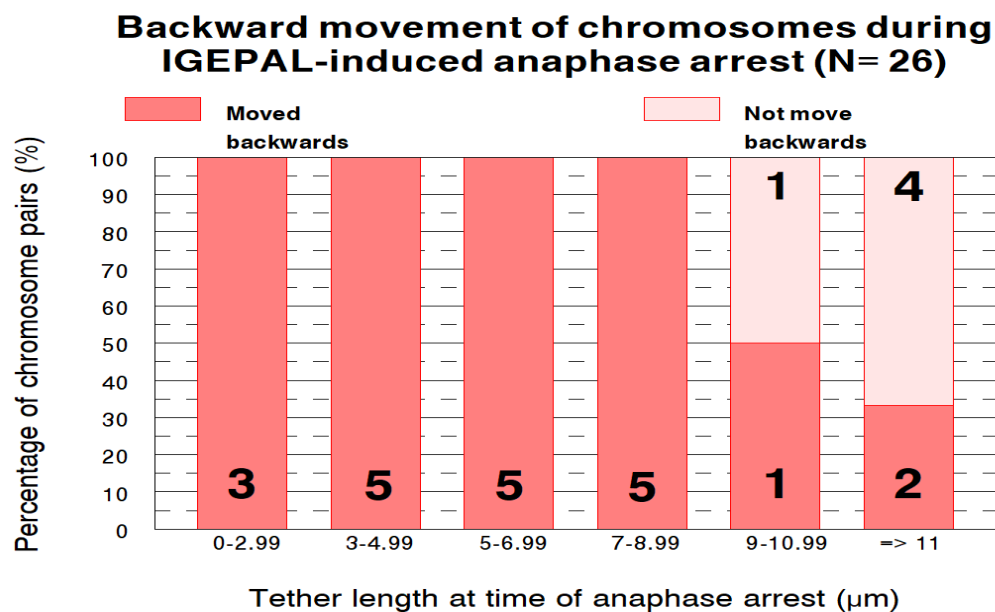


**Figure 2.12B.** Frequency of backward movements at different tether length categories in IGEPAL treated cells. 26 homologous pairs were examined in total (N) and numbers tested in each category are written on the respective bars. When comparing frequencies under IGEPAL with frequencies under full-composition lysis treatment (Figure 2.8), the probability of differences at tether lengths of 3-4, 5-6, and 7-8  $\mu\text{m}$  being due to chance are 0.45, 0.18, and 0.20 respectively (alpha level  $\leq 0.01$ ). Therefore, all differences are statistically insignificant.

## Discussion

The main conclusion of my research study is that elastic tethers can function during dilute lysis buffer-induced anaphase spindle deactivation and segregation arrest. This conclusion assumes that all the backward chromosomal movements seen during lysis-induced anaphase arrest are due to elastic tether functioning and not some other factor associated with the lysis buffer. Several lines of evidence supporting the former explanation rather than the latter have been presented during this study. Typical tether characteristics seen under normal anaphase conditions (LaFountain *et al.*, 2002; Kite and Forer, 2020; Forer *et al.*, 2021) are also seen during anaphase spindle deactivation and segregation arrest as follows; (1) elastic tethers cause backward chromosomal movements which are led by partner telomeres directed towards each other while the kinetochores trail behind (Figures 2.3A, 2.4A); (2) shorter tethers are more consistently elastic causing more frequent backward movements than longer tethers (Figure 2.8); (3) shorter tethers are more consistently elastic causing backward movements over greater fractional distances than longer tethers (Figures 2.9B, 2.9C); (4) tethers of different lengths cause backward movement with velocities that have no statistically significant difference between them (Figure 2.10); (5) early anaphase CalA application enables tethers to remain elastic such that when lysis +CalA is added later, tethers are capable of always moving partner chromosomes backward completely to meet each other (Figures 2.8, 2.9D). All these multifaceted proofs underpin the inference that it is most likely elastic tethers which exert anti-poleward forces on chromosomes causing their backward movements during dilute lysis buffer-induced anaphase arrest; this indicates that elastic tethers can function despite a non-functional anaphase spindle.

Tethers work in dilute lysis buffer-treated cells as they do in untreated control cells, which means that the dilute lysis buffer maintains tether function while it stabilizes the anaphase spindle apparatus. Normally, lysis buffer is used to lyse cells, i.e., break cell membranes and release cell content for analysis (Islam *et al.*, 2017); they can be used at lower concentrations to partially lyse cells, i.e., create holes in the intact cell membrane for molecules to enter the cell (Amidzadeh *et al.*, 2014; Behbehani *et al.*, 2014). The lysis buffer used in my research project contains IGEPAL CA-630 detergent which disrupts cell membrane; PIPES buffer and magnesium sulphate salt which maintain the pH and osmolarity respectively of the cell content environment; and EGTA chelating agent which binds divalent cations making them unavailable for reactions that may

damage the cellular proteins and genetic material (Brennan, 2018). Overall, this lysis buffer at full strength causes the complete disintegration of cell membrane, but maintains proteins in their native state preserving their protein-protein interactions, and stabilizes the cytoskeleton preserving its structure (ThermoFisher, 2023). At reduced concentrations, this lysis buffer could cause cell membrane to remain intact but with holes created in its structure, and could still preserve native-state proteins, protein-protein interactions, and stabilized cytoskeleton. This would explain how tether activity remains unaffected while the anaphase spindle activity is arrested in dilute lysis buffer-treated cells.

In my research reported herein, the dilute lysis buffer's effect seems to be mediated by IGEPAL (Figures 2.12A, 2.12B) via some presently unestablished mechanism. Previous research has described two possible mechanisms of action of mild, non-ionic, non-denaturing detergents which, working either individually or together, could explain how dilute IGEPAL may be causing anaphase spindle deactivation and anaphase arrest. The dilute IGEPAL detergent punches holes in a few areas of the cell membrane instead of completely breaking it down; the tiny pathways thus created could allow some vital intracellular proteins or co-factors such as ATPs to solubilize out of the cell, thereby arresting anaphase (Seddon *et al.*, 2004; Churchward *et al.*, 2005; Sinha *et al.*, 2017; Berlin *et al.*, 2023). Alternatively, the dilute IGEPAL maybe interacts with the intracellular tubulin to inhibit microtubule dynamics, thereby deactivating the spindle apparatus (Mesland and Spiele, 1984; Andreu, 1982). Favoring this alternative hypothesis is the evidence that detergents like IGEPAL can inhibit *in vitro* microtubule assembly reversibly such that removal of detergent leads to restoration of tubulin polymerization abilities (Andreu *et al.*, 1986). Such reversibility is seen 100% of the times in my IGEPAL experiments where IR washout causes the IGEPAL-arrested anaphase to restart and cell division to complete as seen in control cells. Interestingly, IR washout in the 6:1000 lysis buffer-arrested cells, having PEM mixed with the same concentration of IGEPAL as that used alone, does not always yield restoration of anaphase segregation. This suggests that the same detergent concentration, when used in a buffer mixture, causes more permanent irreversible anaphase arrest contrary to when used alone.

In partially lysed cells, elastic tethers cause backward chromosomal movements with typical characteristics which match the characteristics previously documented in non-lysed cells, all except one: the backward chromosomal velocities in lysis and lysis+ CalA treated cells are

smaller than the backward chromosomal arm fragment velocities seen previously in control and CalA-only treated cells respectively (Figure 2.10; Forer *et al.*, 2021). Nevertheless, backward chromosomal velocities in lysis+ CalA treatment are close to those measured before in CalA-only treatment (Figure 2.10; Fabian *et al.*, 2007a). So, with corresponding treatments, chromosomal backward velocities seem to be comparable to each other, but are considerably slower than backward-moving cut arm fragment velocities. Why? The difference is most likely not due to some effect of the partial lysis agent itself since the difference also exists between the CalA-only treatments of Forer *et al.* (2021) and Fabian *et al.* (2007a). I suggest that this discrepancy may be due to chromosomes having to move backward against certain resistance that may not be experienced by cut-arm fragments (Anjur-Dietrich *et al.*, 2021). Arm fragments are not attached to anything; however backward moving chromosomes are firmly attached onto their kinetochore microtubules (kMTs) despite the lysis-induced anaphase spindle deactivation and anaphase arrest (Figure 2.11). Moreover, the kMTs are completely acetylated, hence they are stable and not easily depolymerized (Wilson and Forer, 1989; Wilson *et al.*, 1994; Xu *et al.*, 2017). These stable kMTs holding the chromosomes back from the poleward direction could be preventing them from moving anti-poleward as fast, and as far, as they possibly could without the kMT attachments. Therefore, anti-poleward tether forces causing backward chromosomal movements may be retarded due to the poleward resistance produced against them by the stable kMTs attached to the chromosomes (Figure 2.11).

Chromosomal attachment to kMTs may be causing their backward movements to be slower than the backward movements of cut arm fragments which are not attached to anything. If that is the case, then detaching the chromosomes from kMTs might allow them to move backward as fast as cut arm fragments move. This can be tested by treating cells with microtubule (MT) inhibitors that block MT polymerization, promote their depolymerization, and thereby cause MTs to break into their monomer units. If kMTs are depolymerized into their tubulin subunits and are no longer attached to their chromosomes, the chromosomes should be free to move backwards faster than they could move while being attached to their kMTs.

My partial cell lysis protocol can be further developed into an *in vitro* system for studying tether function in detail. Dilute lysis buffer preparations of 4, 5, and 6:1000 strength can cause consistent anaphase spindle deactivation with anaphase arrest (Figure 2.6); this treatment does

not damage the anaphase spindle because the anaphase arrest can be reversed with IR wash (Figure 2.7). Since tethers remain active during the dilute lysis buffer-induced anaphase arrest, different phosphorylation promoters/inhibitors can be added directly to the partially permeabilized cells, and then their effect on tether elasticity can be analyzed. To confirm that the promoters/inhibitors cross the partially permeabilized cell membrane and enter the cell, the enzymes can be fluorescently tagged, and a sample of the experimental cells can be analyzed by flow cytometry (Amidzadeh *et al.*, 2014), or regular fluorescence microscopy. Besides phosphorylation enzymes, other molecules targeting tether components can be introduced into the partially lysed cells and studied. For example, titin protein has been suggested as being a possible component of tethers, accounting for its elastic nature (Fabian *et al.*, 2007b). Hence, antibodies against phosphorylated titin can be added to partially permeabilized cells, and their relative concentrations bound to tethers during different timings of anaphase can be compared to assess tether titin phosphorylation/dephosphorylation states. Overall, partially permeabilized cells can serve as an *in vitro* system for studying tethers in detail to further understand their function, and possible role in cell division.

To summarize, my research shows that partially lysing cells arrests their anaphase segregation, but does not affect their tether function since elastic tethers produce backward forces on chromosomes in partially lysed cells like they do in non-lysed (control) cells. Therefore, partially lysed cells can be further developed into an *in vitro* system for studying tethers to better understand the contribution of tethers in normal cell division; this can help advance our understanding and management of anomalous cell divisions resulting in abnormal cell death, cancer, and fatal birth defects.

### **Chapter 3. Elastic tethers remain functional during microtubule inhibition, but do not cause faster backward chromosomal movements than the backward movements seen in partially-lysed cells**

#### **Abstract**

During normal anaphase, elastic tethers connect partner telomeres of segregating chromosomes, and they exert anti-poleward forces on those chromosomes. Tethers can cause anti-poleward (backward) movement of chromosomes if poleward forces dissipate, as seen in partially-lysed cells where anaphase spindle is deactivated and anaphase segregation is arrested (Chapter 2). The backward moving chromosomes remain attached to their kinetochore microtubules (kMTs) which may be exerting poleward resistance against chromosomes' anti-poleward movement, thereby slowing them down. Would detaching chromosomes from their kMTs cause faster backward movements, like the backward movements of laser-cut chromosomal arm fragments seen in control cells of Forer *et al.* (2021)? To test this hypothesis, I treated anaphase crane-fly spermatocytes with low-high concentrations of nocodazole, colcemid, and podophyllotoxin to disassemble kMTs. The inhibitor drug treatments led to anaphase segregation arrest, and backward chromosomal movements, similar to the anaphase arrest and backward movements seen in partially-lysed cells. However, the drugs did not disassemble the stable, acetylated kMTs, and backward movements of chromosomes remained slower than the backward movements of cut chromosomal arm fragments. These results prove that elastic tethers can work normally during microtubule inhibition, like they work during partial cell lysis and control conditions. Also, depolymerizing microtubule inhibitors nocodazole, colcemid, and podophyllotoxin disassemble the non-acetylated non-kinetochore microtubules; however, even the higher possible concentrations of these inhibitors do not disassemble the stable, acetylated kMTs during the short time period of anaphase.

## Introduction

This study investigates whether inhibiting microtubules affects the backward forces produced by elastic tethers during anaphase. Elastic tethers are present in various animal and plant cells (Forer *et al.*, 2017; Paliulis and Forer, 2018). They physically connect two out of four corresponding arms (telomeres) of all partner anaphase chromosomes in meiosis-I of crane flies (LaFountain *et al.*, 2002). As partner chromosomes separate during anaphase, they move towards their respective poles led by their kinetochores while their tethered arms trail behind (Adames and Forer, 1996). Laser cutting a trailing chromosomal arm in early anaphase results in the arm fragment moving backward in the anti-poleward direction, telomere moving to its partner telomere in the opposite half spindle (LaFountain *et al.*, 2002). Such backward movement is due to elastic tethers and not microtubules because it occurs only when both partner telomeres are intact (LaFountain *et al.*, 2002; Forer *et al.*, 2021), and occurs in Taxol treated cells having stabilized microtubules (Forer *et al.*, 2018). The backward movement is not caused by ultra-fine DNA bridges because these are not elastic, are found only in a small number of anaphase chromosomes, mostly at the centromeric regions rather than at telomeres, and generally retard or stop anaphase segregation when present (Chan *et al.*, 2007; Barefield and Karlseder, 2012; Gemble *et al.*, 2015; Su *et al.*, 2016). Moreover, actin and myosin too cannot be the backward movement mediators since these movements occur in the presence of actin and myosin inhibition (Fabian *et al.* in 2007a). Therefore, elastic tethers cause backward movement of chromosomal arm fragments cut during early anaphase.

When arm fragments of segregating anaphase chromosomes are cut in later anaphase rather than early anaphase, their backward movements are less frequent, and occur over shorter distances, indicating that tethers become less elastic as anaphase progresses (LaFountain *et al.*, 2002; Forer *et al.*, 2021). Loss of tether elasticity during anaphase is due to tether dephosphorylation; by treating early anaphase cells with Calyculin A (CalA), an inhibitor of serine-threonine protein phosphatase 1 (PP1) and 2A (PP2A), tether dephosphorylation is prevented. The tethers remain phosphorylated and elastic, and cause backward movements of entire chromosomes (or their cut arm fragments) at the end of anaphase (Fabian *et al.*, 2007a; Kite and Forer, 2020; Forer *et al.*, 2021).

Tether activity remains unaffected when anaphase segregation is arrested by partially lysing cells and deactivating their anaphase spindles (Chapter 2). Typical tether features described in previous work (Forer *et al.*, 2021) are found in partially lysed cells as follows; shorter more-elastic tethers cause chromosomes to move backward more frequently, and over greater fractions of tether length than do longer less-elastic tethers (Figures 2.8, 2.9B, 2.9C); tethers of different lengths, having different elasticities, move chromosomes backward with velocities that are statistically similar to each other (Figure 2.10); early anaphase CalA treatment of cells enables tethers to remain elastic throughout anaphase, such that partial lysis of the cells at any tether length causes all partner chromosomes to move backward and meet each other (Figures 2.8, 2.9D). Interestingly, backward velocity of chromosomes in partially lysed cells (Figure 2.10) is less than the backward velocity of cut-arm fragments seen in non-lysed (control) cells (Forer *et al.*, 2021). Similarly, backward velocity of chromosomes in CalA-treated then partially-lysed cells (Figure 2.10) is less than the backward velocity of cut-arm fragments seen in CalA-treated non-lysed cells (Forer *et al.*, 2021). Therefore, backward movements of chromosomes and cut chromosomal arm fragments caused by elastic tethers are similar in most aspects except one; backward velocities are greater for cut-arm fragments than for chromosomes.

Chromosomes are connected to spindle microtubules via their kinetochores while cut arm fragments are not, which could be a possible reason why chromosomes move backward slower than cut arm fragments do. During cell division, the microtubule organizing centers (MTOCs) assemble tubulin monomers into microtubule (MT) polymers, which constitute a part of the spindle apparatus (McIntosh, 2016). The spindle MTs attached to chromosome kinetochores (kMTs) assist the chromosomes in aligning at the metaphase plate, and then separating towards their poles during anaphase (LaFountain *et al.*, 2004). Anaphase chromosomal segregation in crane-fly spermatocytes involves the kMTs treadmilling towards the pole; the kMTs depolymerize at their poleward (minus) ends faster than they polymerize at their kinetochore (plus) ends (LaFountain *et al.*, 2004). Additionally, as new tubulins add to the kMTs at the plus ends, the older tubulins in the kMTs move towards the minus end, and they get acetylated (Wilson and Forer, 1989; Wilson *et al.*, 1994). Partial cell lysis arrests anaphase most likely by deactivating the spindle apparatus (Chapter 2); however, it does not disassemble the kMTs which remain attached to backward moving chromosomes during the anaphase arrest. These kMTs perhaps exert poleward resistance against the chromosomes' anti-poleward motion, thereby

slowing down their backward movement in partially lysed and CalA treated cells. This could explain why chromosomal backward movements are slower than the arm fragment backward movements in CalA treated cells (Fabian *et al.*, 2007a; Forer *et al.*, 2021), and in partially lysed cells with and without early anaphase CalA treatment (Chapter 2).

My present study aimed at answering the following question; does inhibiting/disassembling kMTs allow elastic tethers to cause faster backward movements of chromosomes like they do with chromosomal arm fragments? I treated cells at different stages of anaphase with various MT inhibitors to disrupt MT dynamics, disassemble kMTs, and then I assessed tether dynamics. Frequency and extent of backward chromosomal movements were measured to ensure tether functioning was as documented in control cells, and was not adversely affected by the MT inhibitors. Backward chromosomal velocities caused by elastic tethers were also analyzed and compared with their counterparts in previous studies to evaluate any differences due to MT inhibition. Immunofluorescence study was conducted on the MT inhibited cells to check whether spindle MTs, including kMTs, were disassembled or still intact. The MT poisons used were Nocodazole (NOC), Colcemid and Podophyllotoxin (PPT); NOC promotes MT depolymerization by binding and aggregating free tubulin, thereby inhibiting MT polymerization; Colcemid also promotes MT depolymerization, but, by binding directly onto the MT structural tubulins at the plus end and inhibiting their polymerization; PPT promotes MT depolymerization by binding and blocking the colchicine binding sites on MTs, thus inhibiting their polymerization (Bryan, 1974; Jordan *et al.*, 1992; Hamel, 2003; Jordan and Wilson, 2004; Yang *et al.*, 2010). Using different mechanisms to inhibit MTs and yet obtain similar results with each gives credence to those results being due to MT inhibition and not due to some side effect of the drugs used for the inhibition.

## **Materials and Methods**

### **Living cell preparation**

Living cells of crane flies (*Nephrotoma suturalis* Loew) were prepared as described in detail previously in chapter 2, by Forer (1982), and by Forer and Pickett-Heaps (1998). Briefly, testes of IV-instar larvae were dissected in a drop of halocarbon oil to prevent their dehydration, and washed in insect Ringer's solution (IR) (0.13 M NaCl, 5mM KCl, 1.5 mM CaCl<sub>2</sub>, 3mM phosphate buffer, pH 6.8). Each testis' cells were spread out in a 2.5 µL drop of IR containing fibrinogen (10mg/mL) on a coverslip. Cells were then fixed in place by adding 2.5 µL thrombin to the fibrinogen making a fibrin clot (Forer and Pickett-Heaps, 2005). The clot-embedded cells on the coverslip were inverted over a drop of IR in a perfusion chamber (Forer and Pickett-Heaps, 2005) and sealed with a molten mixture of 1:1:1 Vaseline, lanolin and paraffin. IR was perfused through the chamber covering the clot-held cells as they continued their routine division. Finally, the perfusion chamber was set up on the stage of a phase-contrast microscope for observation.

### **Experimental agent addition**

The cells in the perfusion chamber were observed with the phase-contrast microscope, and once the cells were at the required stage of division (different times during anaphase-I like early, mid, or late), they were perfused according to the treatment group they belonged to. Control cells were treated with IR. Experimental cells were treated with various concentrations of three different microtubule (MT) inhibitors; Nocodazole (NOC), Colcemid, and Podophyllotoxin (PPT) (LaFountain, 1985; Silverman-Gavrila and Forer, 2000; Hamel, 2003; Yang *et al.*, 2010). Inhibitor stock solutions prepared in DMSO and stored frozen were thawed and diluted in IR to make final working concentrations of the experimental drugs. Stocks of NOC were used to make final working concentrations of 20, 30, 60 and 90 µM NOC. Colcemid stocks were used to make final working concentrations of 100 and 200 µM Colcemid. PPT stocks were used to make final working concentrations of 10, 20, 30, 50 and 60 µM PPT respectively. The highest DMSO concentration in experimental agents was 0.55% (v/v) DMSO which was still within the 1% tested in control cells and found to have no effect on normal anaphase-I segregation (Chapter 2). Some of the NOC treated cells were saved for immunofluorescence study. 15-25 minutes after adding NOC, cells were completely lysed using our full-strength lysis buffer as described later in the fluorescent staining and confocal microscopy section.

## Microscopy and data analysis

Phase-contrast microscope with Nikon 100X, 1.25 NA phase-contrast oil immersion objective lens was used to study the living cells in perfusion chambers. Real-time video images were recorded on DVDs and later converted into time-lapse video sequences (.avi files) using freeware VirtualDub 2. Measurements of chromosomal movements were made from individual video sequence frames using an in-house program WinImage (Wong and Forer, 2003). Chromosomal movement graphs were plotted using the commercial software SlideWrite Plus 7.0 (Forer and Berns, 2020).

## Fluorescent staining and confocal microscopy

Fluorescent staining procedure was adapted from chapter 2. Briefly, NOC treated cell preparations on cover slips were lysed in lysis buffer for 15 minutes, and then fixed in 0.25% glutaraldehyde in phosphate-buffered saline (PBS) for 2-3 minutes. Afterwards, cells were rinsed twice in PBS, placed in 0.05M glycine for 10 minutes, rinsed four times in PBS, and stored in PBS-glycerol 1:1 (v/v) mixture at 4°C ready to stain. For immunostaining, stored coverslips were first washed in PBS, and then rinsed with 0.1% Triton X-100 in PBS. All the cells were double-stained for the following; tyrosinated  $\alpha$ -tubulin was stained with primary rat monoclonal antibody YL1/2 (Abcam) diluted 1:200, and then stained with secondary mouse-absorbed Alexa 488-conjugated goat anti-rat antibody (Molecular Probes) diluted 1:50; acetylated  $\alpha$ -tubulin was stained with primary mouse monoclonal antibody 6-11B-1 (Millipore Sigma) diluted 1:50, and then stained with secondary rat-absorbed Alexa 568-conjugated donkey anti-mouse antibody (Invitrogen) diluted 1:200. All antibodies were diluted in PBS, and cells were incubated in each antibody for 1 hour in the dark. At the end of every antibody incubation, cells were rinsed twice in PBS, and then rinsed with 0.1% Triton X-100 in PBS. After the last antibody staining, coverslips were rinsed twice in PBS, and then placed in PBS-glycerol 1:1 (v/v) for 2-3 minutes. Finally, coverslips were mounted in Mowiol solution (Osborn and Weber, 1982) containing 0.2 g/L paraphenylene diamine (PPD) antifading agent, and left to dry in the dark for 24-48 hours. Once dry, coverslips with the stained cells were stored at 4°C ready for analysis. Cells were analyzed using an LSM 700 Zeiss Observer confocal microscope, with a Zeiss Plan-Apochromat 63X 1.4 NA oil-immersion objective lens. Images were collected using ZEN Black software, and further processed using FIJI Image J software.

## Results

### Control cells

Primary crane-fly spermatocytes have three pairs of homologous autosomes and two unpaired sex chromosomes that participate in meiosis-I. During metaphase-I, the bivalent autosomes and the univalent sex chromosomes line up at the equator. Anaphase-I involves the three bivalents disjoining into six half-bivalents (partner homologues) which then move towards their respective poles in opposite directions (Figure 3.1). While the autosomes are segregating, spindle length remains constant, and both sex chromosomes remain stationary at the equator (Forer, 1966; Forer *et al.*, 2013). Once the autosomal partner homologues reach near their respective poles in about 20-30 minutes, the spindle starts elongating, the sex chromosomes start segregating, and the cleavage furrow ingresses.

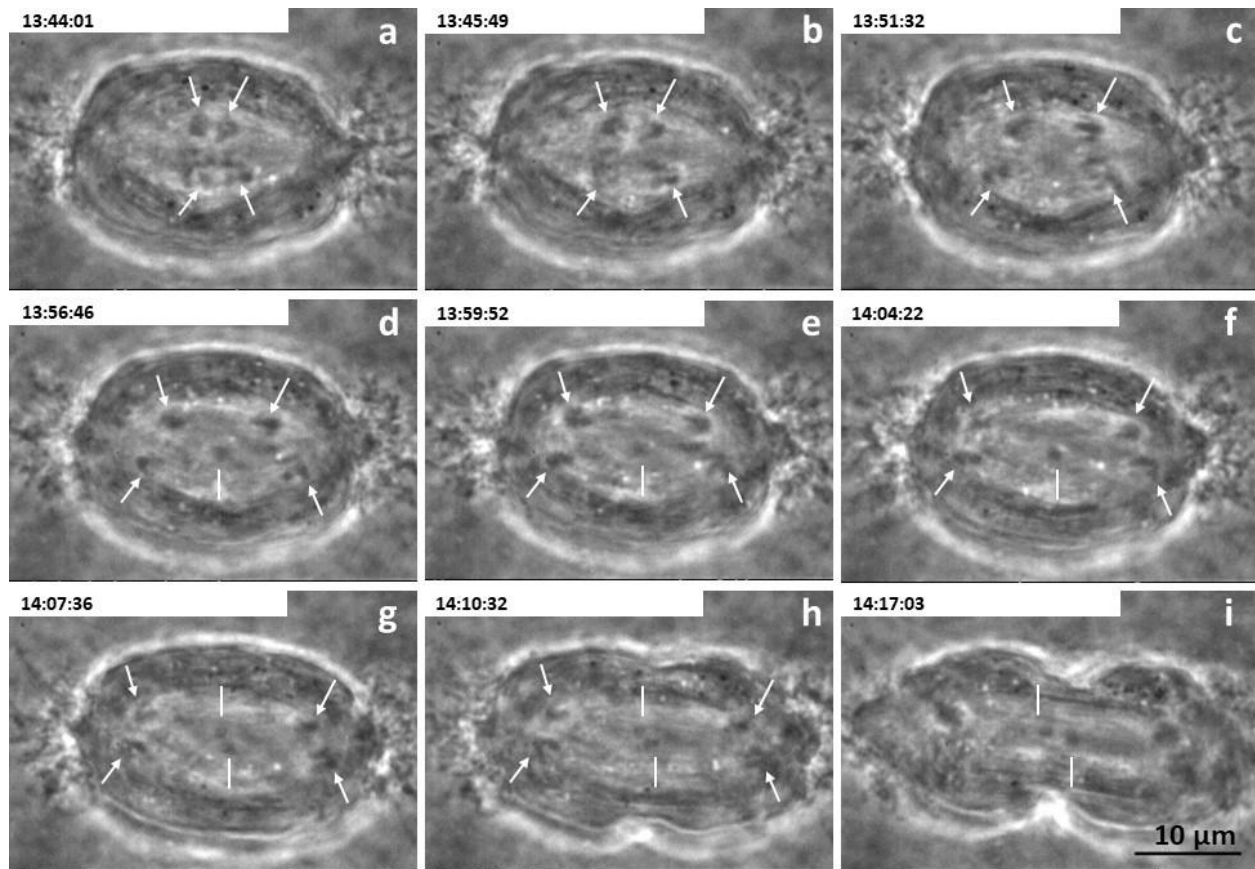


**Figure 3.1.** Meiosis-I in primary spermatocyte of crane flies. Time (hrs: min:sec) is presented at the top of each image panel (a-i). **(a)** Arrows point to two pairs of homologous autosomes just starting anaphase. **(b–c)** Arrows follow the positions of separating partner homologues during anaphase as they move apart from each other and travel to their respective poles in opposite directions. **(d–f)** Arrows follow segregating homologues. Lines indicate position of sex chromosomes which remain stationary while homologues segregate. **(g)** Autosomes reach near the poles while both sex chromosomes remain at the equatorial region **(h–i)** Spindle elongates as both sex chromosomes separate, and the cleavage furrow appears at the equatorial region of the cell cortex. Scale bar in (i) equals 10  $\mu\text{m}$ .

## **Experimental cells**

### **1) Chromosomal segregation stops in all anaphase cells treated with various MT inhibitors**

To study the effect of various MT inhibitors on anaphase chromosomal dynamics, cells at different stages of anaphase were treated with the inhibitors and partner chromosomal movements were studied. In each cell, movements of partner telomeres and kinetochores were measured at regular intervals from a fixed reference point near one spindle pole, and plotted as distance versus time graphs. Figures 3.2, 3.3, and 3.4 illustrate how these graphs were analyzed: immediately after adding MT inhibitor, distance between partner telomeres was measured to represent initial tether length; partner kinetochore separation towards their respective poles was checked to determine whether anaphase stopped or not; and if anaphase stopped, then antipoleward movement of partners was assessed to ascertain whether backward chromosomal movement occurred or not. For partner chromosomes that moved backward, final tether length between partner telomeres was measured at the end of their backward movement. This was subtracted from the initial tether length to give total distance traveled backward by partners towards each other due to elastic tethers. The total distance traveled backward when taken as a fraction of initial tether length quantified the extent of tether shortening and its resultant backward movement. Slopes of kinetochore graphs were taken as corresponding chromosomal movement velocities.

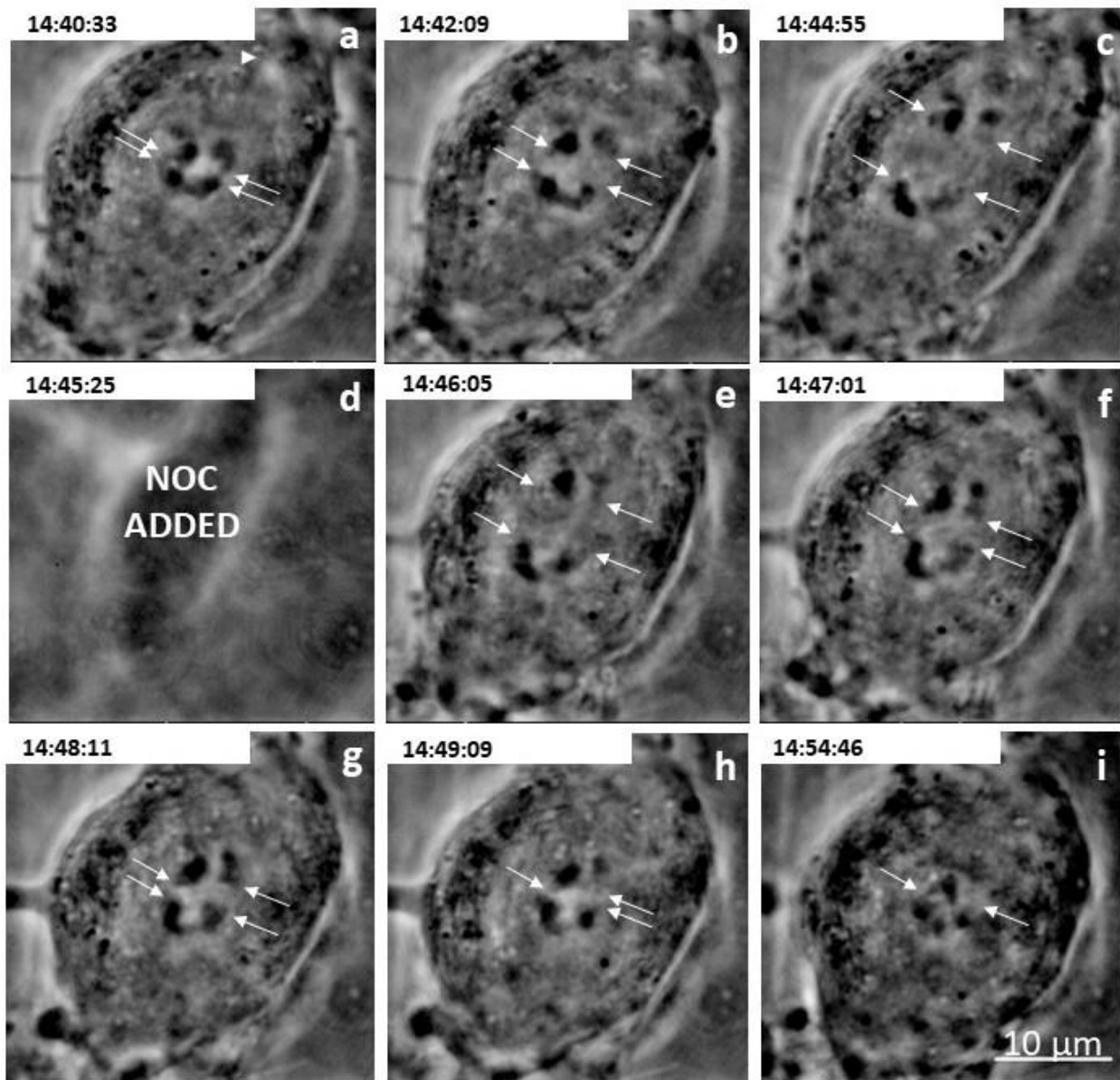


**Figure 3.2A.** 30 $\mu$ M NOC-treated cell montage. Time (hrs: min:sec) is presented at the top of each panel (a-i). **(a)** Two pairs of homologous chromosomes start anaphase separation; each partner homologue is marked by arrows. The single arrowhead points to the fixed point near the top spindle pole used as a fixed reference point for measurements. **(b-c)** Partner homologues continue separating. **(d)** 30 $\mu$ M NOC added. **(e)** Homologues stop separating and start moving backwards towards each other. **(f-h)** partners continue moving backwards towards each other **(i)** Backward movement stops as partners meet up with each other and remain as they are. Scale bar in (i) represents 10  $\mu$ m.

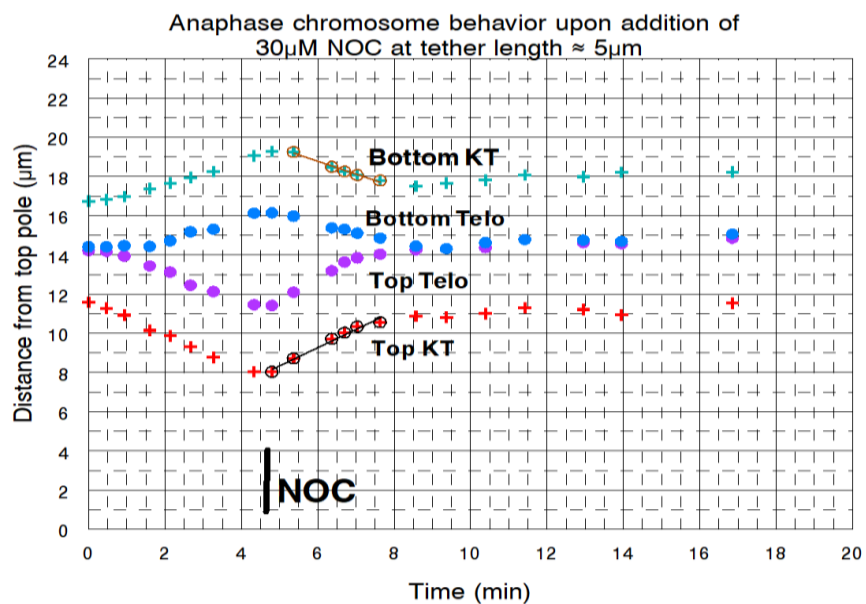


**Figure 3.2B.** Movement graph for the left pair of homologous chromosomes illustrated in Figure 3.2A. The graph time=0 min corresponds to the montage panel (a) image time=14:40:33 (hrs: min:sec). Distance measurements were made from a fixed point near the top pole. Partner kinetochores are marked as Top KT and Bottom KT, partner telomeres are Top Telo and Bottom Telo. Partners were moving apart when NOC was added after which they stopped separating and moved backwards all the way to meet each other. Slopes of the kinetochore graphs represent backward movement velocities.

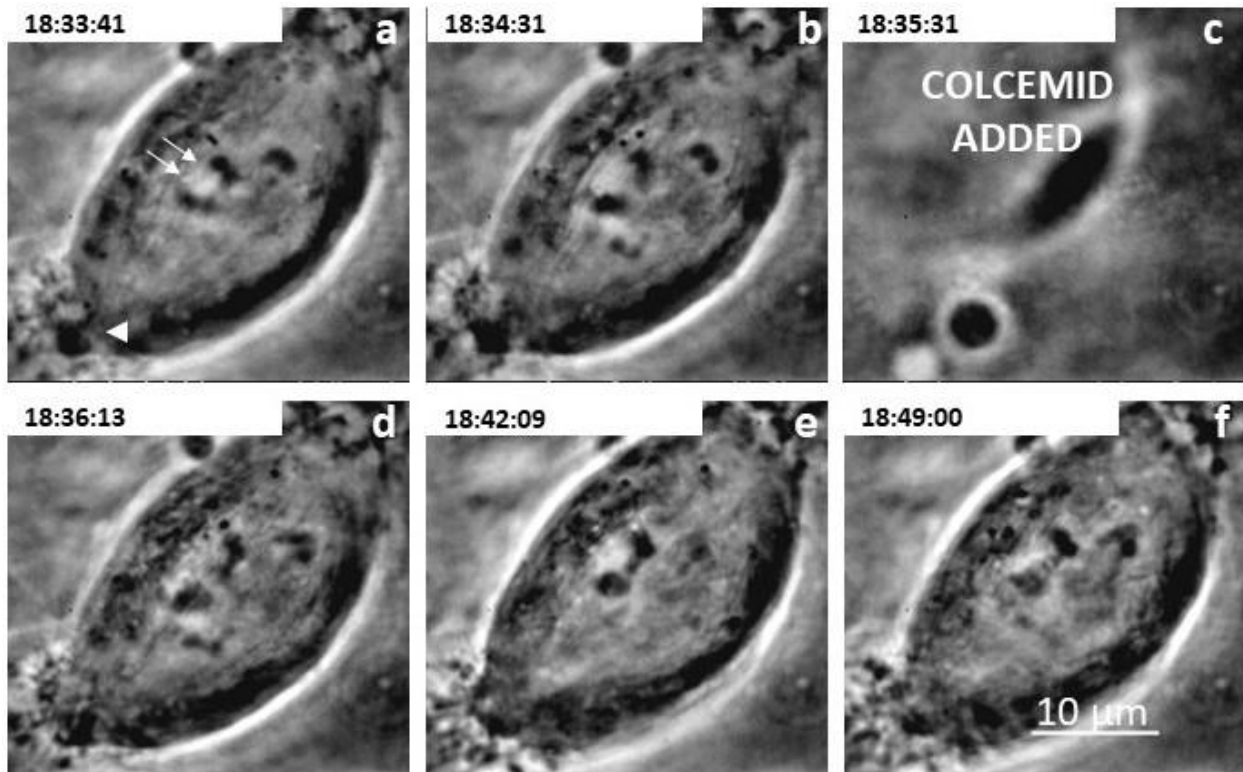


**Figure 3.3A.** 100 $\mu$ M Colcemid-treated cell montage. Time (hrs: min:sec) is presented at the top of each panel (a-f). **(a)** Arrows point to the partners of one pair of homologous chromosomes clearly visible and starting anaphase separation. The single arrowhead points to the fixed point near the bottom spindle pole used as a fixed reference point for measurements. **(b)** Partner homologues continue separating. **(c)** 100 $\mu$ M Colcemid added. **(d)** Homologues stop separating and start moving backwards towards each other. **(e)** Backward movement stops as partners meet up with each other. **(f)** Partners remain as they are. Scale bar in (f) represents 10  $\mu$ m.

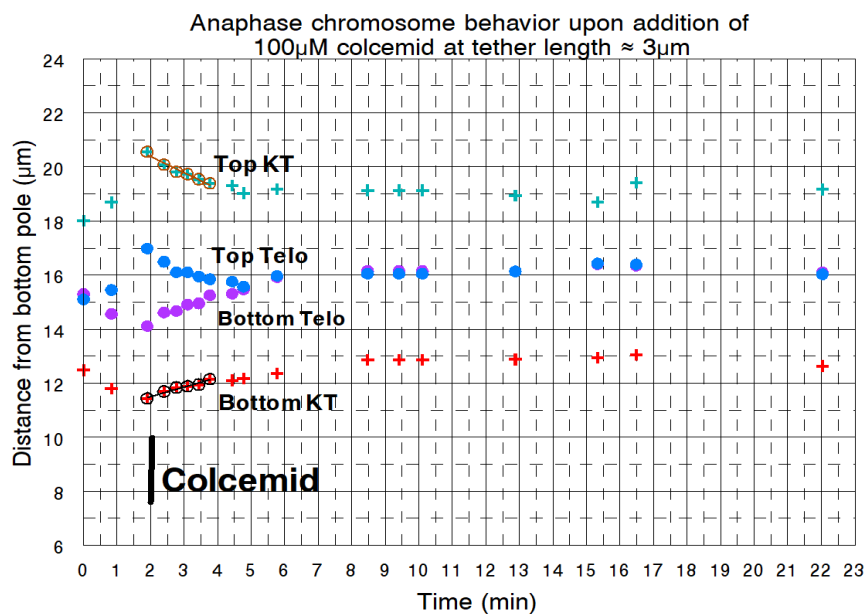


**Figure 3.3B.** Movement graph for the left pair of homologous chromosomes illustrated in Figure 3.3A. The graph time=0 min corresponds to the montage panel (a) image time=18:33:41 (hrs: min:sec). Distance measurements were made from a fixed point near the bottom pole. Partner kinetochores are marked as Top KT and Bottom KT, partner telomeres are Top Telo and Bottom Telo. Partners were moving apart when Colcemid was added after which they stopped separating and moved backwards all the way to meet each other. Slopes of the kinetochore graphs represent backward movement velocities.

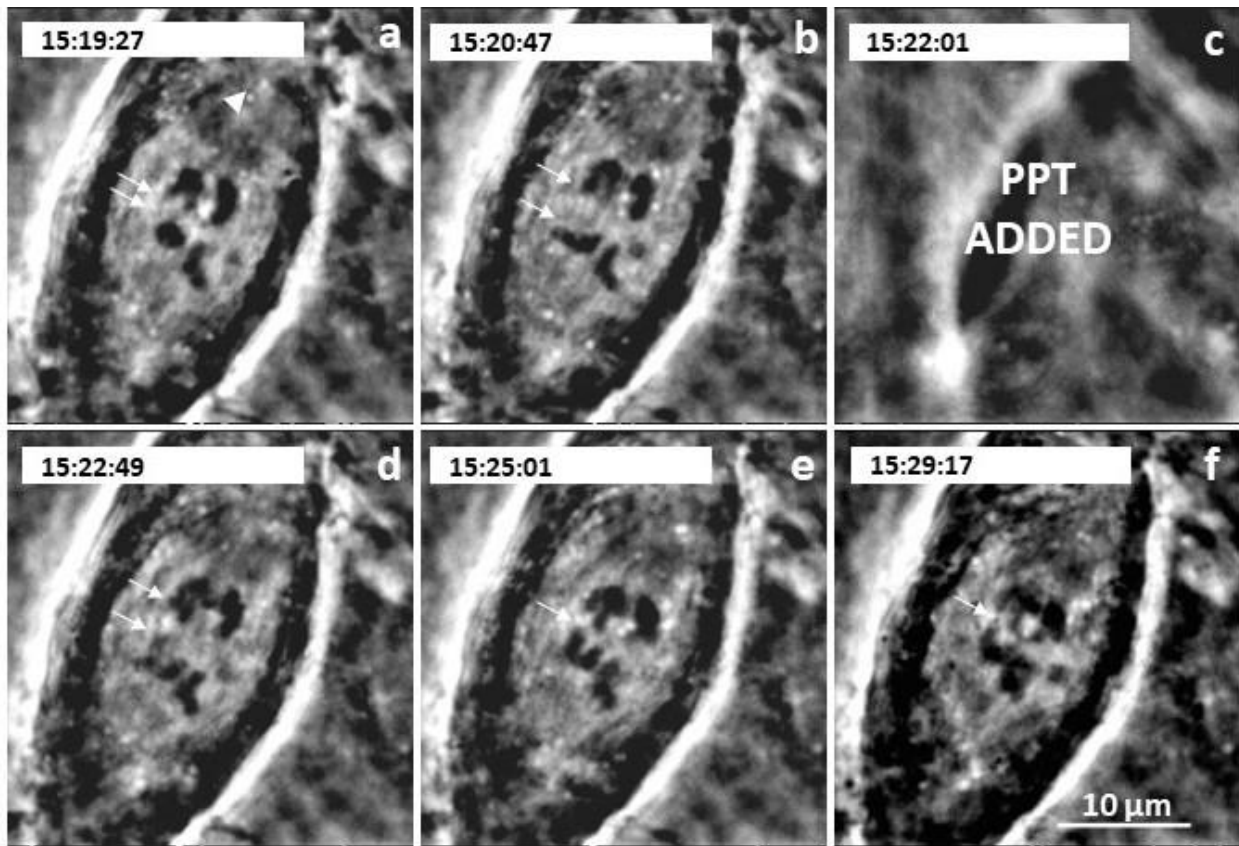


**Figure 3.4A.** 60 $\mu$ M PPT-treated cell montage. Time (hrs: min:sec) is presented at the top of each panel (a-f). **(a)** Arrows point to the partners of one pair of homologous chromosomes next to another pair; both pairs are starting anaphase separation. The single arrowhead points to the fixed point near the top spindle pole used as a fixed reference point for measurements. **(b)** Partner homologues continue separating. **(c)** 60 $\mu$ M PPT added. **(d)** Homologues stop separating and start moving backwards towards each other. **(e)** Backward movement continues. **(f)** Backward movement stops as partners meet up with each other, then remain as they are. Scale bar in (f) represents 10  $\mu$ m.

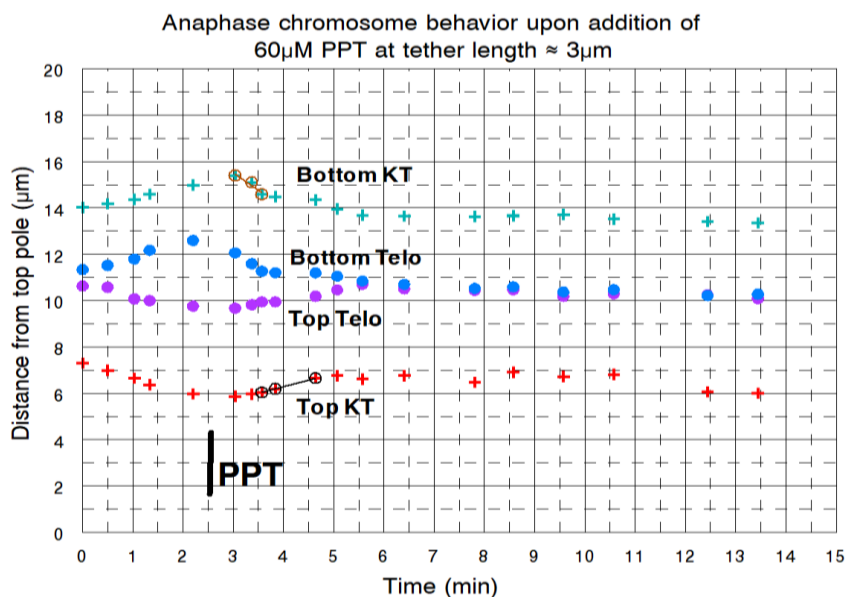


**Figure 3.4B.** Movement graph for the left pair of homologous chromosomes illustrated in Figure 3.4A. The graph time=0 min corresponds to the montage panel (a) image time=15:19:27 (hrs: min:sec). Distance measurements were made from a fixed point near the top pole. Partner kinetochores are marked as Top KT and Bottom KT, partner telomeres are Top Telo and Bottom Telo. Partners were moving apart when PPT was added after which they stopped separating and moved backwards all the way to meet each other. Slopes of the kinetochore graphs represent backward movement velocities.

For each of the MT inhibitors, NOC, Colcemid, or PPT, chromosomal behavior was comparable at all the different drug concentrations used. Furthermore, since all the drugs produced similar effects on the MTs, albeit via different mechanisms, their results could be grouped together. Thus overall, 107 homologous pairs were observed in 38 cells treated with various MT inhibitors, and all inhibitors stopped anaphase chromosomal segregation within 1 minute of drug treatment (Table 3.1).

**Table 3.1.** Anaphase segregation arrest in cells treated with various MT inhibitors

<b>Drug treatment</b>	<b>Treated cells</b>	<b>Homologous pairs that stopped segregating/ homologous pairs observed</b>
20 $\mu$ M NOC	3	9/9
30 $\mu$ M NOC	17	48/48
60 $\mu$ M NOC	4	10/10
90 $\mu$ M NOC	1	3/3
100 $\mu$ M Colcemid	2	6/6
200 $\mu$ M Colcemid	2	6/6
10 $\mu$ M PPT	1	3/3
20 $\mu$ M PPT	1	3/3
30 $\mu$ M PPT	1	3/3
50 $\mu$ M PPT	3	8/8
60 $\mu$ M PPT	3	8/8

## 2) Shorter tethers are more consistently elastic and cause more frequent backward chromosomal movement than longer tethers during MT inhibition

MT inhibition caused anaphase segregation to stop; were tethers still working? A marker of tether function is the correlation between tether length and frequency of backward movement. Shorter tethers are more consistently elastic and cause backward chromosomal movements more often than longer tethers (Forer *et al.*, 2021). Therefore, once partner chromosomes stopped moving towards their respective poles, any anti-poleward movements of  $\geq 0.5 \mu\text{m}$  were considered backward chromosomal movements caused by elastic tethers and not some adverse effect of the drug inhibition. Such backward movements were plotted against tether lengths measured immediately after drug addition (Figure 3.5). All the backward movements started within 1 minute of anaphase arrest, and occurred 100% of the time at short tether lengths of  $< 3 \mu\text{m}$ , about 75% of the times at 3-4  $\mu\text{m}$ , 65% at 5-6  $\mu\text{m}$ , only 20% at 7-8  $\mu\text{m}$ , and 0% of the times at longer lengths  $\geq 9 \mu\text{m}$  (Figure 3.5). This pattern of decreasing backward movement frequencies with increasing tether length is characteristic of elastic tether behavior, and indicates that tethers function in MT inhibited cells as they do in untreated (control) cells.

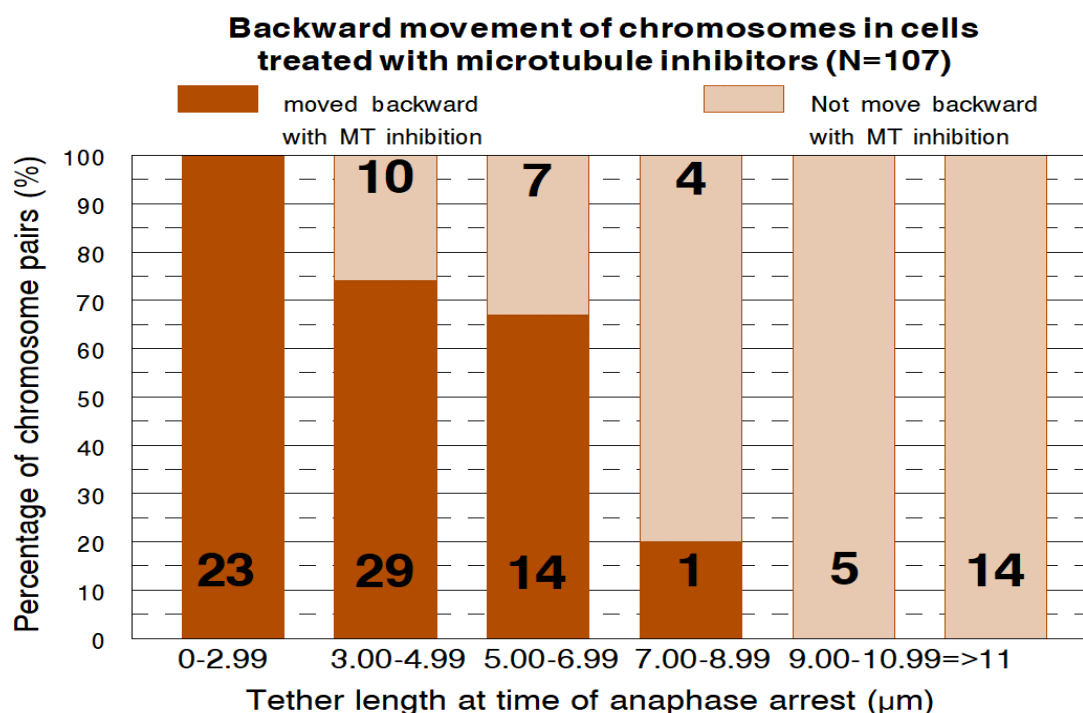


**Figure 3.5.** Frequency of backward chromosomal movements at different tether length categories in cells treated with different microtubule (MT) inhibitors. 107 homologous pairs were examined in total (N) and numbers tested in each category are written on the respective bars.

### 3) Shorter tethers are more consistently elastic and cause backward chromosomal movements over greater distances than longer tethers do during MT inhibition

Tether function was further assessed by evaluating tether elasticity. Shorter tethers tend to be more consistently elastic than longer tethers; so, short tethers shorten and pull back chromosomes more after being stretched than long tethers do (Forer *et al.*, 2021). The extent of tether shortening and backward chromosomal movement was measured by taking the distance moved backward as a fraction of initial tether length (Figures 3.6A, 3.6B). Short tethers of lengths  $<3\mu\text{m}$  caused average fractional backward movement of  $>0.9$  (Figure 3.6B), meaning partner chromosomes often moved backward completely to meet up with each other (Figure 3.6A). Contrarily, long tethers  $\geq 9\mu\text{m}$  caused average fractional backward movement of 0, meaning partners did not move backward at all. Thus, shorter tethers seem to be more consistently elastic causing backward movements over greater fractional distances than longer tethers in MT-inhibited cells, like that described in untreated (control) cells by Forer *et al.* (2021).

Spearman's rank correlation was calculated to verify that shorter tether elasticity was unlike longer tether elasticity, and that the differences between the fractional backward chromosomal movements caused by tethers of different lengths were statistically significant. The correlation coefficient ( $r_s$ ) was found to be -0.724, and with alpha level  $\leq 0.01$ , p value equaled  $1.34 \times 10^{-18}$ . Therefore, with MT inhibition, fractional distance moved backward by chromosomes due to their tether elasticity is negatively correlated to their tether length more than 99.99% of the times (Figures 3.6A, 3.6B). This highly significant correlation further corroborates that tethers work during MT inhibition as they do during uninhibited (control) conditions.

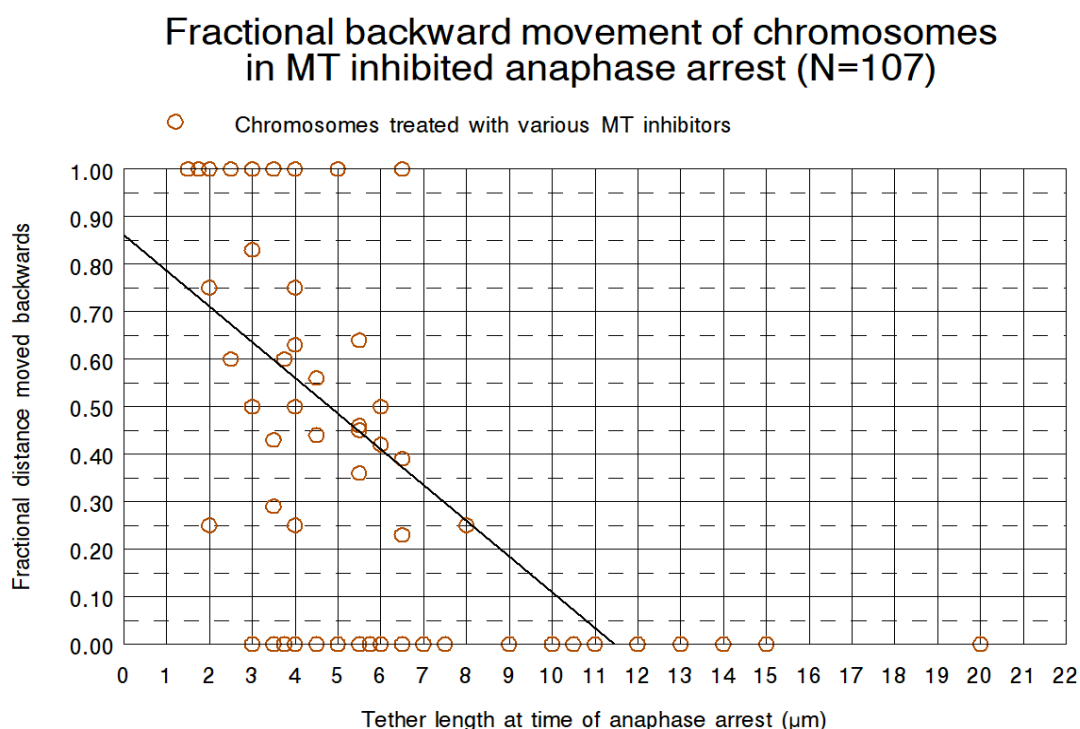


**Figure 3.6A.** Distances moved backwards by chromosomes as fractions of their initial tether length in cells treated with various MT inhibitors. 107 homologous pairs were examined in total (N). Spearman's rank correlation ( $r_s$ ) was calculated to assess the relationship between fractional distance moved backwards and tether length at time of anaphase arrest. A negative correlation was found with  $r_s = -0.724$  and  $p = 1.34 \times 10^{-18}$  (alpha level  $< 0.01$ )

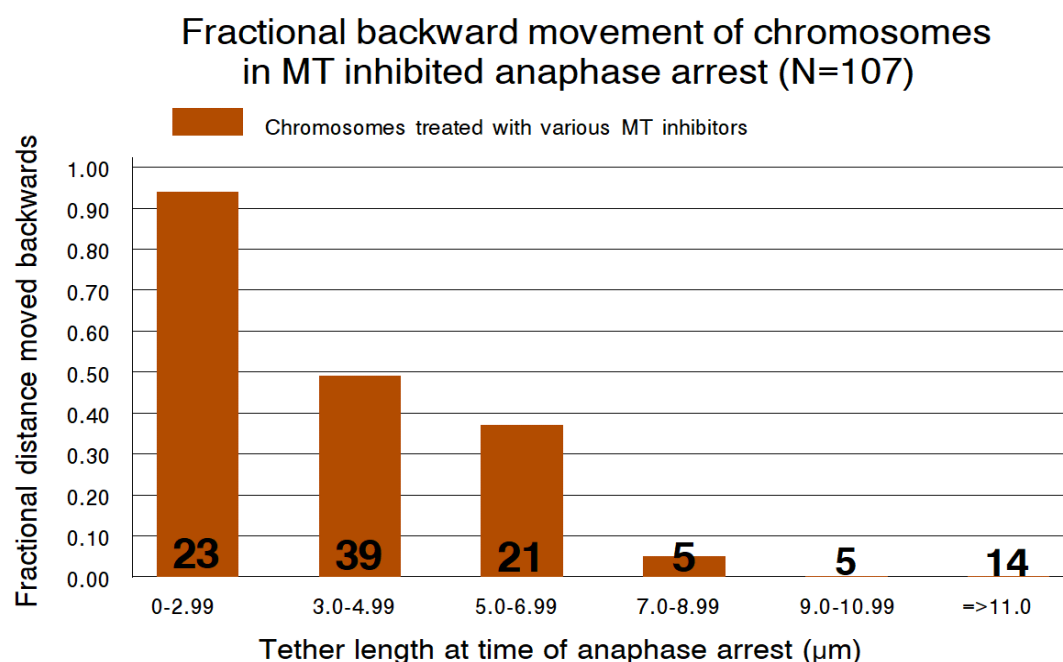


**Figure 3.6B.** Scatter plot data from Figure 3.6A grouped into categories of tether lengths plotted against average fractional distances moved backwards in each category. 107 homologous pairs were examined in total (N) and numbers tested in each category are written on respective bars.

#### **4) Backward chromosomal velocities at different tether lengths are statistically the same during MT inhibition**

Chromosomal arm fragments produced at different tether lengths move backward with statistically similar velocities in both CalA treated (experimental) and untreated (control) cells (Forer *et al.*, 2021). Likewise, chromosomes treated with dilute lysis buffer at different tether lengths move backward with velocities which are not statistically different from each other (Chapter 2). Same is the case with MT inhibition in the present study, which substantiates that the MT poisons used herein do not adversely affect tether function (Figure 3.7). Backward chromosomal velocities obtained with each MT inhibitor, NOC, Colcemid, and PPT, were first examined individually to prevent overlooking any unexpected statistically significant variation between the drug treatments. For each drug, differences between backward velocities at various tether lengths were statistically insignificant, and when compared to the other drugs, the differences were also statistically insignificant. Due to these statistically insignificant differences, backward chromosomal velocity results for the various MT inhibitors used in this study were grouped together for analysis, like the other chromosomal behavior results described already

(Figures 3.5, 3.6). Therefore, the effects of various MT inhibitors used in this study are similar, and MT inhibition does not alter tether function characteristics.

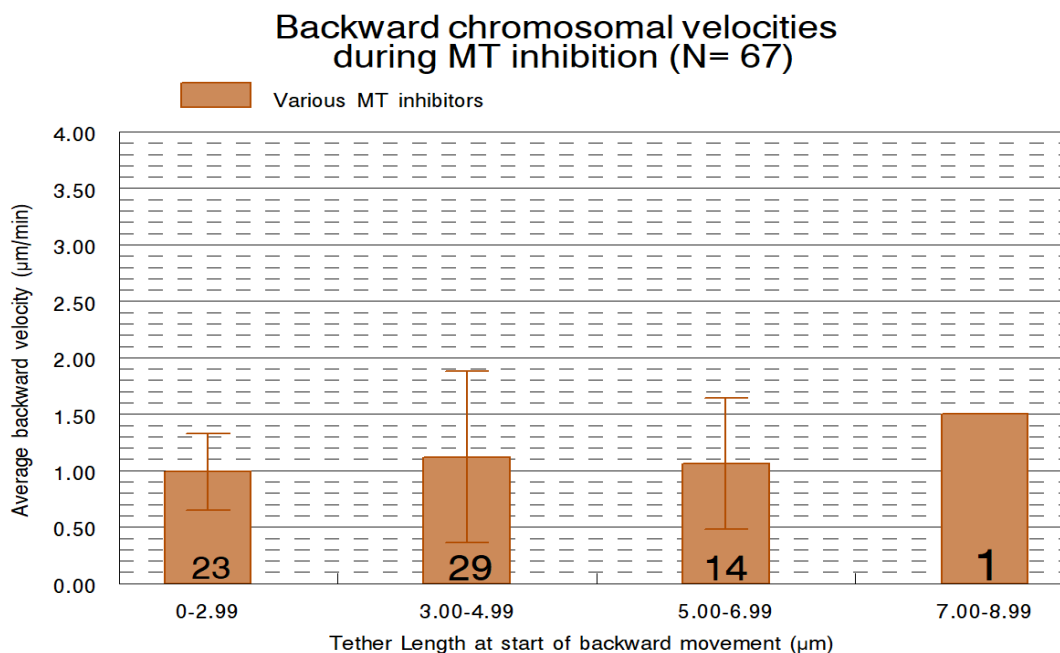


**Figure 3.7.** Average backward velocities with their standard deviations (capped bars) found at different tether length categories during MT inhibition. 67 homologous pairs were examined in total (N) and numbers tested in each category are written on the respective bars. Student's t-test was performed on all data sets and all differences were statistically insignificant (alpha level set at 0.01).

### 5) Backward chromosomal velocities during MT inhibition are statistically similar to backward chromosomal velocities seen with other anaphase arresting treatments

Elastic tethers move chromosomes backward during anaphase arrest in MT inhibited cells as they do during anaphase arrest in partially lysed cells (treated with dilute lysis buffer), and in CalA-treated partially lysed cells (treated with CalA then lysis+ CalA) (Chapter 2). Are backward movement velocities the same under all these treatment conditions? Average backward velocities at corresponding tether lengths during these treatments were compared, and Student's t-test revealed that they were all statistically the same (Figure 3.8). Comparison of MT inhibition and dilute lysis treatment groups at tether lengths  $<5 \mu\text{m}$  had t-test p-value of 0.011, meaning that there was a 0.011 probability of the two groups being from the same distribution (alpha level  $\leq 0.010$ ). The t-test probability for the same two groups at tether lengths of  $5-8 \mu\text{m}$  was 0.55, meaning that the probability of any difference between those two data sets being due to chance was 0.55. Comparing dilute lysis group with CalA then lysis+ CalA group showed a 0.010 t-test

probability of being from the same distribution, while MT inhibition and CalA then lysis+CalA groups had 0.06 t-test probability of being from the same distribution. Thus, backward chromosomal velocities seen with all these anaphase arresting treatments are statistically the same.

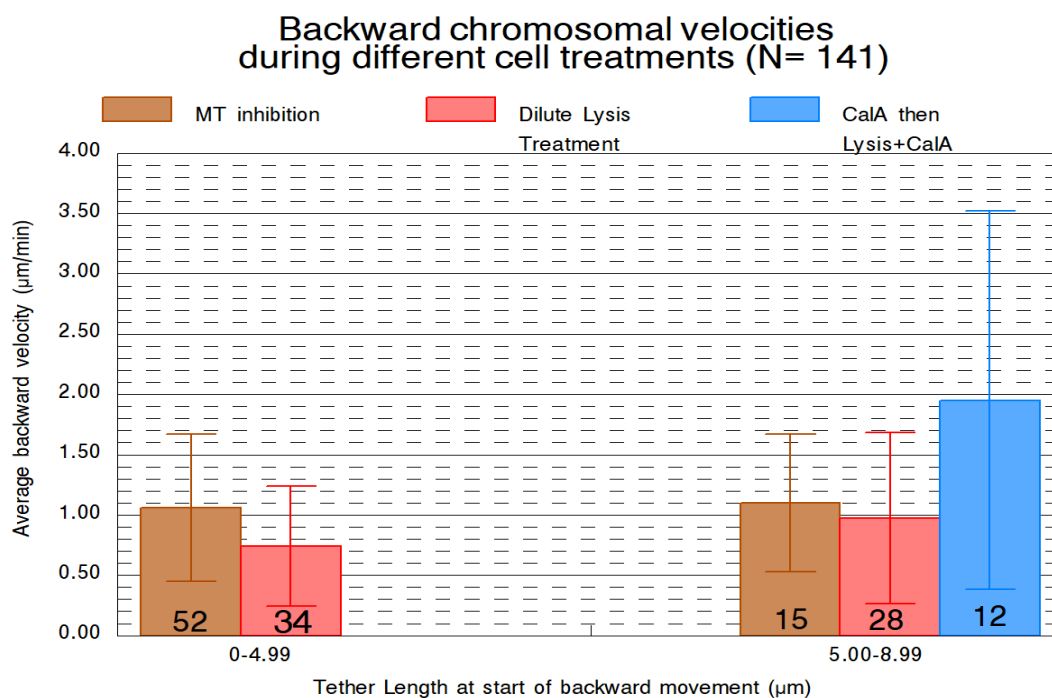


**Figure 3.8.** Average backward velocities with their standard deviations (capped bars) shown at different tether length categories during MT inhibition, dilute lysis treatment, and CalA then lysis +CalA treatment. 141 homologous pairs were examined in total (N) and numbers tested in each category are written on the respective bars. Student's t-test was performed on all data sets and all differences were statistically insignificant (alpha level set at 0.01).

#### 6) Backward moving chromosomes remain attached to their kMTs during MT inhibition; MT inhibitors fail to disassemble the stable acetylated kMTs.

Backward chromosomal velocities in MT inhibited cells were 1-1.5  $\mu\text{m}/\text{min}$  (Figure 3.7), which were less than the backward chromosomal arm fragment velocities of 4-7  $\mu\text{m}/\text{min}$  seen in control cells (Forer *et al.*, 2021). Did the MT inhibitors fail to disassemble kMTs and free the backward moving chromosomes from their poleward resistance? 30  $\mu\text{M}$  NOC-inhibited cells were immunostained for  $\alpha$ -tyrosinated ( $\alpha$ -TYR) and  $\alpha$ -acetylated ( $\alpha$ -AC) tubulin, and compared with similarly stained metaphase control cells (Figure 3.9). The fluorescence intensity in the two immunolabelled channels was obtained from a line drawn along one kinetochore fiber starting from the equator side of its kinetochore and ending near its poleward end (Figures 3.9A.c-d, 3.9B.c-d). The metaphase control cell, about to start anaphase, had both non-kinetochore MTs

(non-acetylated), and kMTs (acetylated) (Figure 3.9A.a-b). The kMT intensity profile extracted from the line along a kMT fiber (Figure 3.9A.c-e) shows that  $\alpha$ -TYR label intensity increases abruptly and is at its maximum starting at the kinetochore at a distance of about  $1\mu\text{m}$ ; the intensity stays more or less at its maximum level till the end of the fiber near its pole at a distance of about  $8.5\mu\text{m}$ , from where it starts to decrease. Contrarily, the  $\alpha$ -AC intensity increases slowly from the kinetochore and reaches its maximum at a distance of about  $2\mu\text{m}$  ( $1\mu\text{m}$  away from the kinetochore where  $\alpha$ -TYR maximum is reached); the intensity remains at maximum level till the end of the fiber near its pole also at a distance of about  $8.5\mu\text{m}$ , from where it starts to decrease. Hence, kMT tubulins in control cell are not acetylated right from the kinetochore as there is a gap of about  $1\mu\text{m}$  in the acetylation of kMTs near the kinetochore end. The  $30\mu\text{M}$  NOC-inhibited cell in early anaphase arrest only had kMTs (acetylated) (Figure 3.9B.a-b); the kMT  $\alpha$ -TYR and  $\alpha$ -AC intensities increase similarly and reach their maximums near the kinetochore at a distance of about  $1\mu\text{m}$ ; both immunolabel signals follow the same pattern until the end of the fiber (Figure 3.9B.c-e). Therefore, MT inhibitors used in this research project disassemble non-kinetochore MTs, but do not disassemble the stable acetylated kMTs, which become completely acetylated and remain attached to chromosomes. These kMTs most likely resist chromosomal backward movements and slow down their backward velocities.

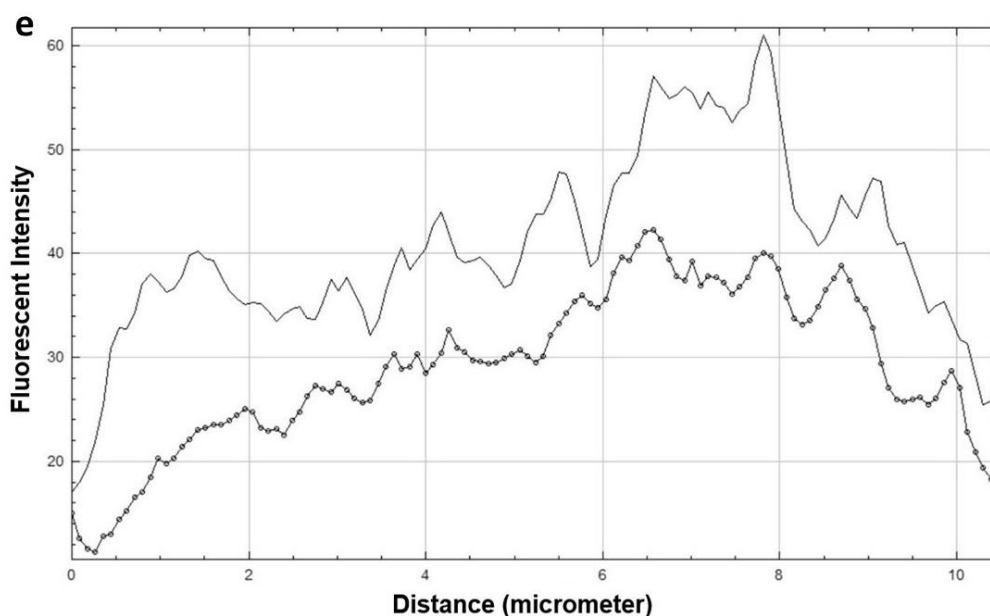
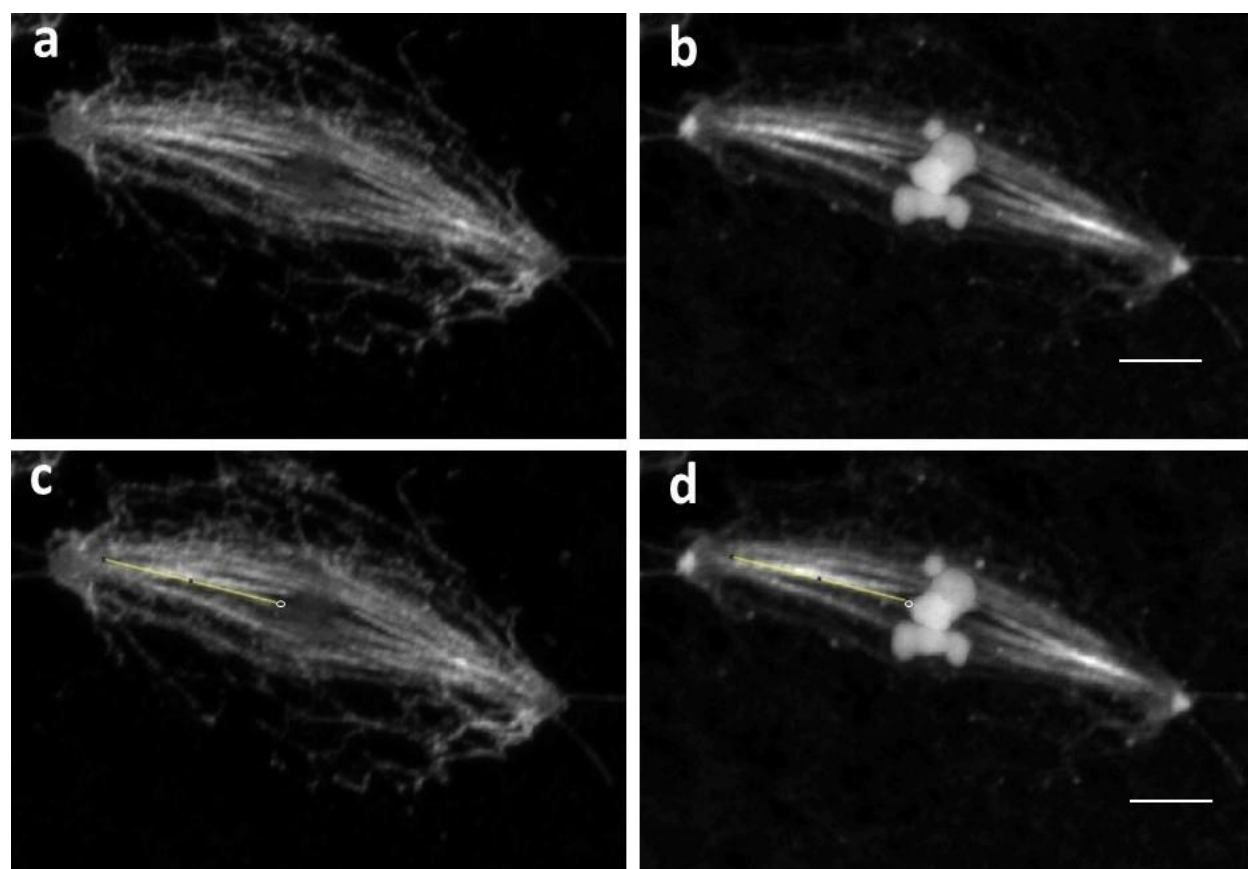


**Figure 3.9A.** Control metaphase spindle dual labeled with  $\alpha$ -TYR (image panels a & c), and  $\alpha$ -AC (image panels b & d). (a-b) 22 optical slices were taken through the cell; slices 6-19 were superposed to form a z-series. (c-d) Same z series as a-b with a line drawn along one kinetochore fiber to measure intensity of the immunostain; O marks the equator side of the kinetochore from where intensity measurement was started (time=0 of graph e). (e) Fluorescent intensity plotted against distance along the measuring line for  $\alpha$ -TYR (smooth line graph) and  $\alpha$ -AC (speckled line graph);  $\alpha$ -TYR is at maximum intensity from kinetochore till the end of the fiber near the pole;  $\alpha$ -AC reaches maximum intensity 1  $\mu$ m away from kinetochore, then it has the same intensity profile as  $\alpha$ -TYR for rest of the fiber. Scale bars= 5  $\mu$ m.

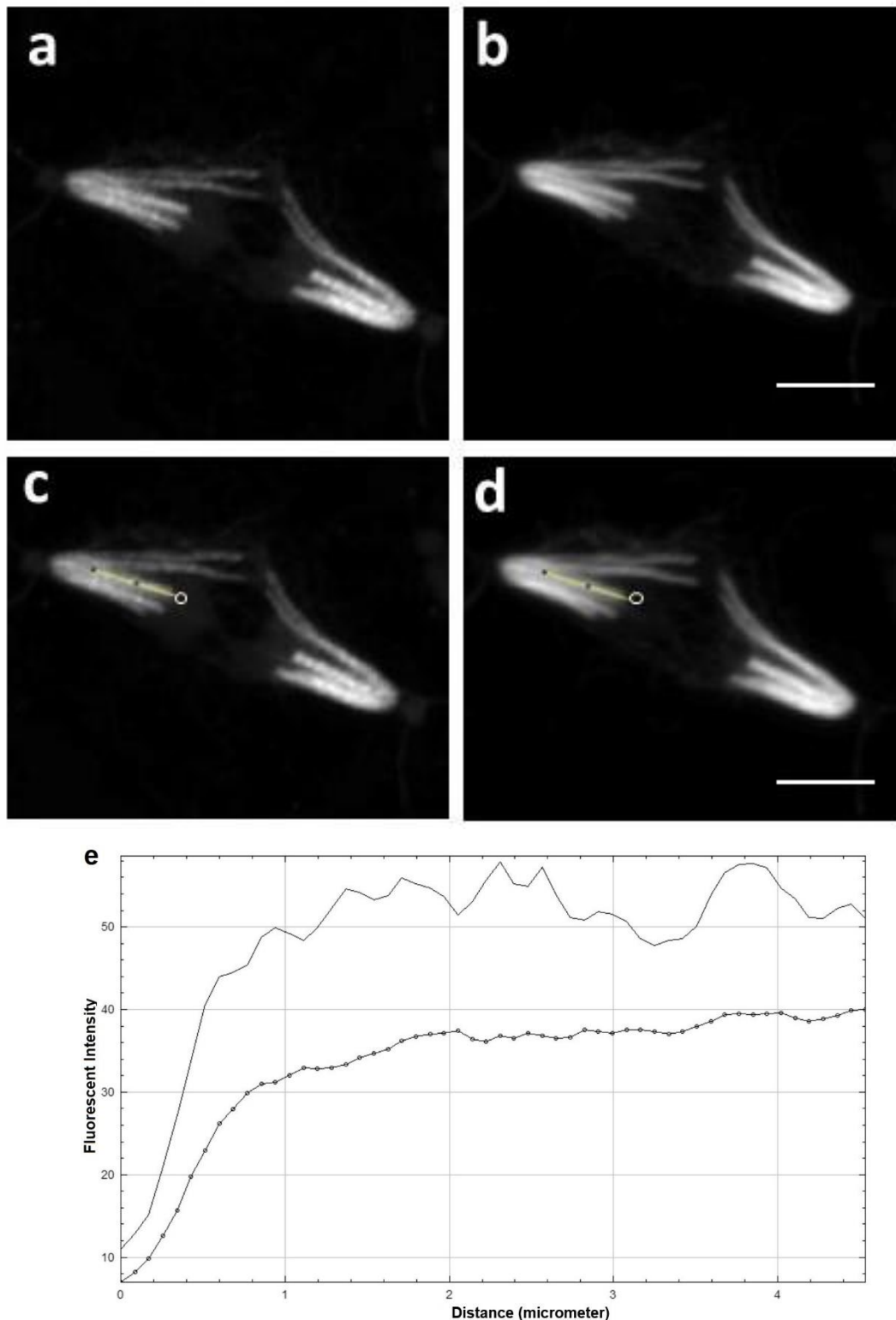


**Figure 3.9B.** 30 $\mu$ M NOC-treated early anaphase spindle dual labeled with  $\alpha$ -TYR (image panels a & c), and  $\alpha$ -AC (image panels b & d). **(a-b)** 19 optical slices were taken through the cell; slices 4-16 were superposed to form a z-series. **(c-d)** Same z series as a-b with a line drawn along one kinetochore fiber to measure intensity of the immunostain; O marks the equator side of the kinetochore from where intensity measurement was started (time=0 of graph e). **(e)** Fluorescent intensity plotted against distance along the measuring line for  $\alpha$ -TYR (smooth line graph) and  $\alpha$ -AC (speckled line graph); both  $\alpha$ -TYR and  $\alpha$ -AC stained similarly indicating kinetochore fiber was completely acetylated from its kinetochore end till its poleward end. Scale bars= 5 $\mu$ m.

## Discussion

The findings of my research project led to the conclusion that MT inhibition does not alter elastic tether function; disabling MTs does not enable elastic tethers to function more efficiently and cause faster chromosomal backward movements compared to the backward movements seen during uninhibited MT conditions. Typical elastic tether features seen during anaphase arrest in partially lysed cells, and in CalA-treated partially lysed cells (chapter 2), remain unchanged during the anaphase arrest in MT inhibited cells. These include shorter tethers causing more frequent chromosomal backward movements than longer tethers (Figure 3.5); shorter tethers causing backward movements over greater fractional distances than longer tethers (Figure 3.6); tethers of different lengths causing backward movements with statistically similar velocities for each MT inhibition group compared within itself, and compared to its counterpart partially lysed and CalA-treated partially lysed groups (Figures 3.7, 3.8). All these tether characteristics are also seen with chromosomal arm fragments in untreated cells (Forer *et al.*, 2021), which supports my conclusion that MT inhibition does not alter elastic tether function.

The different MT poisons used in this study deactivate the MTs and cause anaphase arrest in all the treated cells (Table 3.1), but deactivating MTs does not affect the velocities of backward chromosomal movements caused by elastic tethers during anaphase arrest (Figure 3.8). During anaphase chromosomal segregation in crane-fly spermatocytes, the kMTs treadmill towards the pole (LaFountain *et al.*, 2004). As new tubulins add to the kMTs, the older tubulins already incorporated in the kMTs get acetylated; acetylated MTs are more stable than the non-acetylated MTs (Wilson and Forer, 1989; Wilson *et al.*, 1994). NOC, Colcemid, and PPT halt anaphase segregation by inhibiting MT dynamics; they block MT polymerization and promote their depolymerization (Bryan, 1974; LaFountain, 1985; Jordan *et al.*, 1992; Silverman-Gavrila and Forer, 2000; Hamel, 2003). These MT inhibitors obstruct both the non-kinetochore and kinetochore MT function, but they cause only non-kinetochore (non-acetylated) MT disassembly; the stable acetylated kMTs are resistant to inhibitor disassembly. This is why MT-inhibited anaphase chromosomes stop segregating but they remain attached to their acetylated kMTs (Figure 3.9), just like the lysis buffer treated chromosomes remain attached to their acetylated kMTs (chapter 2). These acetylated kMTs holding onto the chromosomes from the poleward direction probably retard their anti-poleward accelerations in both MT-inhibited and

lysis buffer-treated anaphase arrest. This could explain why the backward chromosomal movements caused by elastic tethers during MT-inhibited and lysis buffer-treated anaphase arrest have statistically similar velocities (Figure 3.8). Hence, disabling MTs with NOC, Colcemid, or PPT arrests anaphase chromosomal segregation, but does not affect backward chromosomal velocities, which remain similar to the backward chromosomal velocities seen during other anaphase arrests.

Inhibiting MTs does not allow the elastic tethers to cause fast backward movements of chromosomes, like tethers do with chromosomal arm fragments. Most of the characteristics of backward chromosomal movements caused by elastic tethers during MT-inhibited anaphase arrest match the characteristics of backward chromosomal arm fragment movements caused by tethers. Nevertheless, though elastic tethers exert anti-poleward forces on chromosomes like they do on chromosomal arm fragments, the effective velocities of backward moving chromosomes are almost three times less than those of backward moving arm fragments (Figure 3.7; Forer *et al.*, 2021). The reason for this could again be related to the kMTs; kMTs are acetylated and stable, thus they are resistant to complete breakdown by inhibitors. Since kMTs do not disassemble under MT inhibitor treatment, backward moving chromosomes remain attached to their kMTs while backward moving chromosomal arm fragments are not. Thus, chromosomes move backward slower, against their kMT's poleward resistance, while chromosomal arm fragments move backward faster, not having any kMT's poleward resistance acting against them.

I used MT inhibitors at their higher possible concentrations to try to disable and disassemble all MTs, and then assess whether tethers can work more efficiently without having MT resistance acting against them. To achieve this objective, I chose MT inhibitors commonly used to depolymerize MTs; NOC, Colcemid, and PPT. NOC used at 10-20  $\mu\text{M}$  concentration in *Mesostoma ehrenbergii* prometaphase spermatocytes causes kMT depolymerization and fragmentation within 5-10 minutes; this leads to chromosomes detaching from their kMTs at one pole and moving to the opposite pole (Fegaras and Forer, 2018). Similar effects are seen with 50-100  $\mu\text{M}$  Colcemid treatments which enable chromosomes to detach from their kMTs at one pole and move to the opposite pole (Fegaras and Forer, 2018). LaFountain (1985) demonstrated that applying 33  $\mu\text{M}$  NOC or 27  $\mu\text{M}$  Colcemid to *Nephrotoma suturalis* testes for 10-60 minutes results in prophase cells entering metaphase without any spindle MTs. Furthermore, the NOC and

Colcemid affect on metaphase and anaphase cells causes non-kinetochore spindle MTs to disassemble, and anaphase segregation to stop within a few minutes of treatment. However, kMTs persist in both metaphase and anaphase cells for at least an hour post-treatment. Therefore, for my experiments with *Nephrotoma suturalis* anaphase spermatocytes, I decided to use NOC at 20, 30, 60 and 90  $\mu\text{M}$  concentrations, and Colcemid at 100 and 200  $\mu\text{M}$  concentrations; these were 2-10 times greater than the concentrations used in previous studies. I selected these higher dosages to increase the probability of attaining the desired effect quickly and completely with the drug treatments. None of the treatments produced any apparent toxic effects on the anatomy and physiology of my experimental cells. As for the PPT, HeLa S3 cells incubated in 15 nM PPT for 20 hours exhibit a 50% reduction in MT polymerization (Jordan *et al.*, 1992). Also, *In vitro* tubulin polymerization assays using 40  $\mu\text{M}$  PPT for 10-20 minutes show a complete blockage of tubulin polymerization (Hamel, 2003). Based on these reports, I used PPT at 10, 20, 30, 50 and 60  $\mu\text{M}$  concentrations to ensure the drug achieved its complete target effect without having any adverse outcomes. Thus, I treated my experimental cells with various (low-high) concentrations of NOC, Colcemid, and PPT, aiming to disable and disassemble all MTs, and then assess whether tethers can work more efficiently than they do in untreated cells.

The MT inhibitor doses I used in my anaphase crane-fly spermatocytes successfully disabled spindle MTs, arrested anaphase segregation, and disassembled non-kinetochore MTs; however, they failed to disassemble kMTs (Figure 3.9). MT inhibitors can disable kMTs and non-kinetochore MTs similarly, but they cannot break down kMTs as easily as they can non-kinetochore MTs when kMTs are acetylated and stable (Bryan, 1974; Wilson and Forer, 1989; Xu *et al.*, 2017). Crane-fly spermatocytes have acetylated kMTs in their metaphase and anaphase spindles; these dynamic kMTs treadmill as they polymerize at their kinetochore (plus) ends where new tubulins are added, and depolymerize at their poleward (minus) ends where old tubulins are removed (Wilson *et al.*, 1994). The new tubulins are not acetylated when they add on to the kMT plus end; they become acetylated later after they have moved along the kMT fiber towards the minus end (Wilson *et al.*, 1994; Wilson and Forer, 1997). Thus, immunostaining for acetylated tubulin in metaphase and anaphase cells shows a gap in the acetylated kMT stain at the kinetochore, indicating the lag in acetylation of new tubulin subunits in the treadmilling kMTs (Wilson *et al.*, 1994; Wilson and Forer, 1997). 10  $\mu\text{M}$  NOC treatment of metaphase cells result in disassembly of all non-kinetochore MTs, while the kMTs are disabled yet remain intact; also,

these intact kMTs become fully acetylated, so the gap in acetylation at the kinetochore disappears (Silverman-Gavrila and Forer, 2000). I treated my anaphase cells with higher concentrations of NOC (up to nine times greater than 10  $\mu\text{M}$ ), and still obtained the same results; all the non-kinetochore MTs disassembled, yet kMTs remained intact, and kMTs became fully acetylated (Figure 3.9). The disappearance of acetylation gap at kinetochore ends of kMTs indicates that new tubulin subunits are no longer adding onto the kinetochore ends, all the previously incorporated tubulins have become acetylated, and the kMTs are not treadmilling anymore, so kMTs are disabled. In case of Colcemid, 10 and 27  $\mu\text{M}$  Colcemid treatments of metaphase and anaphase cells have the same effect on kMTs as NOC has (Czaban and Forer, 1985; LaFountain, 1985). I used higher potency Colcemid dosage in my anaphase cells (up to 200  $\mu\text{M}$ ), but obtained the same results; anaphase was arrested indicating kMTs were disabled, but backward chromosomal velocities were slow indicating kMTs were still intact keeping the chromosomes attached to their poles. These were the results obtained even with all the PPT concentrations applied to my experimental cells. Therefore, NOC, Colcemid, and PPT at high concentrations disable spindle MTs, arrest anaphase segregation, and disassemble non-kinetochore MTs, but they fail to disassemble stable acetylated kMTs.

Besides NOC, Colcemid, and PPT, another possible candidate that I considered using in my experiments, but did not, was vinblastine. Like the other inhibitors, vinblastine suppresses MT dynamics by blocking MT polymerization and promoting its depolymerization (Jordan and Wilson, 2004). Many studies suggest that the stable acetylated MTs that may be resistant to NOC and Colchicine-induced breakdown, may still be sensitive to vinblastine disassembly (Xie *et al.*, 2010; Xu *et al.*, 2017). Yet, some studies have shown that PPT is superior to both NOC and vinblastine when it comes to disassembling MTs (Jordan *et al.*, 1992). Still, the main reason I remained indecisive about using vinblastine was the fact that it has commonly been shown to create tubulin paracrystals both *in vitro* (Na and Timasheff, 1982), and *in vivo* (Behnke and Forer, 1972; Jordan *et al.*, 1992). Moreover, the effect of vinblastine on MT inhibition seems to be irreversible, perhaps due to some permanent damage being caused to the cell by the drug treatment (LaFountain, 1985). Due to the possibility of paracrystal formations, and the irreversibility of vinblastine's effect, I reasoned that vinblastine might adversely affect my anaphase spindles and tethers leading to inaccurate experimental results. Thus, vinblastine was not included in my

experimental protocol; nevertheless, future work on disassembling kMTs to assess tether forces could test vinblastine as a possible kMT disassembly agent.

Laser microsurgery can be used instead of MT inhibitors to devise another method for testing whether kMTs are exerting anti-poleward resistance against tether forces. Chromosomal arms could be laser cut immediately after adding dilute lysis buffer and arresting anaphase. Then, the backward arm fragment velocities in lysis buffer-treated cells can be compared to the velocities in control cells. If the two sets of backward velocities are statistically the same, it would mean that during anaphase arrest, elastic tethers are exerting backward forces on chromosomes with the same magnitude as the magnitude of backward forces exerted on cut chromosomal arm fragments; the reason chromosomal backward velocities are less is probably due to their kMT attachments holding them back.

In conclusion, this research work has revealed that MT inhibition arrests anaphase chromosomal segregation, but the inhibition neither affects tether function, nor increases the velocities of backward chromosomal movements caused by elastic tethers. Although depolymerizing MT inhibitors NOC, Colcemid, and PPT were applied to anaphase crane-fly spermatocytes at higher concentrations than the concentrations used in previous studies, they still disassembled only the non-acetylated non-kinetochore MTs while acetylated kMTs remained intact. This underpins the concept that acetylated MTs are stable, and resistant to inhibitor dissolution. Thus, to further assess kMT resistance against tether backward forces, two possible experiments can be devised: either a more potent MT disassembly agent can be used that can disassemble the stable acetylated kMTs, and allow backward chromosomal movements caused by tethers to occur free of kMT resistance; or laser microsurgery can be used to cut off chromosomal arm fragments soon after anaphase arrest, and then the backward chromosomal movements caused by tethers working free of kMT resistance can be evaluated.

## **Chapter 4. Summary Discussion**

This thesis aimed to devise a partially permeabilized (partially lysed) living cell system where the anaphase spindle apparatus was deactivated, but the tethers still worked so they could be studied. Understanding details of tether mechanics could help improve the management of abnormal cell division conditions like fatal chromosomal birth defects, and cancer. I applied various dilutions of our standard immunofluorescence lysis buffer to anaphase-I spermatocytes of crane flies, and then examined tether function therein. Higher concentrations of lysis buffer dilutions consistently deactivated the anaphase spindle apparatus, and arrested anaphase chromosomal segregation. During the dilute lysis buffer-induced anaphase arrest, elastic tethers caused backward chromosomal movements with typical characteristics, like the characteristics of backward chromosomal arm fragment movements seen in non-lysed (control) cells of Forer *et al* (2021). This proves that the partial lysis treatment of cells does not change the elastic tethers, despite of deactivating the anaphase spindle apparatus. Hence, my dilute lysis buffer preparations can arrest anaphase segregation, and allow elastic tether forces to become effective. This system might be able to be developed into an assay for studying tethers; for example, by applying different enhancer/inhibitor enzymes to the partially lysed cells, then analyzing how they affect tether activity.

IGEPAL detergent (an NP-40 substitute) is the lysis buffer component most likely responsible for arresting anaphase chromosomal segregation, while retaining active elastic tethers capable of exerting backward forces on chromosomes. IGEPAL is a non-ionic, non-denaturing detergent which preserves native proteins in their biologically active state, and maintains protein-protein interactions (Brown and Audet, 2008; Caligur, 2023; Thermofisher, 2023). This could explain how IGEPAL treatment of anaphase cells allows elastic tethers to remain active, and function like they function in non-treated cells. Additionally, two possible mechanisms by which dilute IGEPAL could cause anaphase spindle deactivation and anaphase arrest are as follows: first, dilute IGEPAL can partially permeabilize the cell membrane, which could cause some intracellular proteins playing vital roles in anaphase to solubilize out of the cell (Seddon *et al.*, 2004; Churchward *et al.*, 2005; Sinha *et al.*, 2017; Berlin *et al.*, 2023). Alternatively, dilute IGEPAL maybe interacting with the intracellular tubulin to inhibit MT dynamics, and thereby stabilize the spindle apparatus (Mesland and Spiele, 1984; Andreu, 1982). These mechanisms, working either individually or collectively, could deactivate the spindle apparatus and arrest anaphase

segregation. Moreover, some mild, non-ionic, non-denaturing detergents like IGEPAL have been shown to reversibly inhibit microtubules, such that detergent washout leads to restoration of tubulin polymerization (Andreu *et al.*, 1986). Reversibility is seen 100% of the times in my IGEPAL experiments where IR washout causes the IGEPAL-arrested anaphase to restart, and cell division to complete as seen in control cells. Therefore, previous research supports the possibility of IGEPAL detergent being capable of maintaining elastic tethers in their functional form, while deactivating anaphase spindles and arresting anaphase chromosomal segregation.

Results of my dilute lysis buffer experiments led to a question: why are backward moving chromosomal velocities smaller as compared to backward moving chromosomal arm fragment velocities? This might be due to chromosomes having to move backward (anti-poleward) against poleward resistance; the poleward resistance may be exerted by the kinetochore microtubules (kMTs) which remain attached to backward moving chromosomes during dilute lysis buffer-induced anaphase arrest. Therefore, kMTs keep chromosomes attached to their poles, and they may be holding the chromosomes back from moving anti-poleward as fast, and as far, as chromosomal arm fragments do, since fragments are not attached to anything. This would cause backward chromosomal velocities to be less than backward arm fragment velocities.

If kMTs are retarding chromosomal backward movements during anaphase arrest, then disassembling kMTs should allow the chromosomes to move backward as fast as chromosomal arm fragments do once cut off from segregating anaphase chromosomes. I tested this hypothesis by treating anaphase cells with low-high concentrations of the microtubule (MT) inhibitors NOC, Colcemid, and PPT. These inhibitors prevent MT polymerization and promote their depolymerization, and thereby inhibit MT dynamics (Jordan *et al.*, 1992; Hamel, 2003; Jordan and Wilson, 2004; Yang *et al.*, 2010). All the MT inhibitors used at different concentrations arrested anaphase segregation in all the treated cells. Furthermore, elastic tethers caused backward chromosomal movements with the same characteristics during MT inhibited anaphase arrest as the backward movement characteristics seen during dilute lysis buffer-induced anaphase arrest. The backward chromosomal movement in MT inhibited cells also matched the backward chromosomal arm fragment movements in untreated (control) cells in all aspects except one; backward chromosomal velocities were less with MT inhibition than the backward chromosomal arm fragment velocities seen with control conditions. Chromosomal arm fragments are not

attached to any MTs, so their backward movements are unrestricted; chromosomes remain attached to their kMTs during anaphase arrest, so their backward movements are restricted. The kMTs are completely acetylated, hence they are stable and not easily depolymerized (Wilson and Forer, 1989; Wilson *et al.*, 1994; Xu *et al.*, 2017). So, in spite of applying depolymerizing MT inhibitors at their higher possible concentrations to anaphase cells, the kMTs did not depolymerize and disassemble, even though non-kinetochore MTs completely dissociated, and anaphase segregation stopped. This proves that first, anaphase spindle deactivation and anaphase arrest caused by both partial cell lysis and MT inhibition do not affect elastic tether activity; Second, acetylated kMTs are stable and remain attached to chromosomes during anaphase arrest, and thereby they could prevent backward chromosomal velocities from being greater than the backward velocities of chromosomal arm fragments seen during control conditions. Therefore, elastic tethers work during anaphase arrest like they do during control conditions; tethers cause slower backward movement of chromosomes than the faster backward movement of chromosomal arm fragments probably due to poleward resistance against the antipoleward chromosomal motion.

In order to confirm that it is the stable, acetylated kMTs that resist backward chromosomal motion during anaphase arrest, following protocols can be tested: More potent depolymerizers of MTs can be applied to anaphase cells, like vinblastine, which might be able to disassemble acetylated kMTs that are resistant to NOC and colchicine disassembly (Xie *et al.*, 2010; Xu *et al.*, 2017). However, vinblastine effects are irreversible, and it usually forms paracrystals in treated cells (Behnke and Forer, 1972; Na and Timasheff, 1982; LaFountain, 1985; Jordan *et al.*, 1992), hence the inhibitor may damage cell components leading to inaccurate results. Instead of MT inhibition, laser microsurgery can be applied during dilute lysis buffer-induced anaphase arrest, and cut chromosomal arm fragment backward velocities can be compared to the arm fragment backward velocities in control cells. This would give an accurate comparison of elastic tether forces acting on chromosomes during anaphase arrest, and control conditions. Statistically similar backward moving chromosomal arm fragment velocities during anaphase arrest and control conditions could indicate that chromosomal backward movement velocities are slow due to their kMT attachment.

Summing up my thesis, dilute lysis buffer application to anaphase cells deactivates the anaphase spindle, and arrests anaphase chromosomal segregation. Elastic tethers remain active and cause backward chromosomal movements, like the backward chromosomal arm fragment movements seen in control cells. However, backward chromosomal velocities are less than backward chromosomal arm fragment velocities. This is most probably because the anaphase arrested chromosomes remain attached to their kMTs, and the kMTs exert poleward resistance against chromosomal antipoleward movement. The kMTs are acetylated, stable, and resistant to disassembly by MT inhibitors like NOC, Colcemid, and PPT used at their higher concentrations. So, the backward chromosomal movements occurring during lysis buffer-induced anaphase arrest are similar to the backward chromosomal movements occurring during MT-inhibited anaphase arrest. Still, the lysis buffer-induced anaphase arrest system could possibly be developed further to study tethers in detail; this can improve our comprehension of possible mechanisms causing anomalous cell divisions, and improve our management of disorders with poor prognosis like fatal birth defects and cancer.

## REFERENCES

- Adames KA, Forer A. 1996. Evidence for polewards forces on chromosome arms during anaphase. *Cell motility and the cytoskeleton*. 34(1): 13-25.
- Alberts B, Johnson A, Lewis J, et al. 2002. *An Overview of the Cell Cycle*. Molecular Biology of the Cell. 4th edition. New York: Garland Science. Available from: <https://www.ncbi.nlm.nih.gov/books/NBK26869/>
- Amidzadeh Z, Behbahani AB, Erfani N, Sharifzadeh S, Ranjbaran R, Moezi L, Aboualizadeh F, Okhovat MA, Alavi P, Azarpira N. 2014. Assessment of different permeabilization methods of minimizing damage to the adherent cells for detection of intracellular RNA by flow cytometry. *Avicenna J Med Biotechnol*. 6(1):38-46.
- Anandan A, Vrieling A. 2016. Detergents in Membrane Protein Purification and Crystallisation. In: Moraes, I. (eds) *The Next Generation in Membrane Protein Structure Determination*. Advances in Experimental Medicine and Biology. 922. Springer, Cham. [https://doi.org/10.1007/978-3-319-35072-1\\_2](https://doi.org/10.1007/978-3-319-35072-1_2)
- Andreu JM. 1982. Interaction of tubulin with non-denaturing amphiphiles. *The EMBO Journal*. 1(9): 1105-1110.
- Andreu JM, De la Torre J, Carrascosa JL. 1986. Interaction of tubulin with octyl glucoside and deoxycholate. 2. Protein conformation, binding of colchicine ligands, and microtubule assembly. *Biochem*. 25(18): 5230-5239.
- Andrews FM. 1915. Die Wirkung der Zentrifugalkraft auf Pflanzen. *Jahrb Wiss Bot*. 56:221–253.
- Anjur-Dietrich MI, Kelleher CP, Needleman DJ. 2021. Mechanical mechanisms of chromosomes segregation. *Cells*. 10:465.
- Barefield C, Karlseder J. 2012. The BLM helicase contributes to telomere maintenance through processing of late-replicating intermediate structures. *Nucleic Acid Res*. 40: 7358–7367.
- Barr FA, Gruneberg U. 2007. Cytokinesis: Placing and making the final cut. *Cell*. 131(5):847-860.
- Behbahani GK, Thom C, Zunder ER, Finck R, Gaudilliere B, Fragiadakis GK, Fantl WJ, Nolan GP. 2014. Transient partial permeabilization with saponin enables cellular barcoding prior to surface marker staining. *Cytometry A*. 85(12):1011-9.
- Behnke O, Forer A. 1972. Vinblastine as a cause of direct transformation of some microtubules into helical structures. *Exptl Cell Res*. 73:506-509.

- Berlin E, Lizano-Fallas V, Carrasco del Amor A, Fresnedo O, Cristobal S. 2023. Nonionic surfactants can modify the thermal stability of globular and membrane proteins interfering with the thermal proteome profiling principles to identify protein targets. *Anal. Chem.* 95(8): 4033-4042.
- Brady M, Paliulis LV. 2015. Chromosome interaction over a distance in meiosis. *Royal Society Open Science.* 2(2).
- Brennan J. 2018. Components of lysis buffers. *Sciencing.com*. [Updated 2018 May 21; accessed 2023 June 21, 2023]. <http://www.sciencing.com/components-lysis-buffers-8148370.html>.
- Brown RB, Audet J. 2008. Current techniques for single-cell lysis. *J R Soc Interface.* 5(Suppl 2):S131-8.
- Bryan J. 1974. Microtubules. *Bioscience.* 24(12): 701-711.
- Buonomo SBC, Clyne RK, Fuchs J, Loidl J, Uhlmann F, Nasmyth K. 2000. Disjunction of homologous chromosomes in meiosis I depends on proteolytic cleavage of the meiotic cohesin Rec8 by separin. *Cell.* 103(3):387-398.
- Caligur V. 2023. Detergent Properties and Applications. MilliporeSigma. <https://www.sigmaaldrich.com/CA/en/technical-documents/technical-article/protein-biology/protein-lysis-and-extraction/detergent-properties>
- Carlson JG. 1953. Microdissection studies of the dividing neuroblast of the grasshopper *Chortophaga viridifasciata* (De Geer). *Chromosoma.* 5(3):199–220.
- Carnoy J. 1885. *La cytodierèse ches les Arthropodes.* Aug Peeters Libraire, Louvain.
- Chan KL, North PS, Hickson ID. 2007. BLM is required for faithful chromosome segregation and its localization defines a class of ultrafine anaphase bridges. *EMBO J.* 26: 3397–3409.
- Churchward MA, Butt RH, Lang JC, Hsu KK, Coorsen JR. 2005. Enhanced detergent extraction for analysis of membrane proteomes by two-dimensional gel electrophoresis. *Proteome Sci.* 3(1): 5.
- Coue M, Lombillo VA, McIntosh JR. 1991. Microtubule depolymerization promotes particle and chromosome movement in vitro. *J Cell Biol.* 112 (6): 1165–1175.
- Czaban BB, Forer A. 1985. The kinetic polarities of spindle microtubule *in vivo*, in crane-fly spermatocytes. I. kinetochore microtubules that re-form after treatment with colcemid. *J cell Sci.* 79:1-37.

- Fabian L, Forer A. 2005. Redundant mechanisms for anaphase chromosome movements: crane-fly spermatocyte spindles normally use actin filaments but also function without them. *Protoplasma*. 225: 169-184.
- Fabian L, Troscianczuk J, Forer A. 2007a. Calyculin A, an enhancer of myosin, speeds up anaphase chromosome movement. *Cell & chromosome*. 6(1): 1.
- Fabian L, Xia X, Venkitaramani DV, Johansen KM, Johansen J, Andrew DJ, Forer A. 2007b. Titin in insect spermatocyte spindle fibers associates with microtubules, actin, myosin and the matrix proteins skeletor, megator and chromator. *J Cell Sci*. 120(13): 2190-2204.
- Fegaras E, Forer A. 2018. Chromosomes selectively detach at one pole and quickly move towards the opposite pole when kinetochore microtubules are depolymerized in *Mesostoma ehrenbergii* spermatocytes. *Protoplasma*. 255:1205–1224.
- Forer A. 1966. Characterization of the mitotic traction system, and evidence that birefringent spindle fibres neither produce nor transmit force for chromosomes movement. *Chromosoma (Berlin)*. 19:44-98.
- Forer A. 1980. Chromosome movements in the meiosis of insects, especially crane-fly spermatocytes. *Insect Cytogenetics, Symp. Roy. Entomological Soc. London Number 10*, eds R. L. Blackman, G. M. Hewitt, and M. Ashburner (Oxford; London; Edinburgh; Boston, MA; Melbourne, VIC: Blackwell Scientific Publications): 85–95.
- Forer A. 1982. Crane fly spermatocytes and spermatids: a system for studying cytoskeletal components. *Methods in cell biology Academic Press*. 25:227-252.
- Forer A, Berns MW. 2020. Elastic tethers between separating anaphase chromosomes regulate the poleward speeds of the attached chromosomes in crane-fly spermatocytes. *Front Mol Biosci*. 7:161.
- Forer A, Koch C. 1973. Influence of autosome movements and of sex chromosome movements on sex-chromosome segregation in crane fly spermatocytes. *Chromosoma* 40(4):417–442.
- Forer A, Pickett-Heaps JD. 1998. Cytochalasin D and latrunculin affect chromosome behavior during meiosis in crane-fly spermatocytes. *Chromosome Res*. 6:533-549.
- Forer A, Pickett-Heaps JD. 2005. Fibrin clots keep non-adhering living cells in place on glass for perfusion or fixation. *Cell Biology International*. 29: 721-730.
- Forer A, Adil A, Bern MW. 2021. Blocking protein phosphatase 1 [PP1] prevents loss of tether elasticity in anaphase crane-fly spermatocytes. *Front Mol Biosci*. 8:636746.

- Forer A, Ferraro-Gideon J, Berns MW. 2013. Distance segregation of sex chromosomes in crane-fly spermatocytes studied using laser microbeam irradiations. *Protoplasma*. 250(5): 1045-1055.
- Forer A, Sheykhan R, and Berns MW. 2018. Anaphase chromosomes in crane-fly spermatocytes treated with taxol (paclitaxel) accelerate when their kinetochore microtubules are cut: evidence for spindle matrix involvement with spindle forces. *Front Cell Dev Biol*. 6:77.
- Forer A, Spurck T, Pickett-Heaps JD, Wilson PJ. 2003. Structure of kinetochore fibres in crane-fly spermatocytes after irradiation with an ultraviolet microbeam: neither microtubules nor actin filaments remain in the irradiated region. *Cell Motil Cytoskeleton*. 56: 173–192.
- Forer A, Duquette ML, Paliulis LV, Fegaras E, Ono M, Preece D, Berns MW. 2017. Elastic ‘tethers’ connect separating anaphase chromosomes in a broad range of animal cells. *Eur J Cell Biol*. 96(6): 504-514.
- Garavito RM, Ferguson-Miller S. 2001. Detergents as tools in membrane biochemistry. *Journal of Biological Chemistry*. 276(35):32403-32406.
- Gemble S, Ahuja A, Buhagiar-Labarchède G, Onclercq-Delic R, Dairou J, Biard DS, et al. 2015. Pyrimidine pool disequilibrium induced by a cytidine deaminase deficiency inhibits PARP-1 activity, leading to the under replication of DNA. *PLoS Genet*. 11: e1005384. doi: 10.1371/journal.pgen.1005384.
- Hamel E. 2003. Evaluation of antimetabolic agents by quantitative comparisons of their effects on the polymerization of purified tubulin. *Cell Biochemistry and Biophysics*. 38(1):1-22.
- Ilagan AB, Forer A. 1997. Effects of ultraviolet-microbeam irradiation of kinetochores in crane-fly spermatocytes. *Cell Motil Cytoskel*. 36(3): 266–275.
- Ilagan AB, Forer A, Spurck T. 1997. Backward chromosome movement in anaphase, after irradiation of kinetochores or kinetochore fibres. *Protoplasma*. 198(1-2):20–26.
- Islam MS, Aryasomayajula A, SelvaganapathyPR. 2017. A review on macroscale and microscale cell lysis methods. *Micromachines*. 8: 83.
- Johansen KM, Forer A, Yao C, Girton J, Johansen J. 2011. Do nuclear envelope and intranuclear proteins reorganize during mitosis to form an elastic, hydrogel-like spindle matrix? *Chr Res*. 19:345-365.
- Jordan MA, Wilson L. 2004. Microtubules as a target for anticancer drugs. *Nature Reviews, Cancer*. 4(4): 253-265.

- Jordan MA, Thrower D, Wilson L. 1992. Effects of vinblastine, podophyllotoxin and nocodazole on mitotic spindles; implications for the role of microtubule dynamics in mitosis. *J Cell Sci.* 102:401–416.
- Kite E, Forer A. 2020. The role of phosphorylation in the elasticity of the tethers that connect telomeres of separating anaphase chromosomes. *Nucleus.* 11(1): 19-31.
- LaFountain JR. 1985. Chromosome movement during meiotic prophase in crane-fly spermatocytes: 111. Microtubules and the effects of colcemid, nocodazole, and vinblastine. *Cell Motility.* 5: 393-413.
- LaFountain JR, Oldenbourg R, Cole RW, and Rieder CL. 2001. Microtubule flux mediates poleward motion of acentric chromosome fragments during meiosis in insect spermatocytes. *Mol. Biol. Cell.* 12: 4054–4065.
- LaFountain JR, Cole RW, Rieder CL. 2002. Partner telomeres during anaphase in crane-fly spermatocytes are connected by an elastic tether that exerts a backward force and resists poleward motion. *J Cell Sci.* 115(7): 1541-1549.
- LaFountain JR, Cohan CS, Siegel AJ, LaFountain DJ. 2004. Direct visualization of microtubule flux during metaphase and anaphase in crane-fly spermatocytes. *Mol Biol Cell.* 15(12):5724-32.
- Le Maire M, Champeil P, Møller JV. 2000. Interaction of membrane proteins and lipids with solubilizing detergents. *Biochimica et Biophysica Acta (BBA) – Biomembranes.* 1508(1–2):86-111.
- McIntosh JR. 2016. Mitosis. *Cold Spring Harb Perspect Biol.* 8(9):a023218.
- McIntosh JR, Hays T. 2016. A Brief History of Research on Mitotic Mechanisms. *Biology.* 5(4):55. <https://doi.org/10.3390/biology5040055>
- Mesland DAM, Spiele H. 1984. Brief extraction with detergent induces the appearance of many plasma membrane-associated microtubules in hepatocytic cells. *J cell Sci.* 68(1): 113-137.
- Montgomery TH. 1899. The spermatogenesis in *Pentatoma* up to the formation of the spermatid. *Zool Jahrb Abt f Anat.* 12:1–88.
- Na GC, Timasheff SN. 1982. *In Vitro* vinblastine-induced tubulin paracrystals. *Journal of Biological Chemistry.* 257(17):10387-10391.
- Nakanishi YH, Kato H. 1965. Unusual movement of the daughter chromosome group in telophasic cells following the exposure to ultraviolet microbeam irradiation. *Cytologia.* 30(2):213–221.

- Novus Biologicals. 2023. Plasma membrane markers. [accessed 2023, June 21]. <https://www.novusbio.com/research-areas/cellular-markers/plasma-membrane-markers.html>
- Ohkura H. 2015. Meiosis: an overview of key differences from mitosis. *Cold Spring Harb Perspect Biol.* 7(5):a015859.
- Orwick-Rydmark M, Arnold T, Linke D. 2016. The use of detergents to purify membrane proteins. *Curr Protoc Protein Sci.* 84:4.8.1-4.8.35.
- Osborn M, Weber K. 1982. Immunofluorescence and immunocytochemical procedures with affinity purified antibodies: tubulin containing structures. In: Wilson L (ed) *The cytoskeleton*, part A. Academic Press, London, pp 97–132 (Methods in cell biology, vol 24)
- Paliulis LV, Forer A. 2018. A review of “tethers”: elastic connections between separating partner chromosomes in anaphase. *Protoplasma.* 255:733-740.
- Paliulis LV, Nicklas RB. 2004. Micromanipulation of chromosomes reveals that cohesion release during cell division is gradual and does not require tension. *Curr Biol.* 14(23):2124–2129.
- Pimm ML, Henty-Ridilla JL. 2020. New twists in actin-microtubule interactions. *Molecular Biology of the Cell.* 32:211-217.
- Rogers GC, Rogers SL, Sharp DJ. 2005. Spindle microtubules in flux. *J Cell Sci.* 118: 1105–1116.
- Salmon ED, Segall RR. 1980. Calcium-labile mitotic spindles isolated from sea urchin eggs (*Lytechinus variegatus*). *The Journal of Cell Biology.* 86:355-365.
- Sato, M. 2013. Meiosis. *Encyclopedia of Systems Biology*. New York: Springer. [https://doi.org/10.1007/978-1-4419-9863-7\\_113](https://doi.org/10.1007/978-1-4419-9863-7_113)
- Sauer G, Korner R, Hanisch A, Ries A, Nigg EA, Sillje HHW. 2005. Proteome analysis of the human mitotic spindle. *Molecular and Cellular Proteomics.* 4.1.
- Schaede R. 1930. Zentrifugalversuche mit Kernteilungen. *Planta* 11(2): 243–262.
- Schrader F. 1935. Notes on the mitotic behavior of long chromosomes. *Cytologia.* 6(4):422–431.
- Seddon AM, Curnow P, Booth PJ. 2004. Membrane proteins, lipids and detergents: not just a soap opera. *Biochimica et Biophysica Acta.* 1666:105-117.
- Sharp DJ, Brown HM, Kwon M, Rogers GC, Holland G, Scholey JM. 2000. Functional coordination of three mitotic motors in *Drosophila* embryos. *Mol Biol Cell.* 11: 241–253

- Sheykhani R, Berns M, Forer A. 2017. Elastic tethers between separating anaphase chromosomes in crane-fly spermatocytes coordinate chromosome movements to the two poles. *Cytoskeleton* 74(2): 91-103.
- Sheykhani R, Shirodkar PV, Forer A. 2013. The role of myosin phosphorylation in anaphase chromosome movement. *European Journal of Cell Biology*. 92: 175-186.
- Sillers PJ, Forer A (1981) Analysis of chromosome movement in crane fly spermatocytes by ultraviolet microbeam irradiation of individual chromosomal spindle fibres. II. Action spectra for stopping chromosome movement and for blocking ciliary beating and myofibril contractions. *Canadian J Biochem* 59:777–792.
- Silverman-Gavrila RV, Forer A. 2000. Evidence that actin and myosin are involved in the poleward flux of tubulin in metaphase kinetochore microtubules of crane-fly spermatocytes. *Journal of Cell Science*. 113: 597-609.
- Sinha S, Field JJ, Miller JH. 2017. Use of substitute Nonidet P-40 nonionic detergents in intracellular tubulin polymerization assays for screening of microtubule targeting agents. *Biochem. Cell Biol.* 95: 379-384.
- Spurck T, Forer A, Pickett-Heaps J. 1997. Ultraviolet microbeam irradiations of epithelial and spermatocyte spindles suggest that forces act on the kinetochore fiber and are not generated by its disassembly. *Cell Motil Cytoskel.* 36(2):136–148.
- Su KC, Barry Z, Schweizer N, Maiato H, Bathe M, Cheeseman IM. 2016. A regulatory switch alters chromosome motions at the metaphase-to-anaphase transition. *Cell Rep.* 17: 1728–1738.
- Sudbrack TP, Archilha NL, Itri R, Riske KA. 2011. Observing the solubilization of lipid bilayers by detergents with optical microscopy of GUVs. *J Phys Chem.* 115:269-277.
- ThermoFisher Scientific. 2023. Detergents for cell lysis and protein extraction. [accessed 2023, June 21]. <https://www.thermofisher.com/ca/en/home/life-science/protein-biology/protein-biology-learning-center/protein-biology-resource-library/pierce-protein-methods/detergents-cell-lysis-protein-extraction.html>
- Unity Health Toronto. 2023. Flow cytometry intracellular staining. <https://research.unityhealth.to/staff-services/research-facilities/facilities/flow-cytometry-core/intracellular-staining/>
- Wilson EB. 1905. Studies on chromosomes. I. The behavior of the idiochromosomes in Hemiptera. *J Exp Zool.* 2(3):371–405.

- Wilson PJ, Forer A. 1989. Acetylated  $\alpha$ -tubulin in spermatogenic cells of the crane fly *Nephrotoma suturalis*: kinetochore microtubules are selectively acetylated. *Cell motility and the cytoskeleton*. 14: 237-250.
- Wilson PJ, Forer A. 1997. Effects of nanomolar taxol on crane-fly spermatocyte spindles indicate that acetylation of kinetochore microtubules can be used as a marker of poleward tubulin flux. *Cell motility and the cytoskeleton*. 37: 20-32.
- Wilson PJ, Forer A, Leggiadro C. 1994. Evidence that kinetochore microtubules in crane-fly spermatocytes disassemble during anaphase primarily at the poleward end. *J Cell Sci*. 107:3015-3027.
- Wong R, Forer A. 2003. 'Signaling' between chromosomes in crane-fly spermatocytes studied using ultraviolet microbeam irradiation. *Chr Res*. 11(8): 771.
- Xie R, Nguyen S, McKeehan WL, Liu L. 2010. Acetylated microtubules are required for fusion of autophagosomes with lysosomes. *BMC Cell Biology*. 11:89.
- Xu Z, Schaedel L, Portran D, Aguilar A, Gaillard J, Marinkovich MP, Théry M, Nachury MV. 2017. Microtubules acquire resistance from mechanical breakage through intraluminal acetylation. *Science*. 356(6335):328-332. doi: 10.1126/science.aai8764. PMID: 28428427; PMCID: PMC5457157.
- Yang H, Ganguly A, Cabral F. 2010. Inhibition of cell migration and cell division correlates with distinct effects of microtubule inhibiting drugs. *J Biol Chem*. 285(42): 32242–32250.
- Yang NJ, Hinner MJ. 2015. Getting across the cell membrane: An overview for small molecules, peptides, and proteins. *Methods Mol Biol*. 1266:29-53.
- Yin B, Forer A. 1996. Coordinated movements between autosomal half bivalents in crane-fly spermatocytes: evidence that 'stop' signals are sent between partner half-bivalents. *J Cell Sci*. 109:155–163.